CHAPTER 5

RESULTS AND DISCUSSION

5.1 Description of various physico-chemical parameters during pre and post monsoon seasons along with Spatial Distribution Map showing scattering of few important physico-chemical parameters

Analysis of water quality is one of the most formidable tools in the study of the surface water of the area for evaluating and examining the quality of the water to assess the amount of contaminants contaminating the area. Since, water is considered as one of the most important resources for sustaining life on the earth, it becomes important to monitor its quality on a regular basis. In this study, to analyze the impact of water pollutants the area has been supervised during pre and post monsoon seasons. To represent the changes between various physico-chemical parameters during the pre and post monsoon seasons geostatistical tools are considered as one of the effective treatment for a collection of data set of 60 locations in and around the area under study because of the fact that surface water are considered as an important source of water supply fulfillment not only for drinking purpose but also for agricultural and industrial requirements. Here, GIS can be considered as a beneficial and significant tool for amalgamating spatial and temporal data along with other field survey related statistics for investigating and managing complications related to evaluation of various water quality parameters in their spatial extent. Geostatistical analysis is used for computation of various physicochemical parameters along with the Water Quality Index of the area under study for spatial distribution of sampling sites using ArcGIS 10.1 software. The first step of this geostatistical analysis is the exploratory spatial data analysis (ESDA). The main objective of ESDA is to observe the data quantitatively along with the spatial distribution that ultimately assist in approaching an appropriate conclusion for achieving the interpolation models through ArcGIS software using IDW approach. In this study, IDW technique was used since this technique requires comparatively less inputs from the other methods as

well as this method is simple and easy to operate as compared to the other techniques. The main objective of the study is to perform the assessment of water quality of the surface water based on physicochemical parameters data for both pre and post monsoon seasons using GIS as well as ciphering water quality index map for both the seasons since the entire area under study is under the influence of rapid development due to industrialization through mining and thermal power plants thereby causing deterioration of the quality of the water as well as other resources. The above objective was achieved by comparing the data obtained during survey in both the seasons with that of the drinking water quality standards recommended by WHO & BIS respectively.

In this study, the physicochemical characterization of surface water (reservoir water) along with water from industrial outlets were sampled from 60 locations during pre and post monsoon seasons and analysis of major and minor parameters were done for the construction of spatial distribution map. The water samples collected from the different locations were colourless, odourless & free from turbidity except a few locations such as Balia Nala, Motwani Dam and sump of coal mines (Bina, Dudhichua, Nigahi, Krishnashila, Kakri, Amlohri, Jayant & Jhingurdah) which were slightly brackish in taste, translucent in color with turbidity. This implies that except the said few samples, rest of the samples can be used for drinking purpose after satisfying the other required tests. The temperature of the samples collected ranged between 24 to 30°C which shows that it is suitable for public consumption since according to Zajic (1971) water pursuing temperature above 30°C is not suitable for public consumption. The results of the various physicochemical parameters such as pH, Total Dissolved Solids (TDS), Total Suspended Solids (TSS), Dissolved Oxygen (DO), Electrical Conductivity (EC), Salinity, Oxidation Reduction Potential (ORP), Lithium (Li), Sodium (Na), Potassium (K), Magnesium (Mg), Calcium (Ca), Hardness, Fluoride (F^-), Chloride (Cl^-), Nitrate (NO_3^-), Sulphate (SO_4^{2-}),

Phosphate (PO_4^{3-}), Bicarbonate (HCO_3^-), Iron (Fe), Copper (Cu), Lead (Pb), Zinc (Zn), Nickel (Ni), Chromium (Cr) and Cadmium (Cd) for both the seasons are given in Table A.1 to A.8 along with permissible limit recommended by WHO and BIS. However, the spatial distribution map for few of the important parameters such as TSS, Ca, Mg, Fe, Zn, Cu, SO_4^{2-}, F^-, Cr, Cd and Ni along with WQI were computed using the above said Table.

The water quality of the study area is mainly affected by anthropogenic activities due the presence of various mining and thermal power plants. Land Use Land Cover classification of the area has already been carried out to find out the area distributed in various classes using Landsat data at 30m spatial resolution. Further to access the quality of water present in the area spatial distribution map of various parameters along with quality suitability class map was computed to know the percentage of population with access to different quality of surface water.

5.1.1 Total Suspended Solids (TSS)

Being one of the most important characteristics TSS plays an important role in determination of quality of water both for domestic and industrial purposes. High level of TSS is aesthetically undesirable for domestic as well as industrial purposes. Since, high levels of concentration of TSS may reduce the efficiency of wastewater treatment plants as well as prohibit the working of industrial processes by clogging the devices concerned with the use of raw water. TSS also reduces the clarity of the surface water by decreasing the penetration of light through it thereby affecting the process of photosynthesis by aquatic plants and hence reducing the amount of dissolved oxygen present in it posing harmful effects on survival of aquatic life. Most of the suspended solids come from mining industries, thermal power plants into the adjoining reservoir. This is mainly due to accelerated erosion of overburden dump directly into the reservoir especially during

the rainy seasons. The high concentration of TSS settles out into the form of sediment at the bottom of the reservoir as bedded sediments or bedload consequently increasing the amount of siltation into the reservoir and therefore decreasing the volume of the reservoir in the subsequent years. The estimation of the volume of the reservoir has been described in detail in the subsequent subheading later in this chapter.

The TSS values of the study area had been estimated through the laboratory test as discussed in the earlier chapter in mg/L or ppm. These tests were intended to see the spatial distribution of TSS carried out before. Through spatial distribution map of TSS, the scattering of the enormity of TSS in the study area can be identified. TSS in the study area ranges from 227 to 696 mg/L during pre-monsoon season with a desirable limit of 500 mg/L according to WHO while during post monsoon season it was found to be between 271-719 mg/L. Majority of the areas under study in pre-monsoon season lies within the desirable limit except a few of the areas such as Balia Nala and Motwani Dam where concentration of TSS was higher than that of desirable limit making it to fall under brackish water category. During post monsoon season a moderately higher value of TSS was observed than that of the pre monsoon season in most parts of the study area which might be due to the reason of influence by external sources whether natural or anthropogenic causing influx of sediments into the area (Jain et al 2010). In this season too, a higher TSS was observed in many areas encircling the reservoir along with the streams like Balia Nala and Motwani Dam where the water was very muddy as compared to the other locations taken into consideration. Fig 5.1 and Fig 5.2 show the spatial distribution maps of TSS during pre and post monsoon season in the study area respectively.

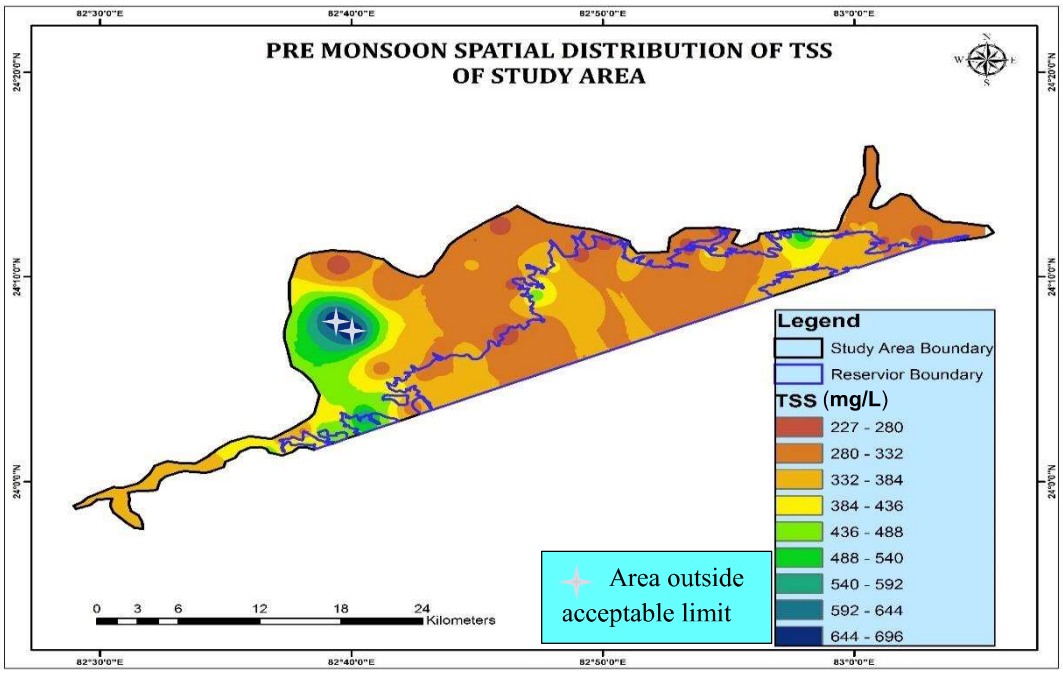

Fig 5.1 Spatial distribution of TSS during pre-monsoon season in the study area.

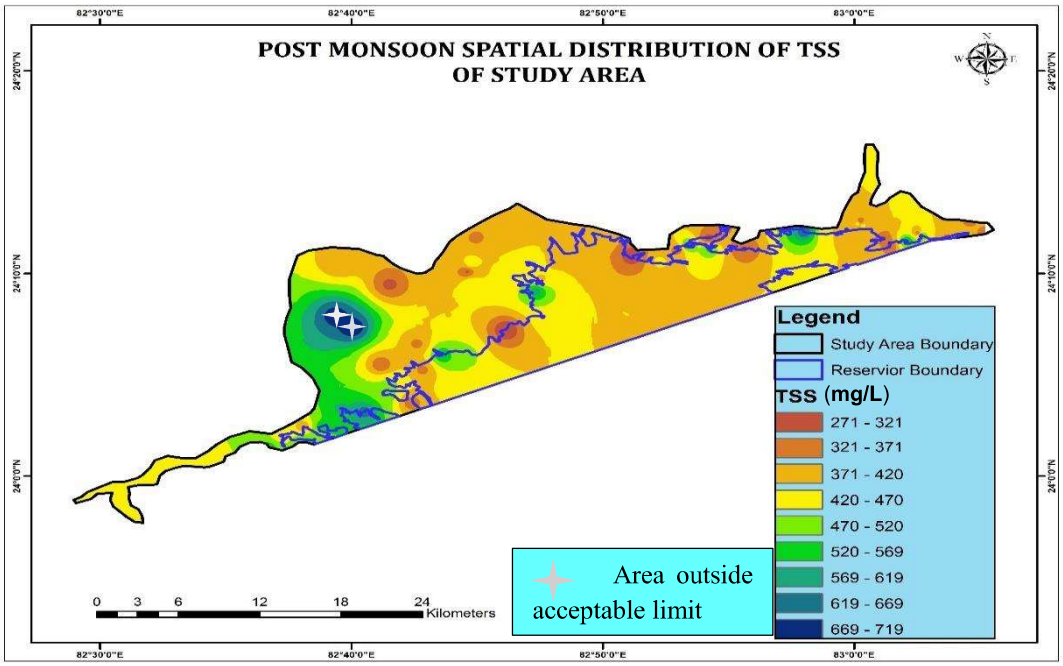

Fig 5.2 Spatial distribution of TSS during post monsoon season in the study area.

5.1.2 Calcium (Ca)

Since, the geology of the area is mainly dominated by sedimentary rocks such as limestone, dolomite and gypsum where the major constituent of it was calcium carbonate thereby making it as one of the important physico-chemical parameters in the area (Younger 2006, Tiwari et al 2016). Being one of the major components of Hardness in water, calcium plays an important role in determining the quality of water. The presence of calcium in surface water (industrial and reservoir water) was well under the limit in almost all of the locations taken into consideration both during pre and post monsoon season. It's value was found to be between 12.75 to 79.77 mg/L and 14.12 to 88.80 mg/L in pre-monsoon and post monsoon seasons respectively. Though, during post monsoon the concentration of it was slightly higher due to fluvial flux in the presence of alluvial environment in the area. Except 2-3 locations as shown in Table A.3 and A.4 the concentration of calcium in all the locations were well within the limit i.e. 75 mg/L as recommended by WHO/BIS in drinking water. As it is one of the essential components of human bones and teeth along with it's significant role in blood clotting and nervous stimulation, it's evaluation in the area has an important role in the study. The deficiency of this ion causes rickets, osteoporosis, hypertension, etc. However it's excess may result in kidney, urinary or gall bladder stones (Daly et al 2010). Fig 5.3 and Fig 5.4 shows the spatial distribution maps of Calcium during pre and post monsoon season in the study area respectively.

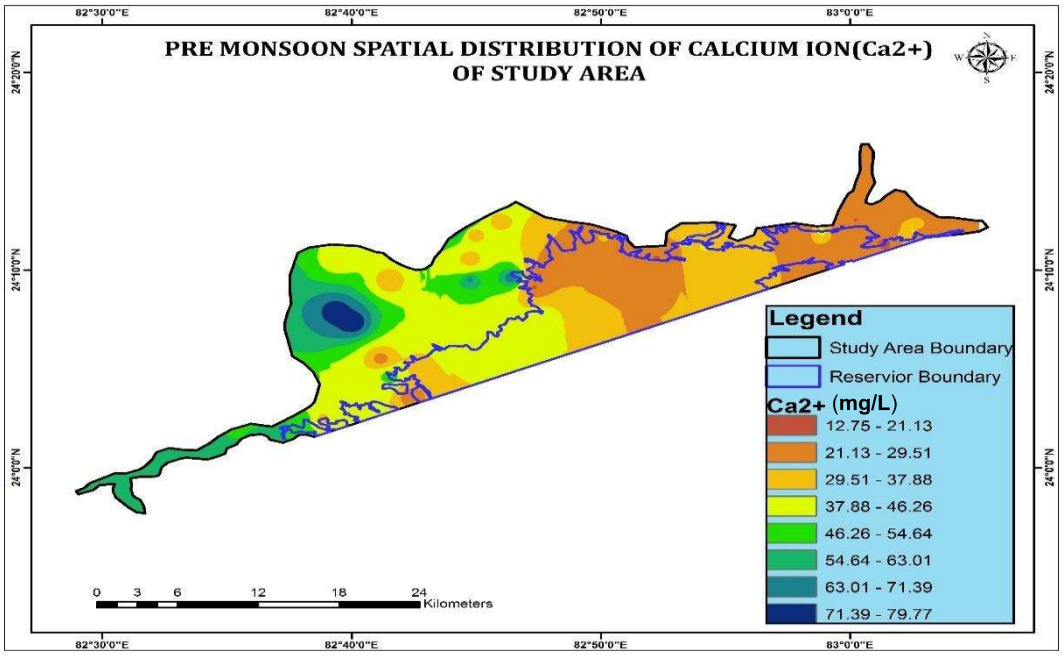

Fig 5.3 Spatial distribution of Calcium during pre-monsoon season in the study area.

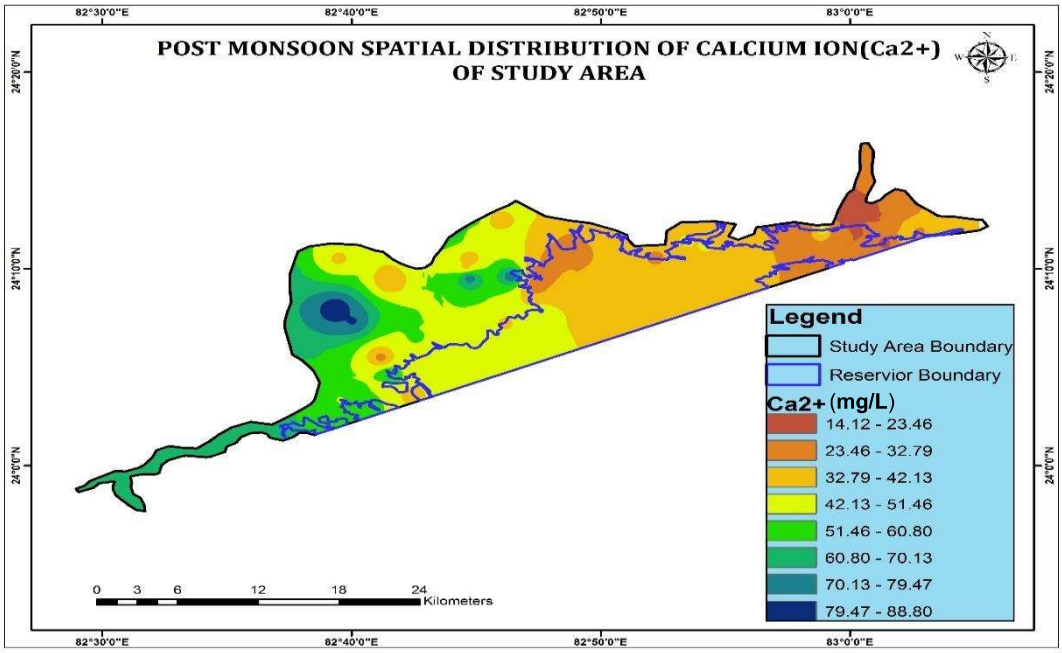

Fig 5.4 Spatial distribution of Calcium during post monsoon season in the study area.

5.1.3 Magnesium (Mg)

The Magnesium ion in the study area was again found to be well under the desirable limit in all the locations of the study area taken under consideration ranging between 15.67-26.11 mg/L and 12.23-23.85 mg/L in pre-monsoon and post monsoon seasons respectively. The desirable limit for this parameter was 50 mg/L as recommended by WHO/BIS for drinking water. The consideration of this ion in determining the water quality of the area becomes important due to the fact that the presence of magnesium in various salts causes cathartic and diuretic alterations along with the laxative effect on human health.(CPCB 2008) (Magesh et al 2013). Also, magnesium acts as a major contributor in determining the hardness of the water present in the area since the geology of the study area is mainly dominated by the presence of the sedimentary rocks like Dolomite thereby making it as one of the principal contributor in determining the water quality for drinking as well as industrial consumptions (Tiwari et al 2016). Fig 5.5 and Fig 5.6 shows the spatial distribution maps of Magnesium during pre and post monsoon season in the study area respectively.

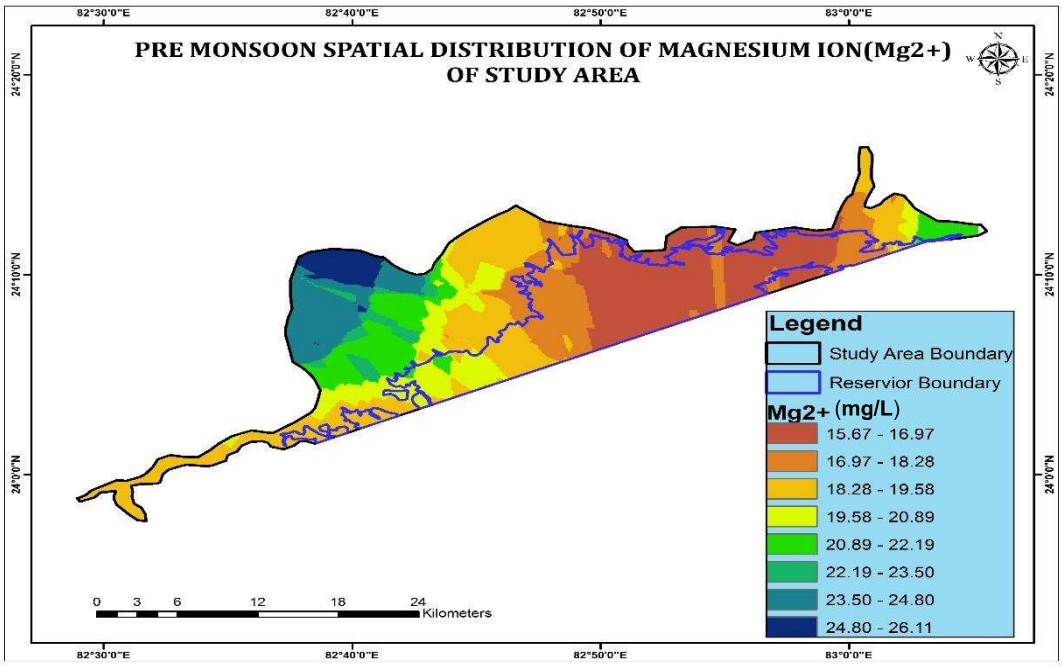

Fig 5.5 Spatial distribution of Magnesium during pre-monsoon season in the study area

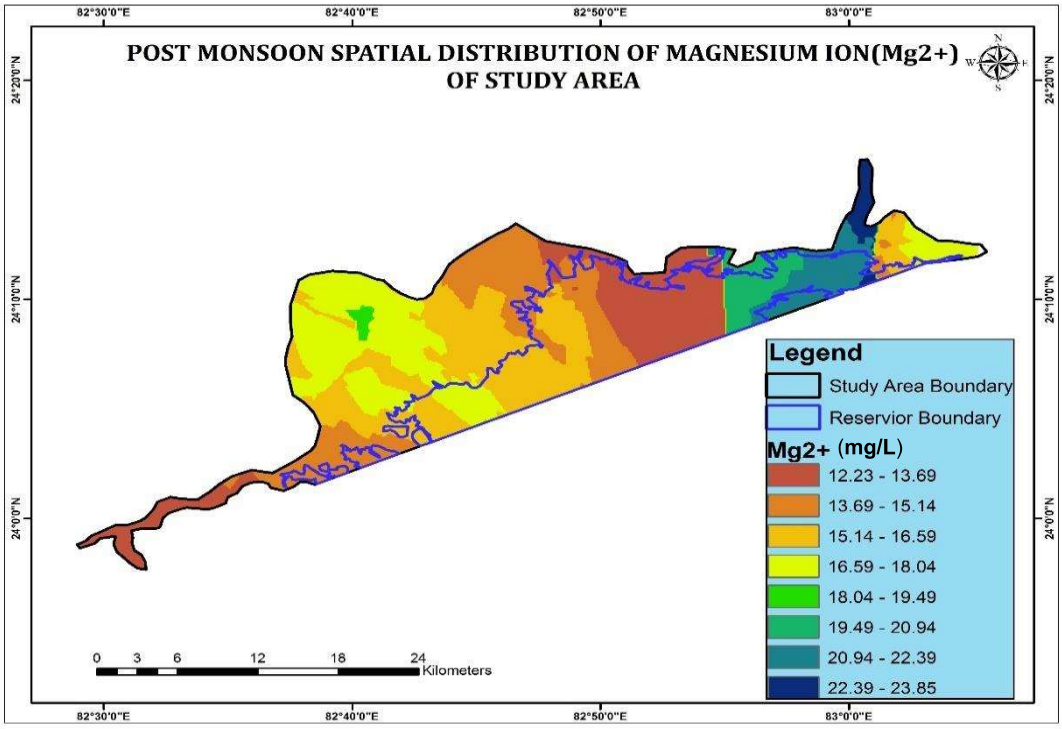

Fig 5.6 Spatial distribution of Magnesium during post monsoon season in the study area

5.1.4 Iron (Fe)

Iron is one of the substantial components present in the earth after oxygen, silicon and aluminum in abundance (Anderson 1983). It is one of the most important constituents of many metallic minerals and rocks. Since, the geology of the area is mainly dominated by sedimentary rocks therefore the mobilization of iron into the adjoining reservoir can be related to weathering of rocks by the runoff (Patel et al 2016). This process causes change in the oxidation–reduction conditions of the rocks as well as overburden present in the area under study hence making it dissolute in the form of Fe(II) (Kumar et al 2019). The spatial distribution of this metal is significant not only due to its role in industrial processes but also its effect on human life. The spatial distribution map shows the range of Fe between 0.12-2.13 mg/L and 0.11-2.10 mg/L during pre and post monsoon seasons respectively. However, the desirable limit of it is 1 mg/L as given by WHO/BIS for drinking water. Only few of the locations show the value above the desirable limit during both the seasons while most of the locations were within the limits during both the seasons. Though, the value of it during the post monsoon season was lower than that in the pre monsoon season. It's assessment is significant since it causes health issues like anemia, mental development of infants in its deficiency while its excess causes diseases like haermosiderosis (Bhaskar et al 2010). Iron is also objectionable in water since it causes rusty color in water along with change of taste. Fig 5.7 and Fig 5.8 shows the spatial distribution maps of Iron during pre and post monsoon season in the study area respectively.

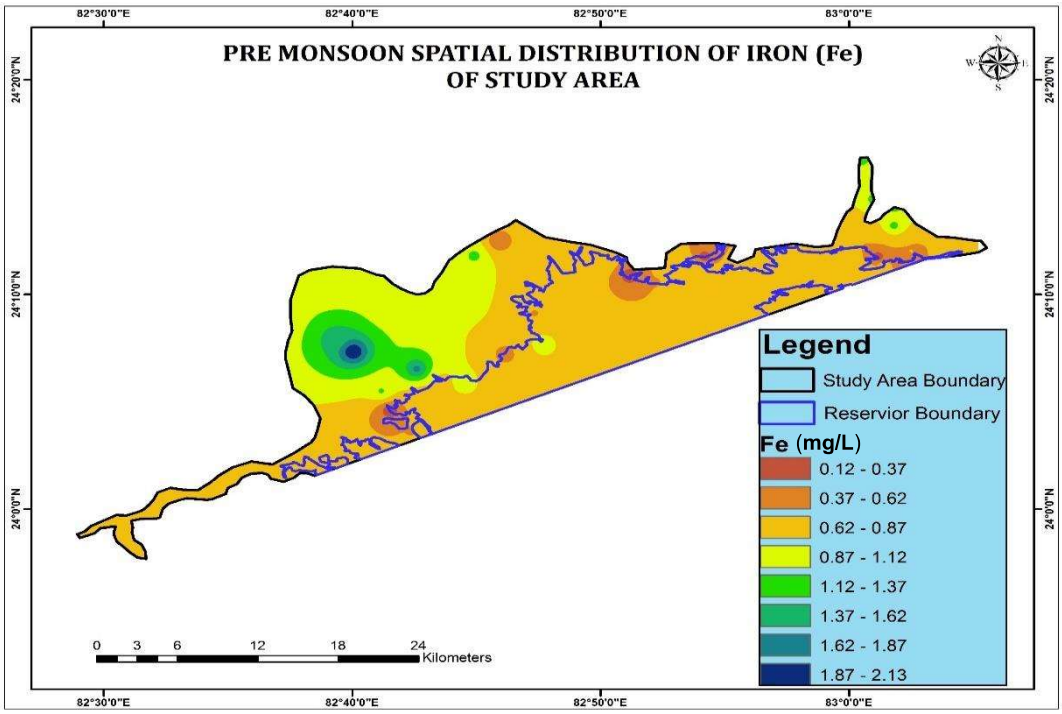

Fig 5.7 Spatial distribution of Iron during pre-monsoon season in the study area

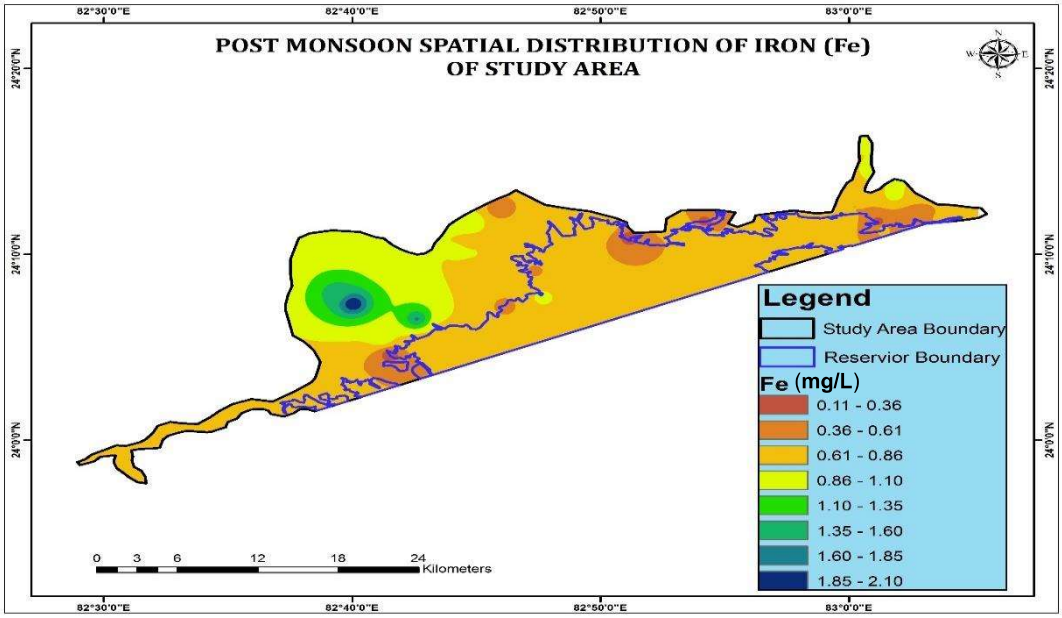

Fig 5.8 Spatial distribution of Iron during post monsoon season in the study area

5.1.5 Zinc (Zn)

As zinc is considered one of the most prolific metals for the human body since it is required for synthesis of various proteins and enzymes (Chrosniak et al 2006). The contamination of zinc in water causes a milky turbid appearance in water in association with change of taste of water thereby making it aesthically unsuitable for human consumption. The major source of pollution of zinc in water is either due to natural or anthropogenic activities such as weathering or runoff from adjoining heap of overburden into the reservoir or due to emissions from power plants, mining industries present around the reservoir in the area under study (Sengupta et al 2002). Zinc is also an important constituent of agricultural fertilizers and manures hence contaminating the surface water by runoff activities (Niagolova et al 2005). Therefore, the computation of its spatial distribution map becomes significant for determining its influential effect on the surface water body. In this study, according to the spatial distribution map it was found that the amount of zinc varied between 1.37 to 5.82 mg/L and between 1.35 to 5.78 mg/L during pre and post monsoon seasons respectively. While the desirable limit of Zn is 5mg/L in drinking water as prescribed by WHO/BIS. Though during post monsoon seasons there was a considerable decrease in concentration of Zn from that of the pre-monsoon but still few of the locations (mainly the sump water pit of mines) showed an enhanced level of concentration of Zn in map during both the seasons. However, there was a slight decrease in conc. Zn during post monsoon season which may be attributed to the increase in hardness of surface water due to addition of suspended solids and other elements in water during rainy season (Chakraborty et al 2015) to the locations under study. Fig 5.9 and Fig 5.10 shows the spatial distribution maps of Zinc during pre and post monsoon season in the study area respectively.

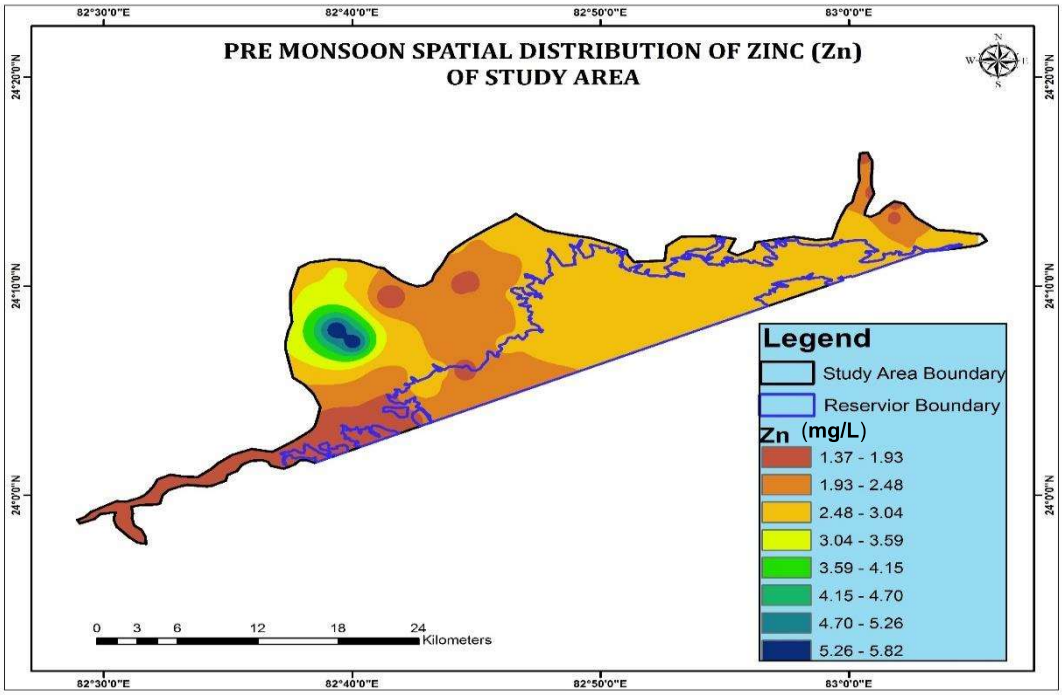

Fig 5.9 Spatial distribution of Zinc during pre-monsoon season in the study area.

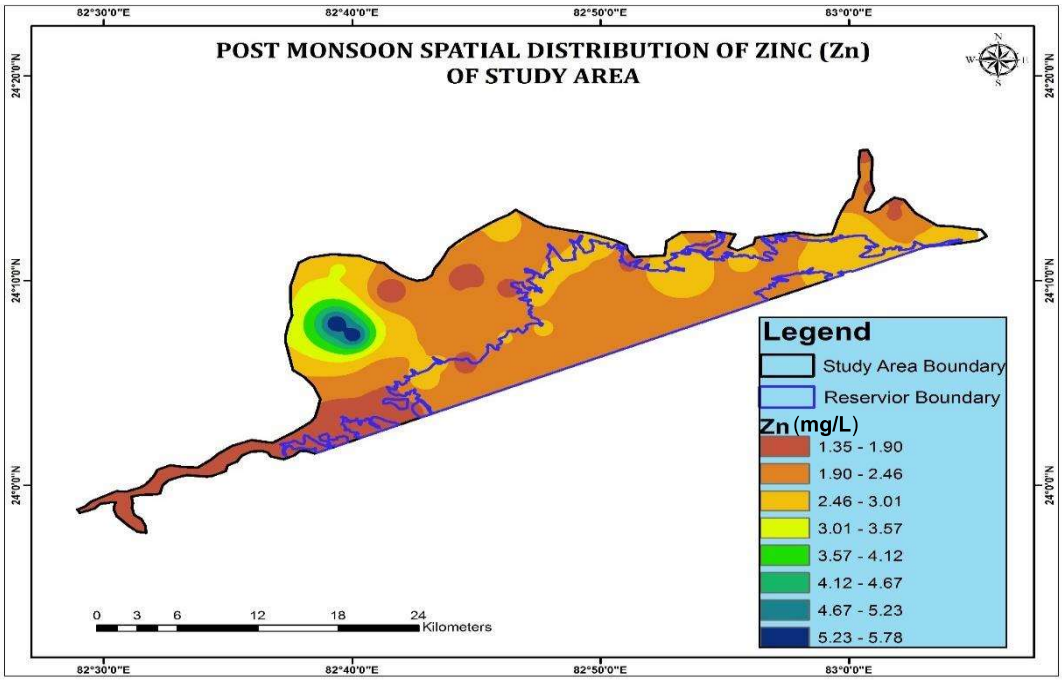

Fig 5.10 Spatial distribution of Zinc during post monsoon season in the study area.

5.1.6 Copper (Cu)

Heavy metal contamination in a watershed is one of the most difficult pollutant to be removed from the ecosystem since it settles into the stream sediments and constantly reconditioned by heavy rains or natural disruption that blend the sediments releasing metals into the solution (Giardina et al 2009). Since, Cu is less soluble in water as compared to Zn therefore it is readily absorbed by organic sediments present at the bottom of the stream or reservoir. One of the major contributor of copper in the study area are mining industries, agricultural runoff, power plant operations, etc (Sengupta et al 2002). During treatment it is mainly concentrated in the form of sludge generated from the wastewater treatment plant. In the present study the concentration of Cu was found to be between 1.00-1.82 mg/L and between 1.00 to 1.72 mg/L during pre and post monsoon season respectively. However, the desirable limit of this ion is 1.5 mg/L as prescribed by WHO/BIS in drinking water. The slight decrease in concentration of Cu during post monsoon is may be due to the reason that the variation of Cu in water is mainly dependent on the variation of pH and hardness which alters during the raining season (Sengupta et al 2002). There were very few locations which showed an enhanced level of concentration from that of the desirable limit which may be probably due to the fact the locations were having standing water and Cu possess a tendency that it is low in concentration in running water as compared to that of the stagnant water (Zlatanović et al 2017). The evaluation of Cu ion through spatial distribution map becomes important because it is mainly required in proper functioning of many enzymatic functioning along with that of the platelet concentration. It's deficiency also causes many genetic disorders such as Menkes Syndrome and excess causes Wilson disease (Wazir et al 2017). Fig 5.11 and Fig 5.12 shows the spatial distribution maps of Copper during pre and post monsoon season in the study area respectively.

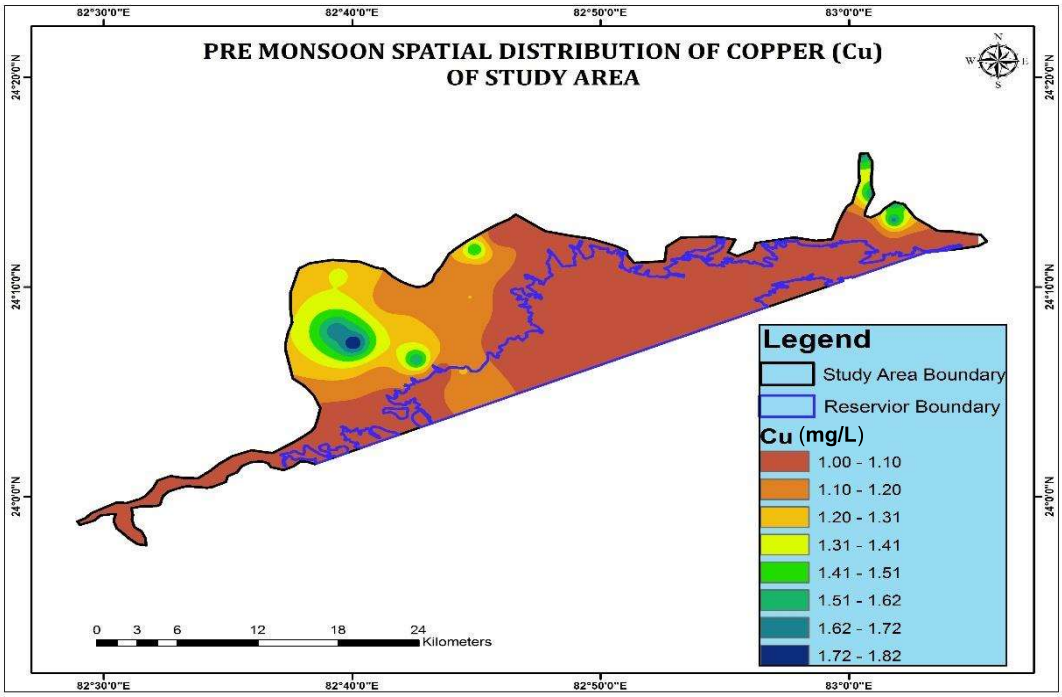

Fig 5.11 Spatial distribution of Copper during pre-monsoon season in the study area.

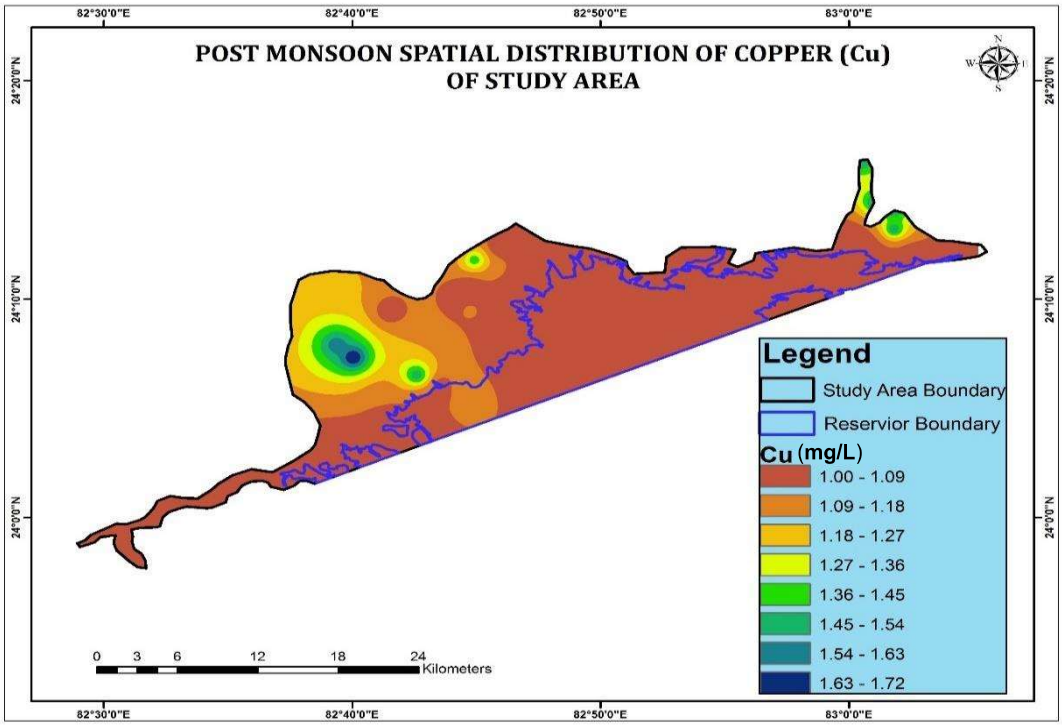

Fig 5.12 Spatial distribution of Copper during post monsoon season in the study area.

5.1.7 Sulphate (SO_4^{2-})

The concentration of sulphate in various locations of study area was found to be between 60.65-735.46 mg/L and between 14.95-728.64 mg/L in both pre and post monsoon seasons respectively. Though the desirable limit as recommended by WHO/BIS was found to be 150 mg/L for drinking water. The concentration of sulphate was beyond the desirable limit in locations around the reservoir and not within the locations of reservoir since most of the locations outside the reservoir were mainly related to mining industries and thermal power plants. Runoff from these industries containing sulphide rich coal flows directly into these location thereby causing a high conc. of sulphate in them (Kumar et al 2019). Also the area is mainly occupied by lithology of sedimentary rock which are mainly associated with gypsum and anhydrite rocks thereby making sulphate content of these rocks to flow directly into sump water present in the coal mines either by weathering or by precipitation and solution of water traversing through the rocks (Younger 2006). The spatial distribution map of this parameter becomes essential since it is mainly associated with acid mine drainage which is one of the most prominent issue in the area of coal mines. Also, it's high concentration in drinking water causes gastrointestinal irritation. When sulphate combines with elements like Mg or Na it can have cathartic effect on the population consuming it along with the laxative effect with Mg (CPCB 2008). Fig. 5.13 and Fig. 5.14 shows the spatial distribution maps of Sulphate during pre and post monsoon season in the study area respectively.

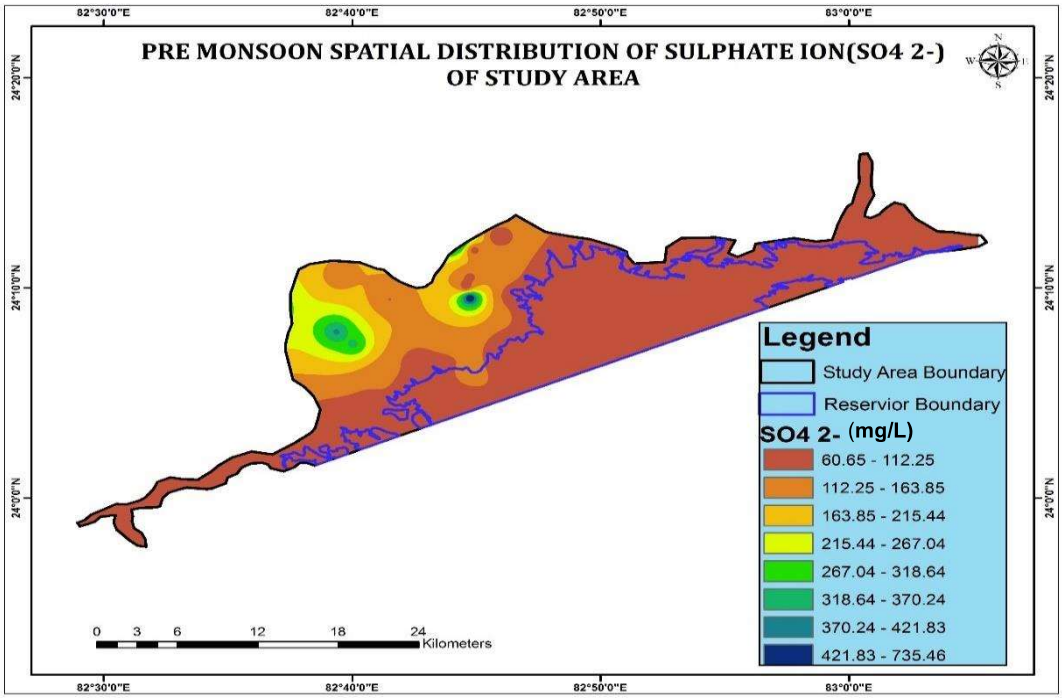

Fig 5.13 Spatial distribution of Sulphate during pre-monsoon season in the study area

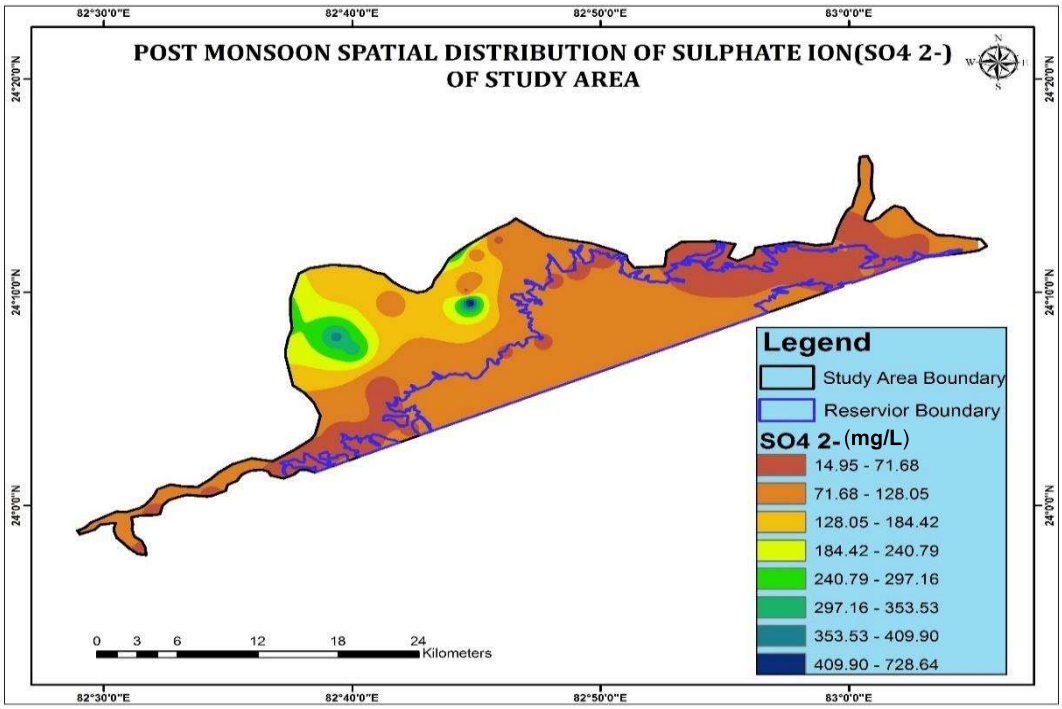

Fig 5.14 Spatial distribution of Sulphate during post monsoon season in the study area

5.1.8 Fluoride (F^-)

Another physico-chemical parameter which is a prominent contaminant and commonly found in surface water is Fluoride. Ingestion of excess fluoride in drinking water causes diseases like Fluorosis, skeletal problems, damaging of enamel, nausea, vomiting or muscle spasms, etc (Dey et al 2016). Though, it is beneficial to human health if taken within the desirable limit i.e. within 1.5 mg/L as prescribed by WHO in drinking water. Here, in this study the spatial distribution map of Fluoride for both pre and post monsoon has been presented. From the map it was depicted that during pre-monsoon season the range of F^- was between 0.648 to 1.896 mg/L and during post monsoon season it was between 0.433 to 1.573 mg/L. Though most of the locations except a few were within the desirable limit of 1.5 mg/L. The slight difference of concentration of F^- in both the seasons was due to the fact that during the rainy season may be due to impoundment of water in sump or reservoir there occurs a dilution in concentration of ions which causes lowering of concentration of F^- during post monsoon season. The presence of F^- in water for the area under study can be both due to natural or anthropogenic activities. It mainly gets into the water because of its geological origin since the lithology is mainly dominated by rocks of sedimentary origin thereby causing its weathering and leaching directly into the nearby water source (Younger 2006). However, the anthropogenic addition of F^- includes the industrial discharges of wastewater into the nearby water body causing an increase in level of F^- into the reservoir (Kumar et al 2019). The various diseases caused by F^- in drinking water makes it one of the most prominent physico-chemical parameters to be considered for the computation of WQI during both the seasons for the area under evaluation. Fig 5.15 and 5.16 shows the spatial distribution maps of Fluoride during pre and post monsoon season in the study area respectively.

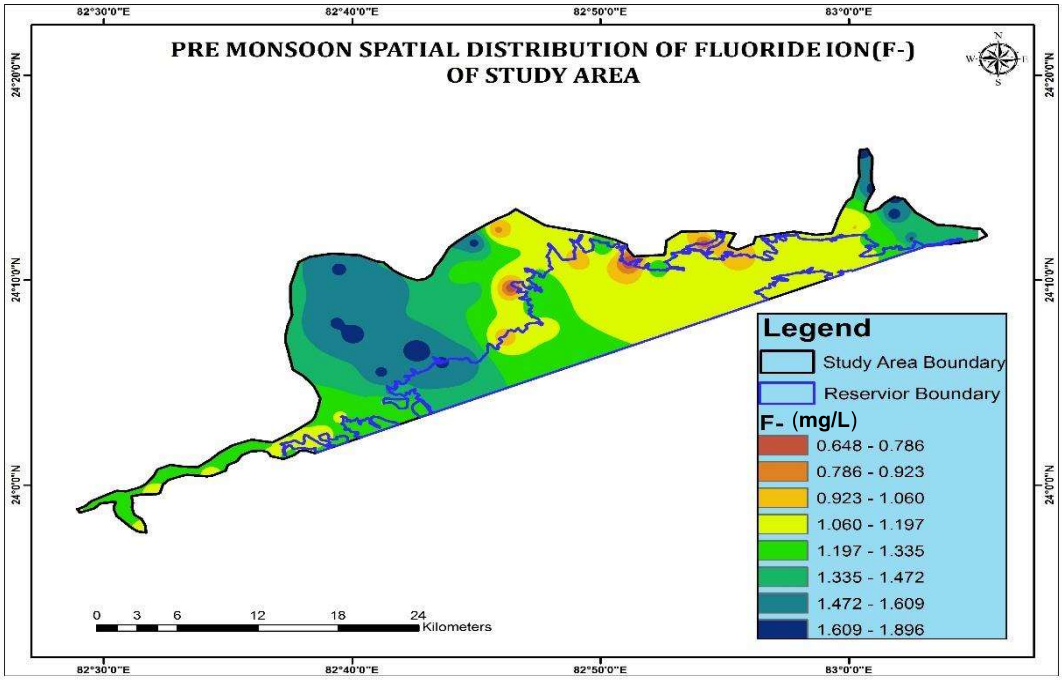

Fig 5.15 Spatial distribution of Fluoride during pre-monsoon season in the study area.

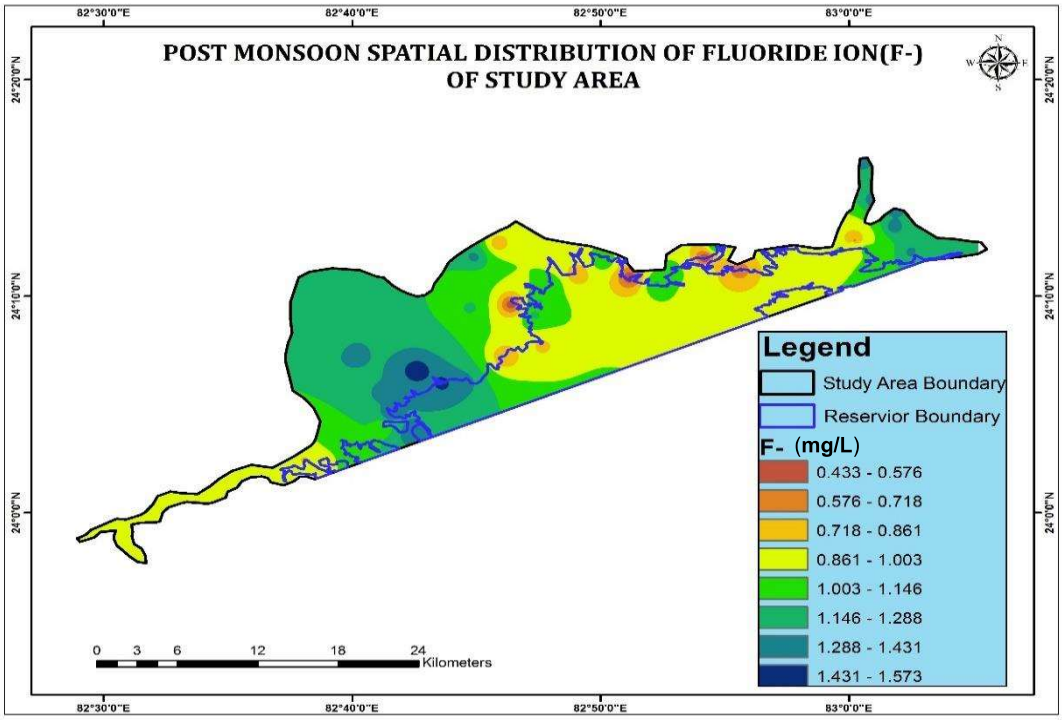

Fig 5.16 Spatial distribution of Fluoride during post monsoon season in the study area.

5.1.9 Chromium (Cr)

Being extensively dispersed in the crust of the earth, chromium makes an indispensable part of many rocks & minerals. In rocks & minerals it is mainly found in its trivalent oxidation state while in surface water it occurs in hexavalent oxidation state (Oliveira 2012). The presence of Cr (VI) in surface water can be both due to anthropogenic and natural sources. The natural sources include erosion and weathering of nearby rocks and coal present in and around the reservoir or other surface water sources (Ali et al 2016). While the anthropogenic sources comprises mining activities, burning of coal for power generation through thermal power plants, leaching of minerals through heaps of overburden present in the vicinity of the reservoir or through inadequate disposal of waste by various industries (Kumari et al 2013). Here, in this study, the chromium is measured in the form of total Cr encompassing both Cr(III) and Cr(VI) since both these ions are interconvertible into each other in water depending on the environmental conditions i.e. aerobic and anaerobic conditions (Kimbrough et al 1999). Though Cr is one of the major dietary components required by the organisms for sustaining life but if it's concentration increases beyond a level of 0.01 ppm it is toxic to human health as prescribed by WHO for drinking water. The preparation of its spatial distribution map becomes important because it is not one of the main but it is regarded as one of the most severe environmental pollutants if present in excess. As depicted from the spatial distribution map, the value of Cr in surface water lies between 0.001 to 0.058 mg/L during pre-monsoon season while during post monsoon it's range lies between 0.001 to 0.056 mg/L. This slight decrease in value of concentration of Cr during post monsoon season is may be because of the dilution of surface water by rainwater during the preceding rainy season. Most of the locations showed concentration beyond the desirable limit of 0.01 mg/L or ppm during both the seasons there by stating that the area is highly affected by Cr pollution & the water is not

suitable for drinking purpose in those locations. Fig. 5.17 and Fig 5.18 shows the spatial distribution maps of Chromium during pre and post monsoon season in the study area.

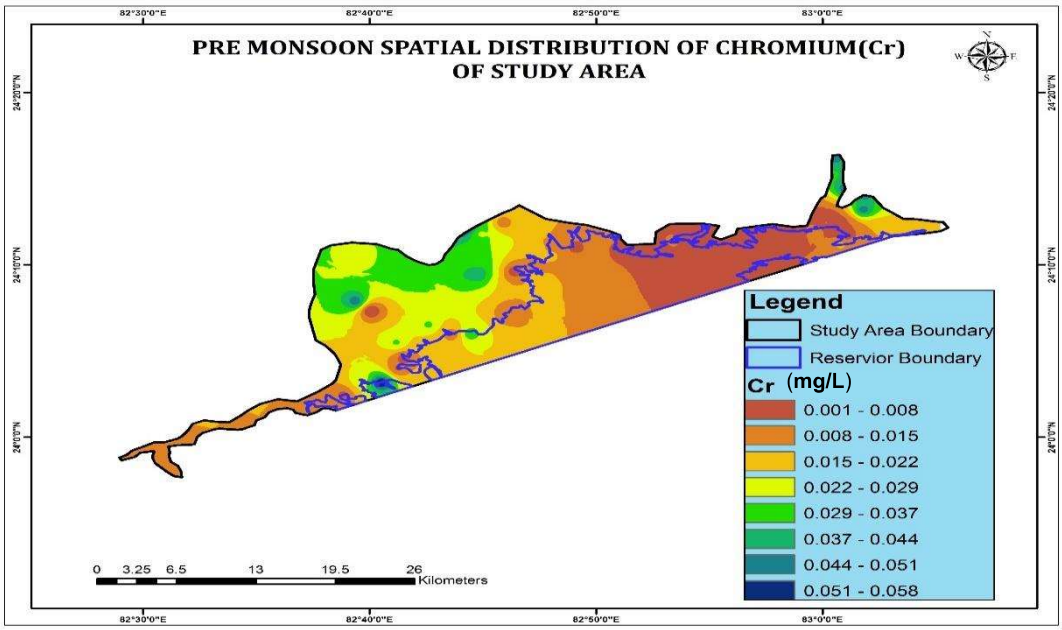

Fig 5.17 Spatial distribution of Chromium during pre-monsoon season in the study area

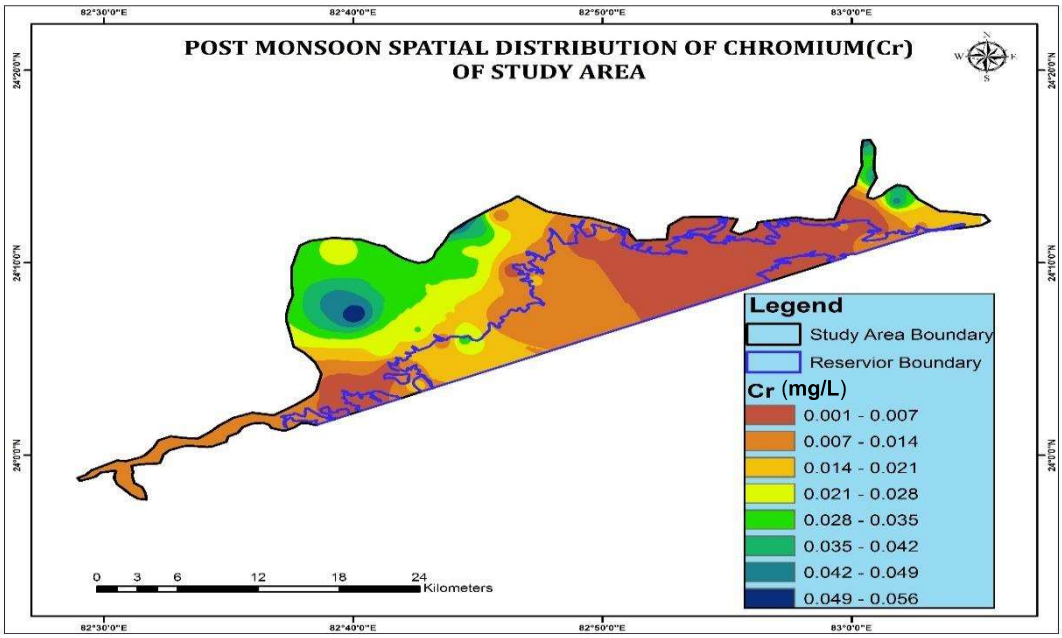

Fig 5.18 Spatial distribution of Chromium during post monsoon season in the study area

5.1.10 Cadmium (Cd)

The next trace constituent which possesses serious health issues when exceeded beyond a limit of 0.1 ppm as prescribed by WHO for drinking water is Cd. This element is also present abundantly on the earth crust like that of Cr. When an individual is chronically exposed to it, it causes diseases like proteinuria, Kidney dysfunctioning, Osteoporosis, Osteomalacia etc (Krajnc et al 1987). The main sources of contamination of surface water by cadmium is also through both natural and anthropogenic sources. The natural sources include erosion and weathering of adjoining sedimentary rocks directly into the surface water while the anthropogenic sources inculcates runoff of industrial discharge through mining activities and thermal power plants as well as through corrosion of galvanized pipes etc (Agrawal et al 2011). Due to these many reasons it became important to prepare a spatial distribution map of the study area for this trace element. From the map it can be concluded that during pre-monsoon season it was in the range of 0.001-0.259 mg/L while during post monsoon season it was in between 0.001 to 0.229 mg/L. The slight difference in concentration during the post monsoon season is again due to presence of the rainy season just before the time of sample collection. Though, most of the locations were free from Cd contamination and only few sites showed its presence beyond the limit of desirable concentration. Hence, it is advisable to utilize the water of these sites after proper treatment. Fig. 5.19 and Fig. 5.20 shows the spatial distribution maps of Cadmium during pre and post monsoon season in the study area respectively.

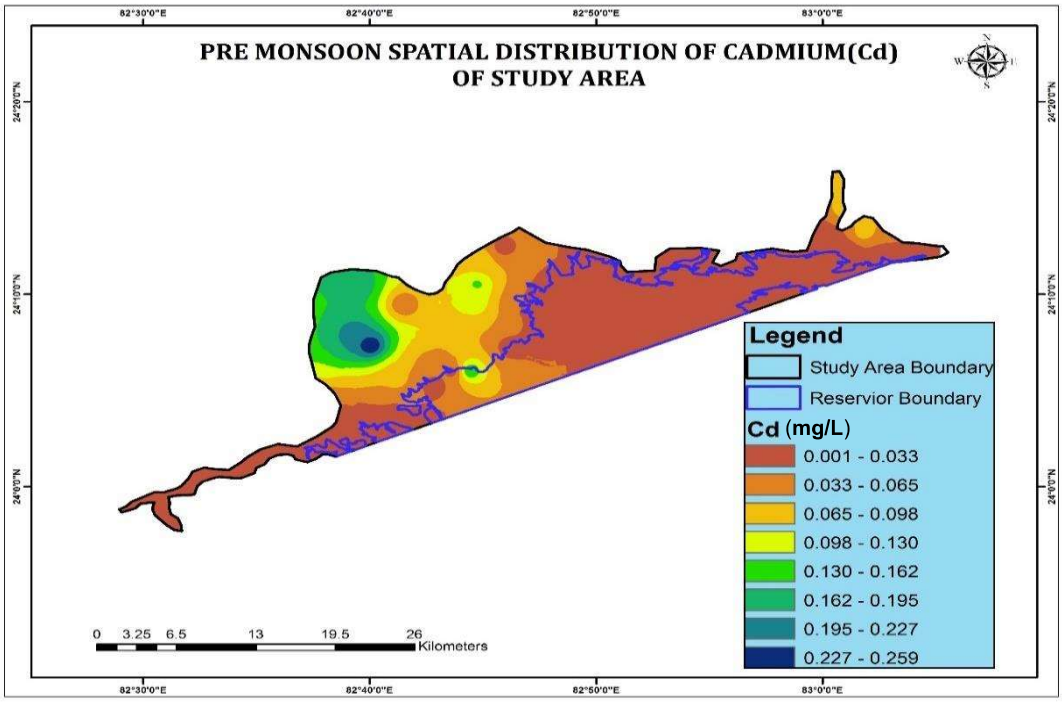

Fig 5.19 Spatial distribution of Cadmium during pre-monsoon season in the study area

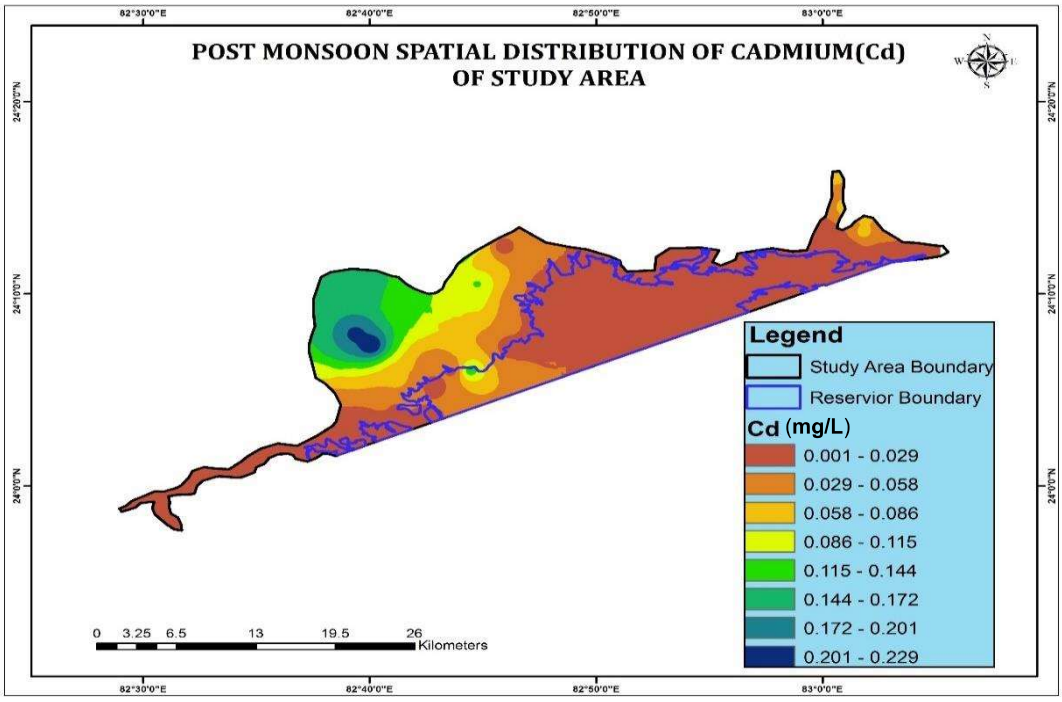

Fig 5.20 Spatial distribution of Cadmium during post monsoon season in the study area

5.1.11 Nickel (Ni)

The succeeding trace element after Cd is Ni which is to be evaluated in the area of study. Unlike the other elements discussed before this element too enters into the surface water either by natural or anthropogenic sources. The source of natural contamination is through erosion and deposition of sandstone since Ni is mainly associated with sandstone & the geology of the area is dominated by the presence of sandstone (Gupta et al 2012). However, the anthropogenic source of contamination is burning of fossil fuel by thermal power plants and through washing of coal from coal washery directly into the surface water (Finkelman 2007). Though it is required by many organisms as their dietary supplements but it's excess causes many diseases in them. The most common diseases caused by intake of Ni is lung cancer or nasal tumors. Ni is also carcinogenic in nature causing alterations in structure of DNA by replacing Mg & Zn ions in DNA polymerase enzymes (Guo et al 2019). Due to these reasons, the computation of Ni through spatial distribution maps of the study area becomes significant. The range of Ni during pre-monsoon season was 0.012-0.29 mg/L with most of the locations falling within the desirable limit of 0.2 mg/L as prescribed by WHO for drinking water and only 2-3 locations showed results beyond it. However, during post monsoon season the range lies between 0.010-0.26 mg/L again with most of the locations lying under the suggested limit of WHO and the locations which were beyond the desirable limit are very limited in number like those in the preceding pre-monsoon season. Fig. 5.21 and Fig. 5.22 shows the spatial distribution maps of Nickel during pre and post monsoon season in the study area.

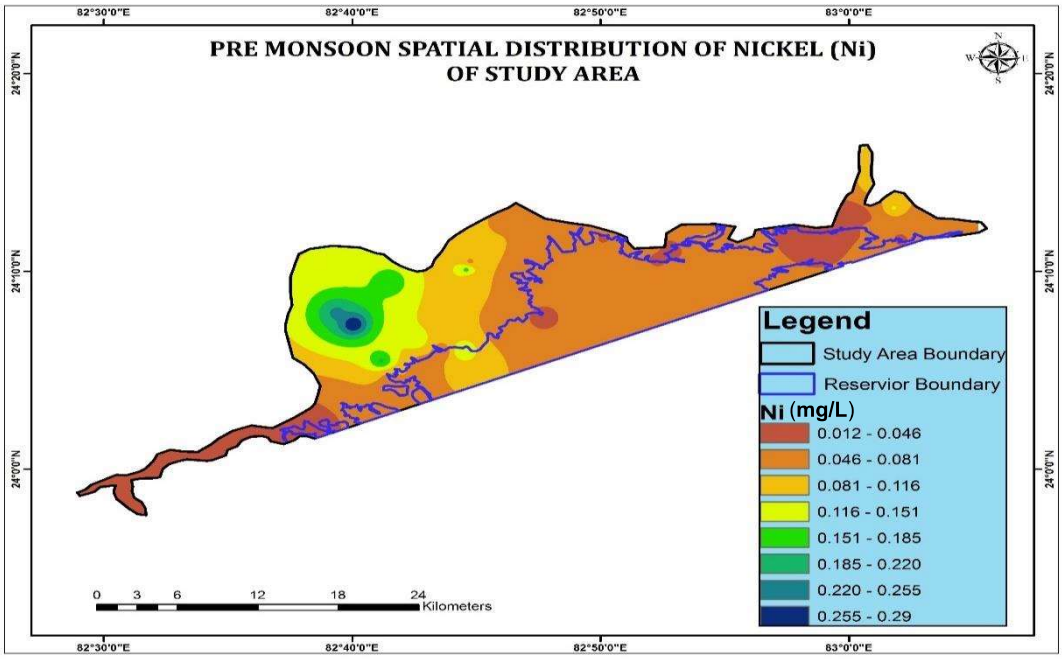

Fig 5.21 Spatial distribution of Nickel during pre-monsoon season in the study area

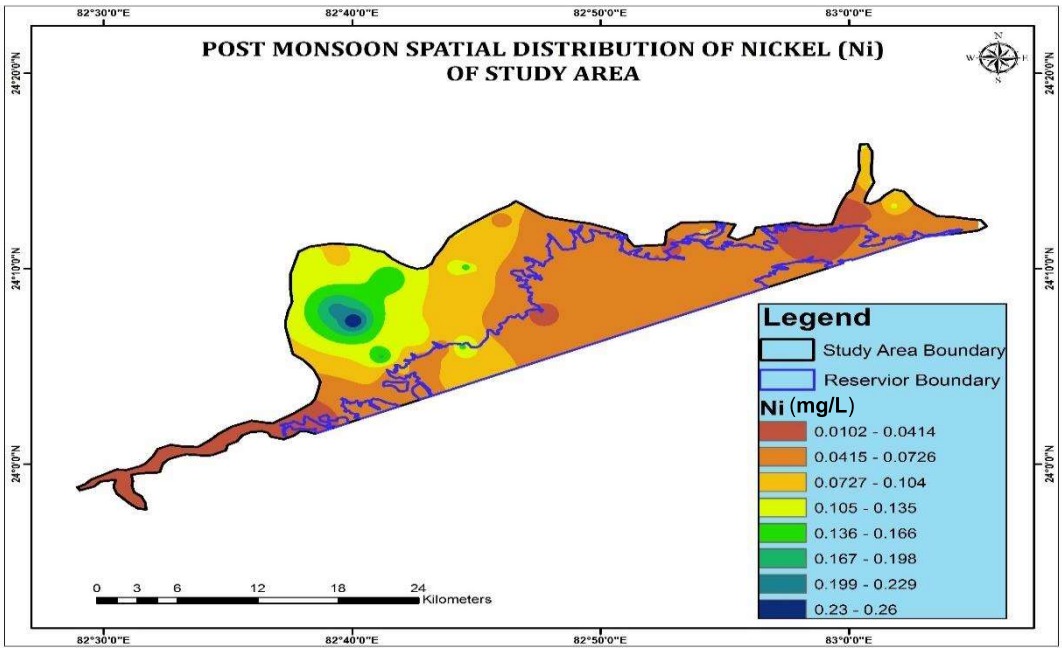

Fig 5.22 Spatial distribution of Nickel during post monsoon season in the study area

5.1.12 Water Quality Index (WQI)

As an outcome of rapid industrial growth, increase of population and agricultural activities, the surface water sources are facing many confrontations. In this context, reservoirs & lakes are facing immense challenges due to increase of urbanization & industrialization by escalation of sediments or nutrients deposition into it thereby making it unsuitable for human consumption. Since, surface water is an important source of water for not only drinking purposes but also for agricultural and industrial utilization (Egbueri et al 2019). Therefore, the evaluation of its quality becomes significant for better utilization in all these purposes. In the area under study due to rapid expansion of opencast mining activities and other industrial activities such as power generation through thermal power plants have led to the degradation of the surface water resources (Singh et al 2014). In this area, reservoir water is the main water resource not only for irrigation and domestic utilization but it plays a major role in fulfilling the industrial water demand for socioeconomic development of the country as well as the region under investigation (Egbueri et al 2018). For assessing the suitability of water for both domestic and industrial applications as well as for scrutinizing the level of water pollution prevailing in the reservoir under study, the computation of Water Quality Index becomes prominent for the evaluation. Here, in this study the quality of water for various locations has been estimated by using 26 physicochemical parameters for both pre and post monsoon seasons. Along with this for assessing the extent of vulnerability and quality of surface water the distribution and physicochemical changes of various parameters on reservoir water spatial distribution maps have been enumerated using geostatistical analysis in Geographic Information System software. Since, the conventional techniques for evaluation of water quality was expensive, difficult, time consuming and inadequate for furnishing spatial & temporal interpretation of the surface water resources having

restricted number of sample location points. Here, in this study, IDW technique was utilized with 60 sample location points for surface water resources with the help of ArcGIS 10.1 software. During the pre-monsoon season, most of the locations of the area under study exhibited good water quality followed by Fair to Marginal quality and only very few locations displayed poor quality of water. However, during the post monsoon season, the maximum number of locations expressed Good to Fair quality while the number of locations with Marginal to Fair quality were more than those during the Pre Monsoon Season. However, none of the locations expressed Poor water Quality during the post monsoon season. Fig 5.25 and 5.26 graphically represents Water Quality Index during pre-monsoon and post monsoon season whereas Fig 5.27 and 5.28 represents Pie charts of WQI during Pre and Post Monsoon Season. It therefore depicts that the quality of water got better during the post monsoon season as compared to the pre monsoon season depending on the physico-chemical parameter which played an important role in determining the quality of water in the area under study. This change in quality of the water samples may perhaps be due to dilution of pollutants due to heavy rainfall in the area in the years taken into consideration. Though, there is addition of pollutants due to surface runoff but dilution is dominating over the addition of pollutants. Fig. 5.23 and 5.24 shows the spatial distribution maps of Water Quality Index during pre and post monsoon season in the study area respectively.

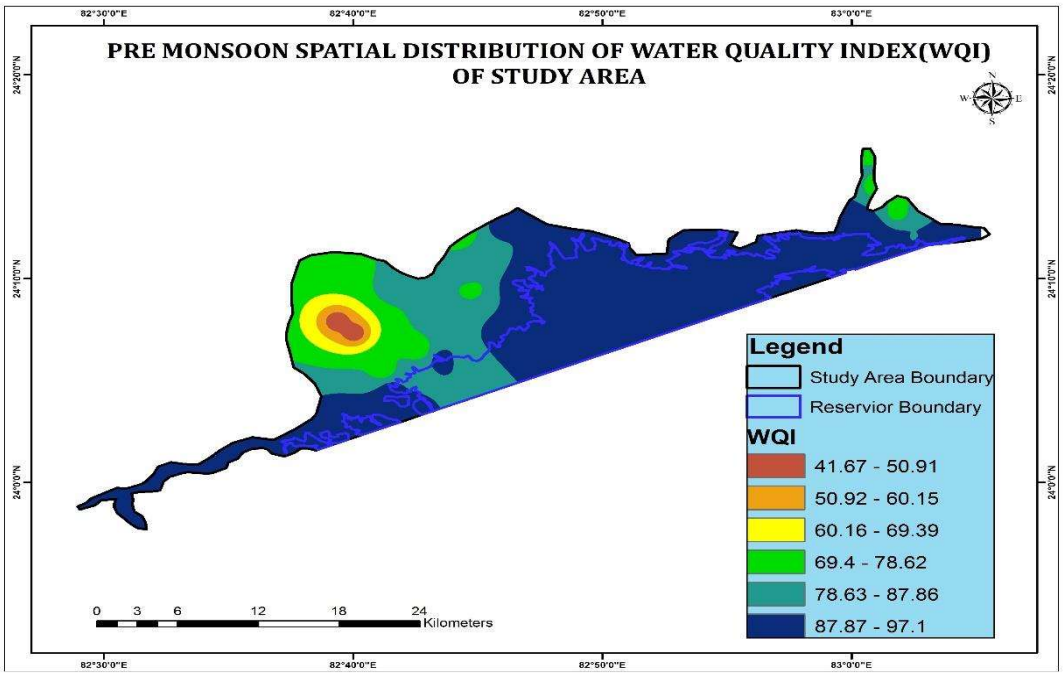

Fig 5.23 Spatial distribution of Water Quality Index during pre-monsoon season in the study area

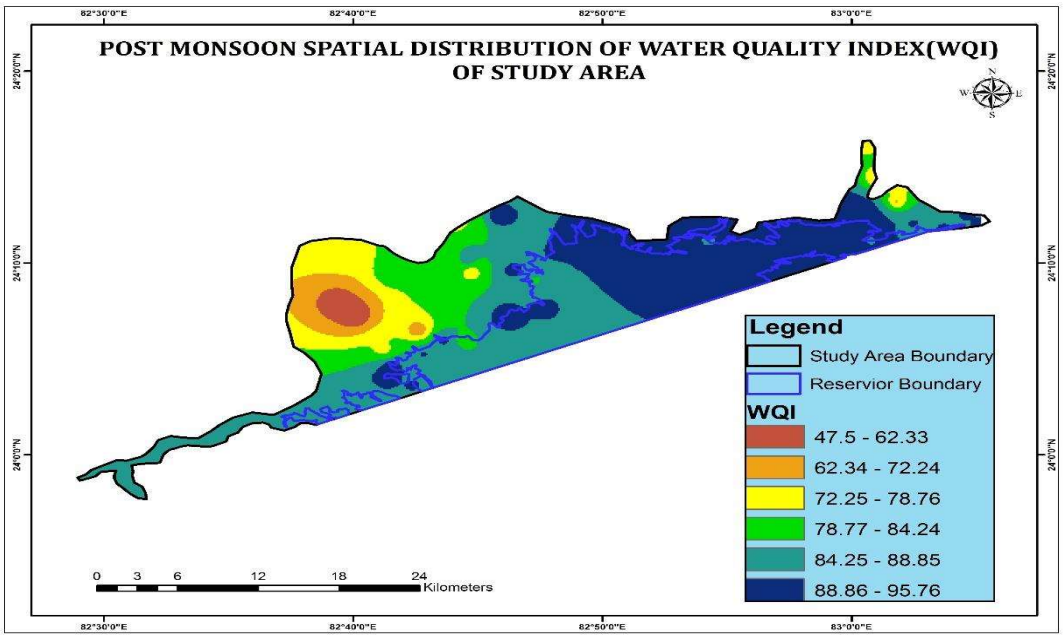

Fig 5.24 Spatial distribution of Water Quality Index during post monsoon season in the study area

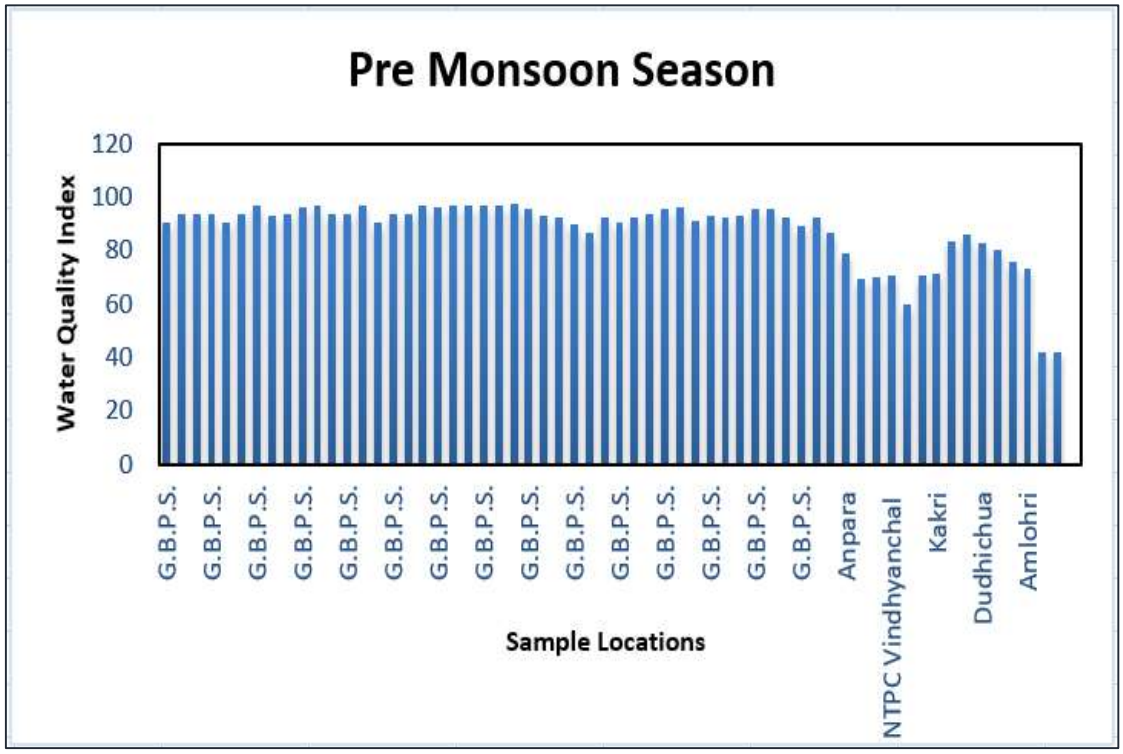

Fig 5.25 Graphical Representation of WQI during Pre-Monsoon Season

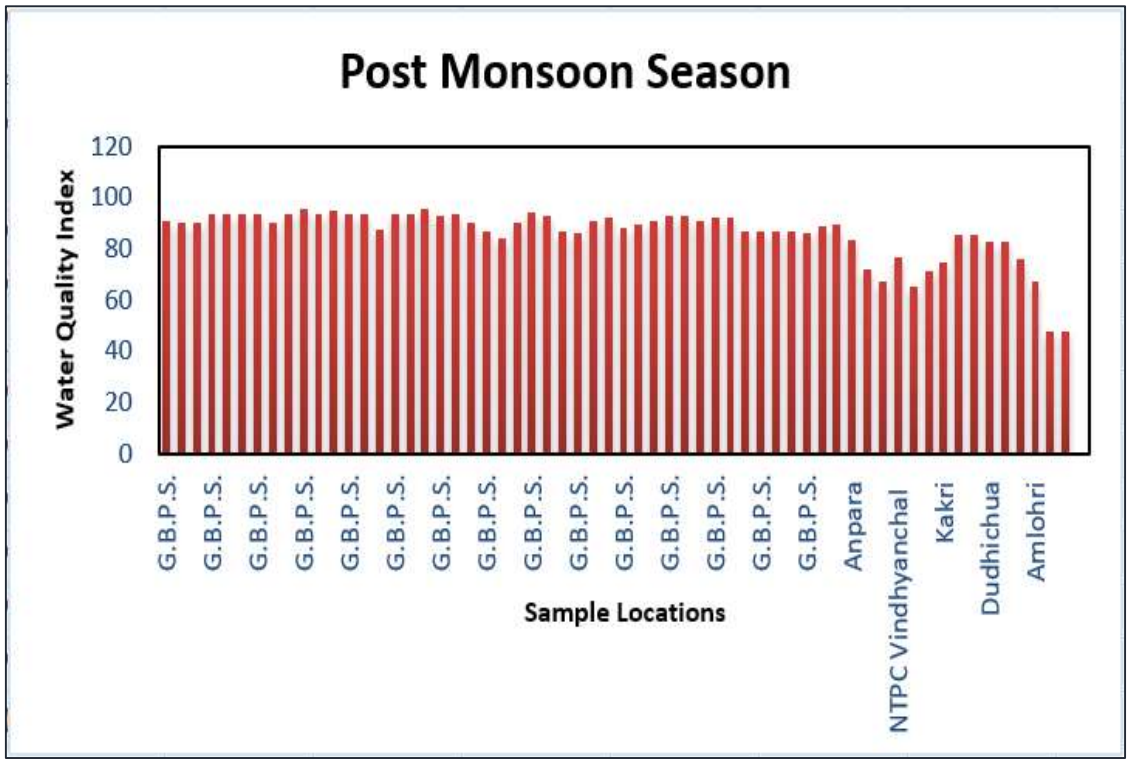

Fig 5.26 Graphical Representation of WQI during Post Monsoon Season

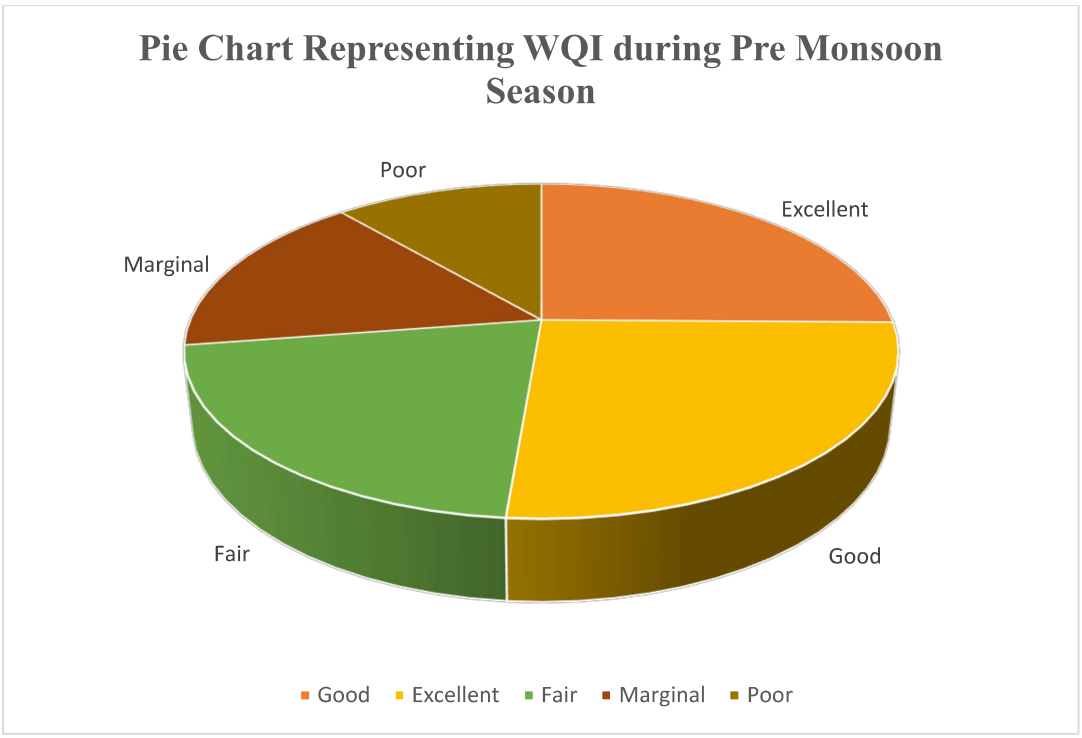

Fig 5.27 Pie Chart Representing Water Quality Index during pre-monsoon season

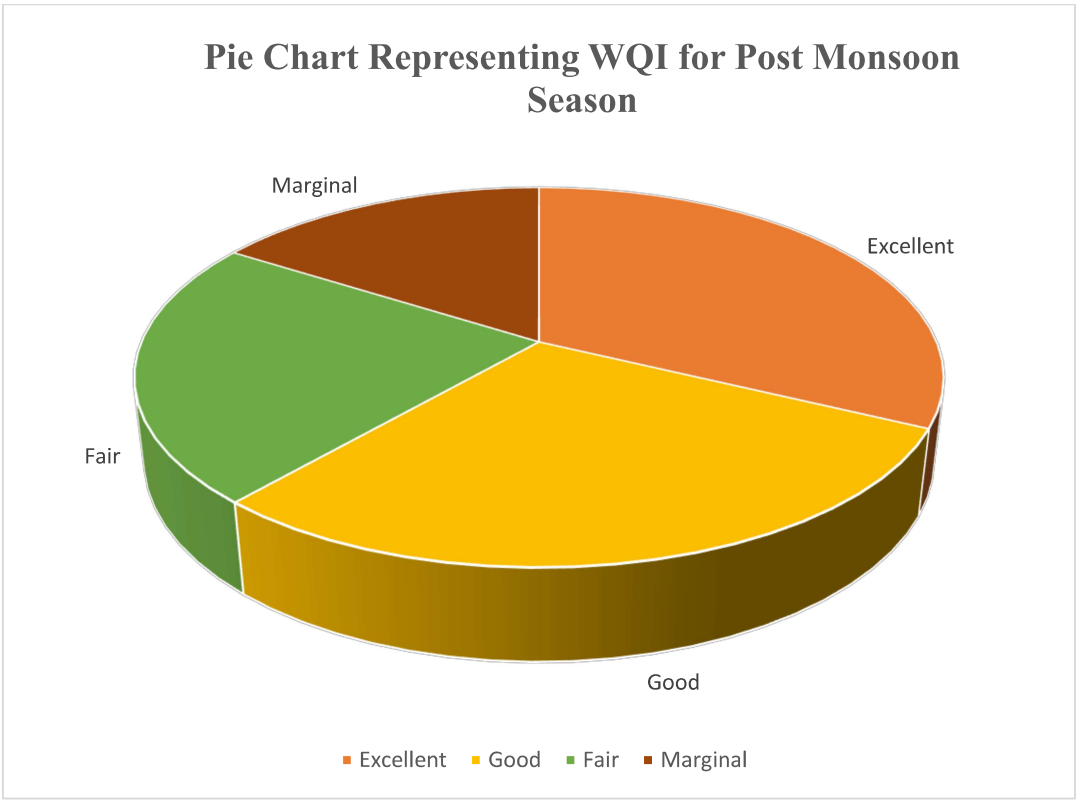

Fig 5.28 Pie Chart Representing Water Quality Index during post monsoon season

5.1.13 pH

The next important parameter which helps in ascertaining whether the surface water present in the area taken into account is acidic or alkaline is pH. The pH of a solution can be defined as a measure of the activity of hydrogen ions i.e. the negative logarithm of the concentration of hydrogen ions and is expressed in powers often to show the concentration of hydrogen ion (Bates 1973). Thus, indicating the acidity or alkalinity of the solution taken into consideration. The interaction of minerals with organic matter leads to the increase or decrease of pH values. This decrease in pH leads to the dissolution of the metal salts, dissolution of retention phases and desorption of the cations and anions (Lions 2004, Ahmed et al 2017). According to the WHO guideline, the recommended limit of pH for drinking water should range between 6.5-8.5. In the present study, the value of the pH was found to be between 8.82 to 6.33 during pre-monsoon season while during post monsoon season it was between 8.52 to 7.49. The value of pH was beyond the desirable limit at one location only while the rest of the locations were within the desirable limit in and around the reservoir during both the seasons. Therefore, it can be concluded from the study that a neutral to alkaline pH characterizes the surface water present in and around the reservoir along with the sump water discharged from mining and thermal power plant industries. However, during the post monsoon season the average value of pH was higher when compared with the value during pre-monsoon season. This could be mainly due to utilization of carbon dioxide by increase in photosynthetic activities of the macrophytes present in the area during the influx of freshwater in the preceding rainy season, thus making it more alkaline as compared to the pre-monsoon season.

5.1.14 Oxidation Reduction Potential (ORP)

The oxidation reduction potential can be described as a representative of oxidation conditions. It can be defined as a measure of the relative chemical potential of electrons accepted or donated by a particular type of molecule (Nobel 2009). The measured redox potential values were between 365-109 during pre-monsoon season while during post monsoon season its value ranged between 149.6-121.5 in the area under study. Since, the value of ORP is low in the area. The ORP of the area was well within the limit thereby indicating a low to moderate affinity for metal dissolution and its mobilization.

5.1.15 Total Dissolved Solids (TDS)

Being one of the most important parameters in determining the quality of water for drinking and other purposes, the computation of TDS becomes important for assessing the water quality of the study area. It gives an indication about the suitability of the water for drinking, agricultural and industrial uses (APHA 1992). TDS can be defined as the compounds of inorganic salts such as Calcium, Magnesium, Sodium, Potassium, Bicarbonate, Chloride and Sulphate and small amounts of organic matter dissolved in water (Sadat-Noori et al 2014). Owing to differences in solubility of minerals due to differences in geological regions, the concentration of TDS in water varies accordingly (WHO 2004). Here, in this study, the range of TDS during pre-monsoon season was found to be between 574-107 mg/L while in post monsoon season it lies between 616-177 mg/L. However, the desirable limit of TDS as prescribed by WHO is 500 mg/L for drinking water. Most of the locations in the study area fall within the desirable limit while only few of the locations were beyond it. The value of TDS during post monsoon season showed an increase due to dissolution of surrounding rocks and overburden present in the

vicinity of the area during the preceding rainy season. The high concentration of TDS at few places may be due to presence of sedimentary rocks in and around the reservoir consisting of a relatively high amount of bicarbonates, sulphates, chlorides, calcium, sodium, etc (Murkute 2014). The presence of high amounts of TDS in water may cause diseases like gall stones, kidney stone, arthritis, stiffness in joints, etc. Due to these reasons the evaluation of TDS during the study becomes significant for both the seasons.

5.1.16 Electrical Conductivity (EC)

EC can be described as the ability of a substance to conduct electrical current (Pande et al 2018). This ability to conduct electric current in water is due to the presence of various cations and anions. EC is usually measured to estimate the amount of TDS present in water which in turn helps in estimating the EC since both EC and TDS are directly proportional to each other (Rusydi 2018). Therefore, if TDS increases then EC increases and vice versa. In this present study, the concentration of EC in water samples during pre-monsoon season was between 1148-214 µS/cm while during post monsoon season it ranged between 1231-354 µS/cm. At most of the locations, the EC of the samples were higher than the desirable limit as prescribed by WHO for drinking water is 300 µS/cm. This high value of EC corresponds to presence of sedimentary rocks and its dissolution in the area of study during both the seasons.

5.1.17 Salinity

The Salinity of the water samples collected during pre-monsoon and post monsoon seasons ranged between 0.4-0.02 and 0.08-0.03 mg/L respectively. While the desirable limit as prescribed by WHO was found to be 200 mg/L for drinking water. Since, Salinity is positively related to various cations and anions taken into study therefore its evaluation becomes important for consideration. Here, in this study, all the samples were well within

the desirable limit during both the seasons as prescribed by WHO. Therefore, it can be concluded that the Salinity of water in the area has no adverse effect on the health of local population either by drinking or through domestic or industrial uses.

5.1.18 Dissolved Oxygen (D.O.)

Dissolved Oxygen (DO) is one of the key parameters in determining the surface water chemistry of an area as well as an indispensable parameter for survival of aquatic life. Any kind of variation in the concentration of dissolved oxygen can be attributed due to change in interaction among physical, chemical and biological processes (Ibanez et al 2008). According to WHO, the limit of DO should not be less than 5 mg/L for drinking water. Hence, if the value of concentration of DO is less than 3mg/L then it is defined as hypoxia and if the concentration of DO is below 0 mg/L then it is known as anoxia (Wang et al 2012). The results of the present study shows that the DO concentration during pre-monsoon season ranges between 6.03-0.26 mg/L while that during post monsoon season the concentration of DO varied from 5.48 to 4.02 mg/L. It was lower during pre-monsoon at few of the locations because of the reason that hypoxia is more likely to occur in summer during pre-monsoon season than that during post monsoon season. This is due to the reason that with increase in temperature, the microorganism activities turns more active as compared to that during post monsoon season.

5.1.19 Chloride (Cl^-)

The next parameter which shows a prominent effect on water quality is Chloride. Cl^- is one of the common ions in estimating the quality of water. It also occurs as a cementing material in sedimentary rock (Hem 1985). The contamination of Cl^- in surface water can be attributed to discharge of industrial effluents directly into the reservoir and due to the other anthropogenic activities. In the present study, the value of Cl^- during pre-monsoon

season was between 96.33 to 43.79, while during the post monsoon it ranged between 91.01 to 31.57 mg/L. However, the permissible limit as recommended by WHO for drinking water is 250 mg/L. The results of the study exhibit that during both the seasons all the samples were well within the desirable limit as prescribed by WHO. Though the value of Cl^- during pre-monsoon was quite higher as compared post monsoon season which may be attributed to evaporation of surface water during summer season due to rise in temperature as compared to post monsoon season. The estimation of Cl^- becomes important since its high value in water can lead to a laxative effect on human health when combined with other elements present in water (McCallum et al 2015).

5.1.20 Nitrate (NO_3^-)

In this study, during the pre-monsoon season, the value of nitrate varied between 97.21 to 10.02 mg/L while during post monsoon season, the value was within the range of 93.43 to 7.4 mg/L. Though, the desirable limit of NO_3^- concentration is 45 mg/L as prescribed by WHO for drinking water. The derivation of nitrate in aquatic environments is mainly caused by terrestrial runoff including that of industrial discharge and agricultural runoff. Concentration of nitrate in aquatic environments is mainly dependent on land use practices in drainage basins since nitrate moves easily through soils and is rapidly lost from land through natural drainage systems (Nazneen et al 2019). It can be concluded from the study that few of the locations showed high concentration of nitrate as compared to the described limit as prescribed by WHO. During pre-monsoon season it's value was relatively higher than that during post monsoon season which may be due to input of fresh water during the preceding rainy season. The evaluation of nitrate becomes important since its high concentration causes various diseases like infant methemoglobinaemia (blue baby syndrome), gastric cancer, cardiovascular diseases and adversely affects Central Nervous System (CPCB 2008).

5.1.21 Phosphate (PO_4^{3-})

During the pre-monsoon season the value of phosphate was in the range of 18.106-0.122 while during post monsoon season its value was within the range of 1.83-0.009 mg/L. Being one of the limiting nutrients in determining the condition of an aquatic environment its evaluation becomes important in determining the water quality of an area. It is mainly derived from agricultural runoff and domestic sewage as well as weathering of rocks present in the vicinity of the reservoir (Jain et al 2010). The concentration of phosphate during pre-monsoon season was higher than that during post monsoon season which might be due to increase in amount of sediment due to evaporation in pre-monsoon thereby increasing it's content in the area while during post monsoon season its value decreases due to increase in surface runoff in the preceding rainy season.

5.1.22 Bicarbonate (HCO_3^-)

Another important parameter which is considered for evaluation of water quality of the area under study is bicarbonate. This ion is the main contributor in determining the alkalinity of surface water of the area. Bicarbonate also plays a significant role in determining the electrical conductivity of the area (Tiwari et al 2016). In the present study, the value of bicarbonate was between 362 to 122 mg/L during pre-monsoon season while during post monsoon it value was between 389 to 145 mg/L. While the permissible limit for bicarbonate as prescribed by WHO is 200 mg/L. The study shows that except few of the locations, most of the locations were under the desirable limit as prescribed by WHO for drinking water. However, during the post monsoon season. This may be due influence of precipitation and surface runoff passing through the geographical formations present in the area (Rose 2002).

5.1.23 Sodium (Na)

Being a major constituent of sedimentary rocks present in the area, the next parameter taken into consideration is sodium. Sodium is mainly added to the reservoir by weathering of sedimentary rocks such as feldspar, clay, halites and industrial waste (Tiwari et al 2016). Since, this cation is harmful to human health if taken in excess by affecting a person with diseases like renal, heart or circulatory impairment. However, it's deficiency causes headache, poor appetite, dehydration, fatigueness, etc (Selinus et al 2005). It's high concentration in soil causes formation of alkaline soil. The observation of the sodium value in study ranges between 49.89 and 11.98 mg/L during pre-monsoon season while that during post monsoon season it varies between 59.2 to 20.9 mg/L. While the desirable limit as recommended by WHO was 50 mg/L for drinking water. During pre-monsoon all the samples were well within the permissible limit while during post monsoon season except few most of the locations were within the permissible limit. The increase of value during the post monsoon season is attributed to the addition of sediments during the preceding rainy season due to weathering, erosion and agricultural drainage in the catchment area.

5.1.24 Potassium (K)

During the pre-monsoon season the value of potassium was between 26.23 to 10.63 mg/L while during post monsoon season the value of it lies between 25.10 to 7.45 mg/L. The desirable limit of it is 15 mg/L as recommended by WHO. This ion is mainly added to the surface water due to weathering of rocks present in the area (Murkute 2014, Li et al 2013). The value of it was higher during pre-monsoon season as compared with that of the post monsoon season with many locations lying beyond the desirable limit. The higher value is either due to addition of industrial effluent or due to weathering of rocks present

in the area. The excess of this ion causes severe problems to human health like that of kidney dysfunctioning, hypertension as well as changes in heart rhythm, etc.

5.1.25 Lithium (Li)

The results of the study showed that during the pre-monsoon season the value of the ion was within the range of 0.14 to 0 mg/L while that during the post monsoon season it was between 0.151-0.03 mg/L. Thereby indicating that during both the seasons the value of the cation was nearly the same with slightly higher value during the post monsoon season. The reason for this excess can be due to large runoff of the rainwater through surrounding rocks present in and around the reservoir catchment area. It's excess in drinking water causes health issues like dysfunctioning of kidney, thyroid gland, heart disease, failure of nervous system, etc (Glitin 2016).

5.1.26 Lead (Pb)

Due to discriminate disposal of heavy metals in water, the analysis of heavy metals including lead becomes important. This is due to the fact that even a small amount of it is significantly toxic to human health. Being a general toxicant it accumulates in the skeleton and causes damage to both Central and Peripheral Nervous System inducing subencephalopathic neurological and behavioral effects (WHO 2008). Here, in this study, the value of lead during pre-monsoon ranged between 0.48 to 0.011 mg/L while during post monsoon season it was found to be between 0.45 to 0.001 mg/L. However, the desirable limit as recommended by WHO is 0.15 mg/L showing that most of the locations possess concentration of lead well above the maximum permissible limit. The value of lead during both the seasons was approximately the same as seen from Table A.7 and A.8. Therefore, it could be depicted that the dissolution of lead in water might be due to influx of domestic and industrial effluents and application of agricultural chemicals in the

adjacent region around the reservoir (Sahoo et al 2016). It can also be analyzed that the geology of the area might also be the influencing factor in raising the concentration of lead in the reservoir under study (Das et al 2018).

5.1.27 Hardness

The hardness of water contemplates the nature of the geological formations with which it has been in contact (Sawyer & McCarty 1967). It results from the presence of divalent metallic cations such as calcium and magnesium which is abundantly found in drinking water (Todd, 2004). According to the classification given by Sawyer & McCarty (1967) as shown in Table 5.1 for hardness.

S.No.	Hardness, mg/L as $CaCO_3$	Water Class
1)	0-75	Soft
2)	75-150	Moderately Hard
3)	150-300	Hard
4)	Over 300	Very Hard

Table 5.1 Classification of Hardness in water (After Sawyer & McCarty 1967)

In this present study, the hardness of water sample ranges between 206.39 to 82.15 mg/L during pre-monsoon season while during post monsoon season its value was between 202.32 to 95.36 mg/L. During both the seasons, the surface water of the area under study falls under moderately hard categories. This exhibits that the hardness of water might be due to leaching of minerals present in the rocks of the surrounding area by the process of weathering as well as due to pouring of effluent from mining and thermal power plants present in the vicinity of the study area (Jain et al 2010).

5.2 Statistical Analysis

The chemical characteristics of surface water are affected by various factors such as surrounding rock constituents, water retention time, influx of industrial waste, surface runoff, amount of rainfall, etc. Therefore, to analyze a large scale of data robustly, multivariate statistics is one of the most useful techniques. This technique not only helps in identification of anomalous patterns but it also acts as an important tool for interpretation of complex data matrices, indication of water quality, ecological status as well as providing a rapid solution to the environmental pollution taking place in the area. The various elements present in the analysis of surface water shows similar or different co-existing patterns and behavior with each other. Hence, the multivariate analysis acts as an essential tool in identifying the similar and dissimilar components used for the analysis of water samples during pre and post monsoon seasons in the study area. Hence, in this study multivariate analysis such as Correlation Analysis, Box plot Analysis, Hierarchical Cluster Analysis and Piper Analysis have been taken into consideration.

5.2.1 Correlation Analysis

Pearson correlation coefficient matrix can be described as the measure of variance of each component used in water analysis along with its relationship with each other (liu et al 2003). This technique reveals the statistical relationship between two or more variables thereby helping to analyze the primary reactions that have formed current water chemistry (Li et al 2011). The correlation also helps in describing the degree of association between two variables as well as providing preliminary information about their relationship for the area under study (Peat et al 2009). In this study, the correlation matrix is important since it exhibits the interrelationship between the variables showing the coherence of the dataset as well as stipulating the involvement of various chemical parameters using several

influencing factors in its study. Here, temporal variation during pre and post monsoon seasons were considered for evaluating the correlation matrix during these two seasons. If the value of the correlation is above ±0.5 between the two parameters then it is considered as a good correlationship between the two variables while a value of around ±1 is termed as a very strong relationship between the two parameters. The correlation between various parameters used in the study both during pre and post monsoon seasons is shown by Fig 5.29 & 5.30 respectively.

During pre-monsoon season, a strong positive correlation was observed between Electrical Conductivity (EC), Total Dissolved Solids (TDS), Salinity, Sulphate (SO_4^{2-}), Bicarbonate (HCO_3^-), Magnesium (Mg^{2+}), Cadmium (Cd), Chloride (Cl), Nitrate (NO_3^-), Sodium (Na), Nickel (Ni), Chromium (Cr) and Hardness indicating that the surface water of the area is the major source of these constituents. A strong positive correlation was observed between Salinity with Sulphate and Bicarbonate where r=+0.816 and r=+0.831 respectively which may be due gradual weathering of surrounding rocks into the nearby water sources. Another set of parameters which shows strong positive correlationship between them were TDS and EC imparting the fact that concentration of dissolved salt in water increases there will be an increase in value of EC (r=+0.997). The next set of parameters which shows a strong relationship between them are TDS and Mg^{2+} (r=+0.810) indicating the presence of Mg^{2+} in freshwater. Sulphate and Bicarbonate too showed a value of r=+0.855 thereby showing a dependency on each other due to presence of anthropogenic activity in the study area. The other sets of parameters which exhibit a strong positive correlationship amongst themselves were bicarbonate and Sodium (r=+0.823), Bicarbonate and Cadmium (r=+0.864), Nitrate and Cadmium (r=+0.855), Chloride and Cadmium (r=+0.832), Potassium and Hardness (r=+0.939), Calcium and Hardness (r=+0.811), Nickel and Cadmium (r=+0.838), Chromium and Cadmium

(r=+0.827) showing their predominance in freshwater due to leaching of nutrients through agricultural or industrial practices into the nearby water bodies as well as due to weathering of sedimentary rocks present in the area surrounding the reservoir.

During the post monsoon season again a strong positive correlation of r=+0.989 was seen between Electrical Conductivity and Total Dissolved Solid owing to the dissolution of various salts and minerals in surface water present in the area and a direct relationship between them. Hence, like that of the pre-monsoon season on increasing the value of Total Dissolved Solids the value of Electrical Conductivity also increases simultaneously. The another set of parameters which showed a positive correlation between them were Sulphate and Bicarbonate with a value of r=+0.838 which may be due to dependency of these ions on mineral dissolution, solubility of minerals, ion exchange and anthropogenic activities like mining, etc taking place in the area. Bicarbonate and Cadmium too exhibited a strong positive correlationship (r=+0.875) showing the effect of human economic activities such as excavation and burning of coal in mining and thermal power plant respectively present in the area. Sodium and Hardness displayed a strong positive correlationship of r=+0.906 thereby showing the dependence of Hardness on Magnesium for its computation which is probably due to the geology of the area having dolomite as the main mineral constituent. This relationship is followed by another set of parameters showing strong positive relationships are Nickel with Cadmium and Chromium with Cadmium having the value of r=+0.836 and r=+0.828 respectively. This increase is due to industrial activities such as mining and other chemical industries present in the area thereby showing a significant increase of their concentration in the area. Fig 5.29 and 5.30 illustrate the correlation during pre and post monsoon season.

	pH	DO	Salinity	ORP	EC	TDS	TSS	Cl^-	F^-	SO_4^{2-}	NO_3^-	PO_4^{3-}	HCO_3^-	Na^+	K^+	Ca^{2+}	Mg^{2+}	Li^+	Pb	Fe	Cu	Zn	Ni	Cr	Cd	Hardness
pH																										
DO	0.301698	1																								
Salinity	0.090794	-0.19943	1																							
ORP	0.066106	0.002773	0.39004	1																						
EC	0.293339	-0.01935	0.5138	0.124376	1																					
TDS	0.306514	-0.01972	0.531721	0.132624	**0.99781***	1																				
TSS	0.105154	0.032497	0.254718	-0.02338	0.34506	0.340318	1																			
Cl^-	-0.1006	-0.50946	0.658253	0.304661	0.354066	0.355526	0.205253	1																		
F^-	0.15394	-0.42575	0.403006	0.170022	0.369294	0.369225	0.182689	0.592869	1																	
SO_4^{2-}	0.295547	0.009128	**0.81634***	0.281452	0.666704	0.687037	0.253678	0.518625	0.396151	1																
NO_3^-	0.066405	-0.04283	0.648509	0.320524	0.392819	0.397207	0.238084	0.793726	0.47661	0.549497	1															
PO_4^{3-}	-0.25295	-0.64825	0.355625	0.019065	0.324176	0.314772	0.229274	0.520852	0.389485	0.111391	0.216458	1														
HCO_3^-	0.096618	-0.23382	**0.83117***	0.32221	0.603267	0.624702	0.277053	0.791973	0.512295	**0.85504***	0.741873	0.345733	1													
Na^+	-0.18852	-0.3945	0.539836	0.107434	0.423719	0.416238	0.369176	0.591599	0.483821	0.379354	0.494222	0.611676	0.505004	1												
K^+	0.104429	-0.29209	0.764908	0.226341	0.503714	0.517652	0.280667	0.663212	0.405112	0.660719	0.61043	0.430289	**0.82264***	0.562553	1											
Ca^{2+}	0.268814	0.111039	0.661733	0.276228	0.699762	0.71326	0.343741	0.407383	0.332564	0.741237	0.467971	0.219318	0.662618	0.348354	0.479244	1										
Mg^{2+}	0.197644	-0.13947	0.620954	0.192568	0.790793	**0.81022***	0.301084	0.430655	0.335802	0.697776	0.405815	0.323369	0.722234	0.301797	0.642933	0.663494	1									
Li^+	0.130372	-0.02154	0.384467	-0.35538	0.466931	0.466451	0.178579	0.275683	0.215486	0.553367	0.314241	0.092649	0.427683	0.287955	0.296801	0.405336	0.376228	1								
Pb	0.086302	-0.23294	0.610848	0.189634	0.518387	0.512331	0.446659	0.58745	0.511207	0.589041	0.48594	0.34289	0.601417	0.586681	0.431918	0.527253	0.486911	0.379224	1							
Fe	-0.20134	-0.36728	0.546667	0.29338	0.374717	0.36651	0.348075	0.704163	0.534739	0.365568	0.532493	0.633108	0.574238	0.630181	0.510925	0.43612	0.321247	0.130778	0.543821	1						
Cu	-0.08938	-0.4691	0.583167	0.237526	0.5252	0.523678	0.358043	0.775666	0.583247	0.424722	0.579542	0.623263	0.711706	0.626884	0.622554	0.439732	0.550856	0.209626	0.643362	0.778302	1					
Zn	-0.08763	0.137408	0.500632	0.227998	0.466146	0.455225	0.339109	0.328178	0.135933	0.387583	0.458913	0.246131	0.419547	0.381051	0.430246	0.317756	0.365846	0.126087	0.472299	0.426302	0.48409	1				
Ni	0.107059	-0.29847	0.515776	0.260723	0.522408	0.51852	0.336202	0.784871	0.545985	0.499223	0.718149	0.460687	0.665326	0.611199	0.534335	0.480712	0.466743	0.274686	0.647319	0.64024	0.749434	0.412674	1			
Cr	0.08492	-0.32391	0.629563	0.272041	0.559527	0.565117	0.194966	0.719106	0.678708	0.715051	0.601477	0.349021	0.764684	0.565501	0.499753	0.549964	0.488839	0.427195	0.672916	0.660925	0.717621	0.272204	0.756529	1		
Cd	0.163352	-0.12619	0.671654	0.349861	0.549431	0.558114	0.29891	**0.83286***	0.559459	0.719374	**0.85486***	0.260707	**0.86414***	0.491189	0.599939	0.636929	0.54056	0.407166	0.630877	0.621644	0.746471	0.415127	**0.838268***	**0.82740***	1	
Hardness	-0.09012	-0.39974	0.698035	0.169566	0.507915	0.508389	0.377111	0.692582	0.50964	0.541471	0.601899	0.610458	0.69728	**0.93973***	**0.81131***	0.444506	0.479275	0.326351	0.593458	0.656888	0.700719	0.447363	0.653147	0.606533	0.595417	1

Fig 5.29 Correlation Analysis during pre-monsoon season

	pH	DO	Salinity	ORP	EC	TDS	TSS	Cl^-	F^-	SO_4^{2-}	NO_3^-	PO_4^{3-}	HCO_3^-	Na^+	K^+	Ca^{2+}	Mg^{2+}	Li^+	Pb	Fe	Cu	Zn	Ni	Cr	Cd	Hardness
pH	1																									
DO	-0.10175	1																								
Salinity	-0.36409	0.076833	1																							
ORP	0.078613	-0.05739	-0.04489	1																						
EC	-0.13955	0.067604	0.257678	0.057821	1																					
TDS	-0.13261	0.050808	0.269817	0.039542	**0.98847***	1																				
TSS	-0.08132	-0.04297	0.057125	0.072142	0.25386	0.254244	1																			
Cl^-	-0.009	0.005709	0.110129	-0.27188	0.399338	0.3985	0.322453	1																		
F^-	0.121573	-0.0979	0.041066	-0.01882	0.3356	0.330918	0.267048	0.28981	1																	
SO_4^{2-}	-0.03367	-0.17192	0.061449	-0.15148	0.435664	0.469749	0.287715	0.467099	0.282794	1																
NO_3^-	0.070803	0.000752	-0.01627	-0.21149	0.299159	0.301443	0.171908	0.706219	0.195776	0.254095	1															
PO_4^{3-}	-0.01035	-0.1254	0.149926	-0.21184	0.33966	0.352185	0.039041	0.395421	0.340675	0.066777	0.157293	1														
HCO_3^-	-0.04167	-0.14643	0.04886	-0.24377	0.484873	0.50439	0.263637	0.715949	0.36106	**0.83793***	0.546499	0.304577	1													
Na^+	-0.2032	-0.14028	0.326448	-0.06429	0.474047	0.491849	0.160207	0.439229	0.353955	0.155407	0.236666	0.562515	0.376534	1												
K^+	-0.06225	-0.04866	0.005051	-0.25693	0.212562	0.255348	0.310327	0.473707	0.115366	0.700753	0.349325	0.129763	0.759805	0.110496	1											
Ca^{2+}	0.058463	-0.02161	0.106871	-0.16276	0.500109	0.527347	0.422911	0.432956	0.26202	0.694494	0.235966	0.188484	0.64051	0.318028	0.562695	1										
Mg^{2+}	-0.07579	0.033261	0.174379	-0.06736	0.29631	0.326845	0.311576	0.346518	0.325396	0.442447	0.071471	0.218145	0.530798	0.195608	0.570498	0.397799	1									
Li^+	0.033103	-0.06462	0.181077	0.091381	0.305115	0.299136	-0.04613	0.183194	0.149392	0.454043	0.268275	0.103744	0.402875	0.15764	0.343444	0.275037	0.17673	1								
Pb	-0.32733	0.013568	0.300968	-0.13409	0.491458	0.493957	0.297191	0.599986	0.390293	0.620789	0.390951	0.284264	0.669592	0.392023	0.389503	0.433222	0.244527	0.26871	1							
Fe	-0.19205	0.016331	0.049941	-0.05503	-0.12347	-0.12391	0.140645	0.012147	-0.05061	-0.03504	-0.03042	-0.01889	-0.01214	-0.12247	-0.00588	0.03346	-0.09397	-0.4831	0.114982	1						
Cu	-0.15146	-0.00851	0.20333	-0.21451	0.627893	0.620846	0.303068	0.649483	0.426434	0.390678	0.514654	0.566821	0.667232	0.562813	0.486132	0.412335	0.352247	0.255678	0.65723	-0.02491	1					
Zn	-0.23864	0.075384	0.140953	-0.00343	0.462936	0.473143	0.338745	0.451035	0.204571	0.407347	0.551655	0.188705	0.448352	0.064747	0.431579	0.221054	0.17466	0.279093	0.589324	0.039903	0.537846	1				
Ni	-0.14252	0.110287	0.09666	-0.03847	0.615502	0.611077	0.213557	0.664942	0.448219	0.47401	0.493475	0.391153	0.695785	0.497183	0.369257	0.464446	0.297998	0.315025	0.668377	0.004414	0.715965	0.402177	1			
Cr	-0.03749	-0.03899	0.079921	-0.07928	0.569219	0.561898	0.190537	0.5614	0.555684	0.715287	0.348285	0.297367	0.777856	0.471857	0.398103	0.54627	0.37613	0.409248	0.743927	-0.09476	0.677157	0.320464	0.767586	1		
Cd	0.019226	-0.02454	0.012283	-0.10398	0.54147	0.543098	0.274352	0.703656	0.395855	0.721534	0.656627	0.197353	**0.87522***	0.37341	0.566268	0.607599	0.276427	0.453335	0.689988	-0.04003	0.670303	0.457905	**0.83572***	**0.82784***	1	
Hardness	-0.20112	-0.14126	0.282822	-0.16431	0.497794	0.531259	0.269447	0.578687	0.35329	0.431016	0.351737	0.538719	0.646202	**0.90668***	0.519402	0.512246	0.410301	0.281295	0.502364	-0.1078	0.690217	0.238831	0.584188	0.574655	0.561379	1

Fig 5.30 Correlation Analysis during post monsoon season

5.2.2 Box Plot Analysis

The graphical representation of data distribution for observing it by simple means for large numbers of dataset is known as Box Plot (Koster et al 2008). This technique basically uses median value for analysis of data dispersion and not the mean value (Stoimenova et al 2006), (US-EPA 2009). Therefore, it helps in exhibiting the hydrochemistry of the samples collected for both pre and post monsoon seasons. It also provides information about the quality of samples collected for various parameters by comparing them over a span of time. Box Plot roughly provides an idea about the shape of the unimodal distribution (Rossiter 2007). This statistical technique envisages the quartiles distribution of various water quality parameters for estimating the water quality for both the seasons. It shows the median, range and shape of the data dissemination. Here, the horizontal middle line of the box represents the median of the data, the top and bottom of the box represents the median of the data, the top and bottom of the box are the first and third quartile respectively while the end of the whiskers exhibit the 10^{th} and 90^{th} percentiles of the data. However, the 95% confidence level of the median is shown by the notch. Hence, the box plot acts as an alternative of graphical, nonparametric ANOVA.

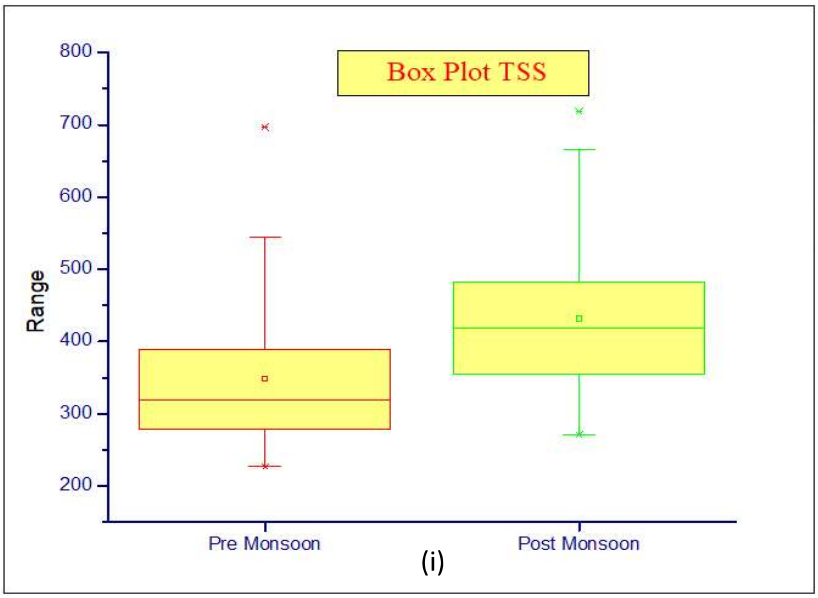

(i)

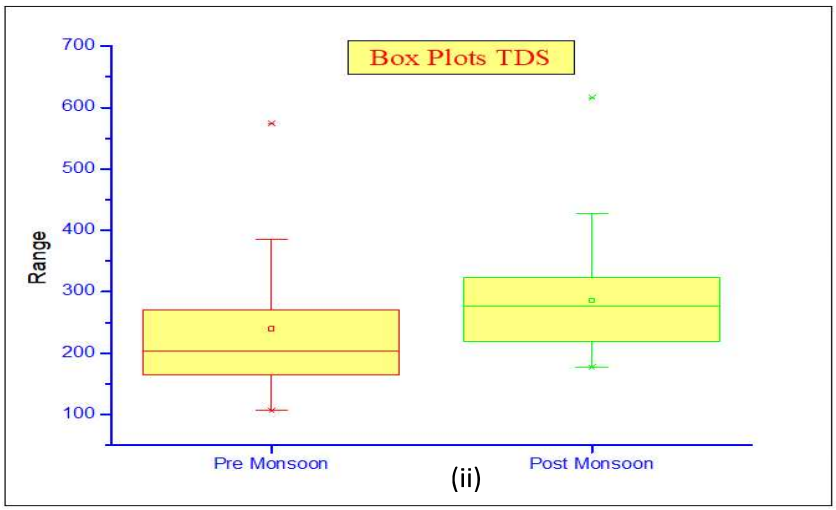
Box Plots TDS
Range
700
600
500
400
300
200
100
Pre Monsoon
Post Monsoon

(ii)

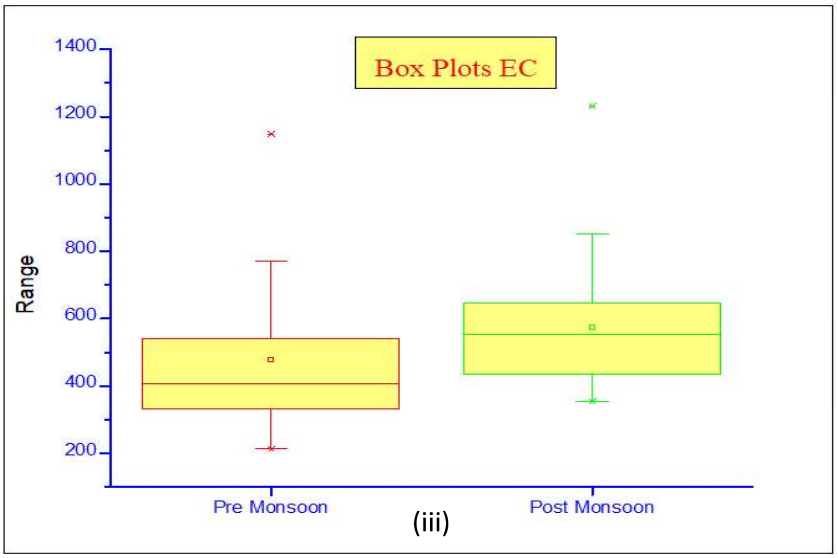
Box Plots EC
Range
1400
1200
1000
800
600
400
200
Pre Monsoon
Post Monsoon

(iii)

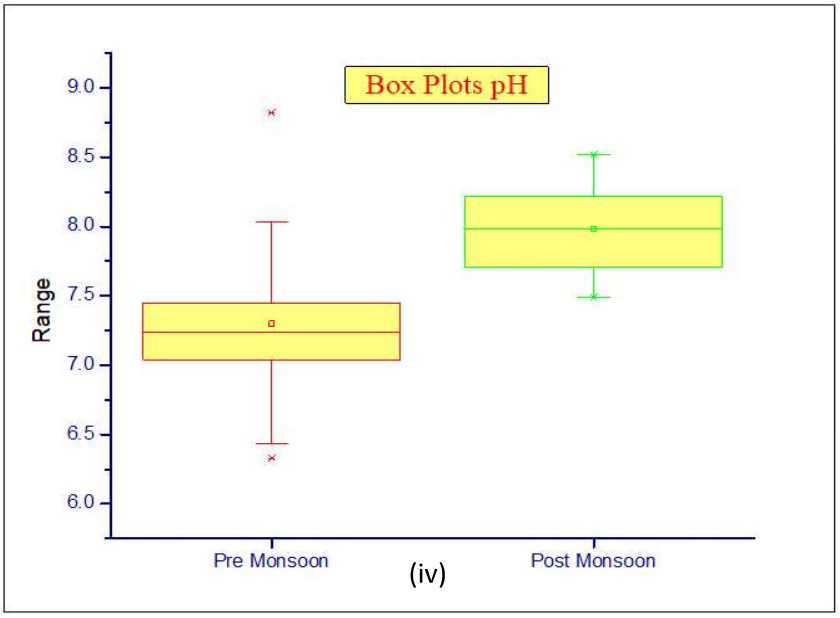
Box Plots pH
Range
9.0
8.5
8.0
7.5
7.0
6.5
6.0
Pre Monsoon
Post Monsoon

(iv)

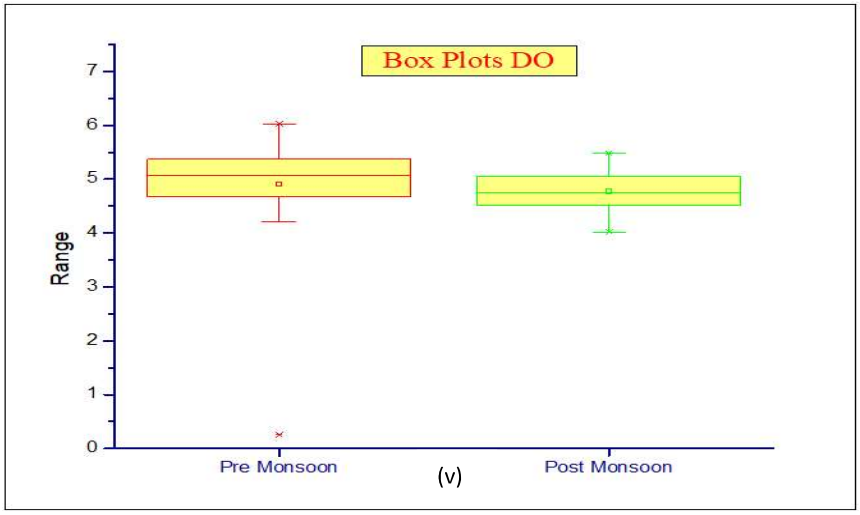
Box Plots DO
Range
7
6
5
4
3
2
1
0
Pre Monsoon
Post Monsoon

(v)

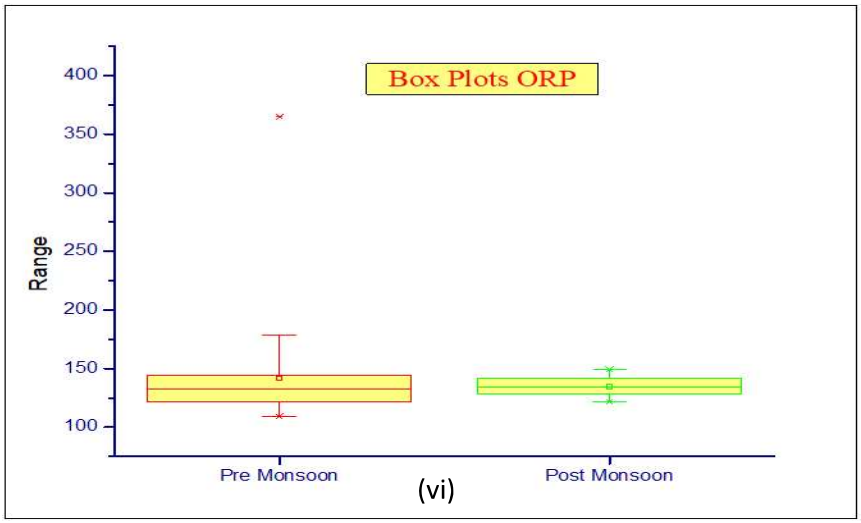
Box Plots ORP
Range
400
350
300
250
200
150
100
Pre Monsoon
Post Monsoon

(vi)

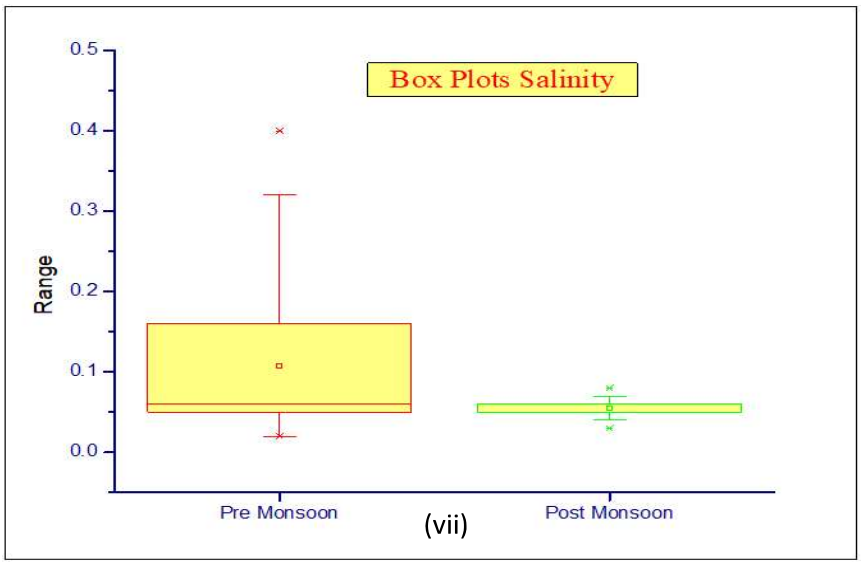
Box Plots Salinity
Range
0.5
0.4
0.3
0.2
0.1
0.0
Pre Monsoon
Post Monsoon

(vii)

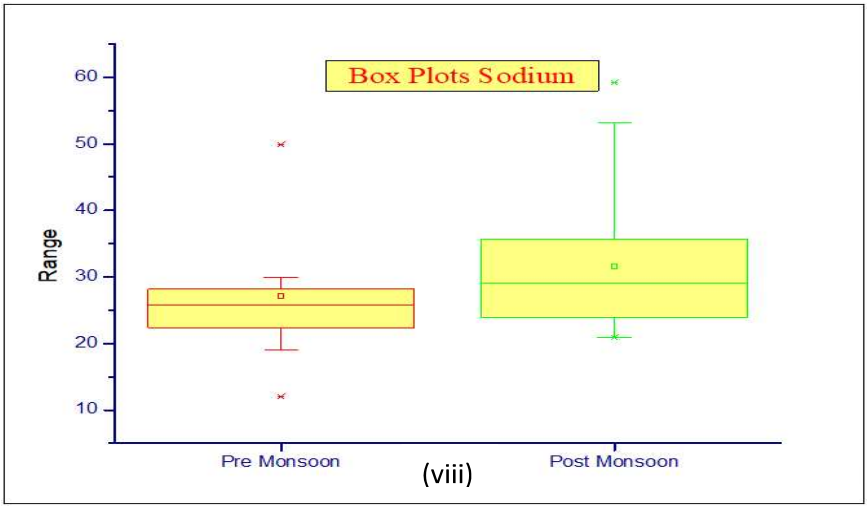
Box Plots Sodium
Range
60
50
40
30
20
10
Pre Monsoon
Post Monsoon

(viii)

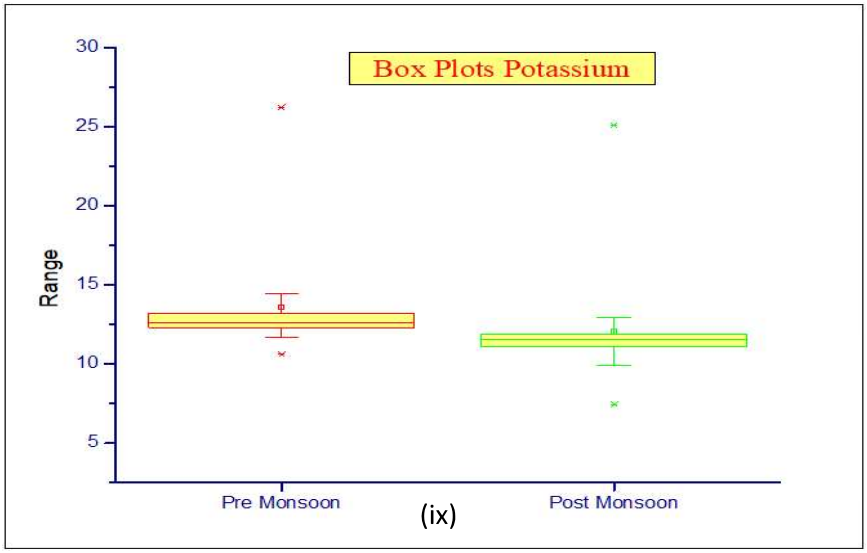
Box Plots Potassium
Range
30
25
20
15
10
5
Pre Monsoon
Post Monsoon

(ix)

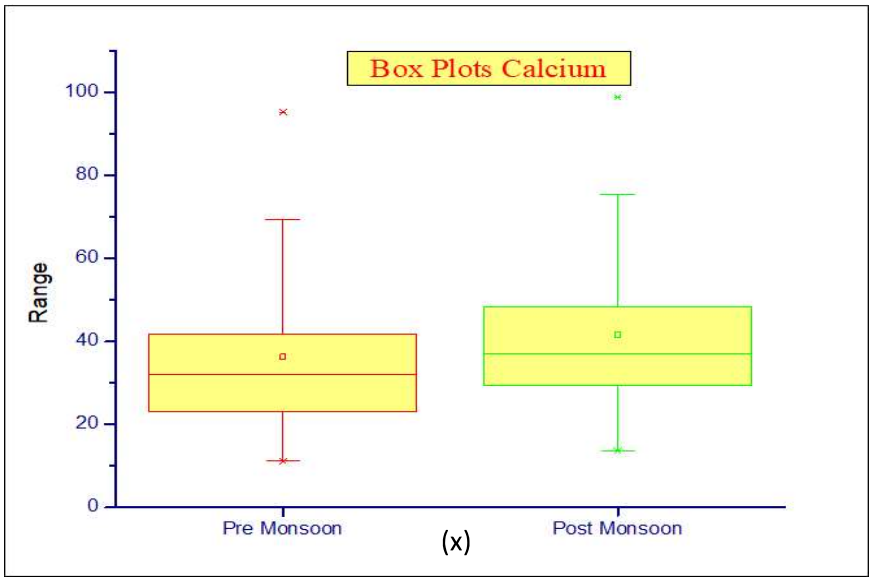
Box Plots Calcium
Range
100
80
60
40
20
0
Pre Monsoon
Post Monsoon

(x)

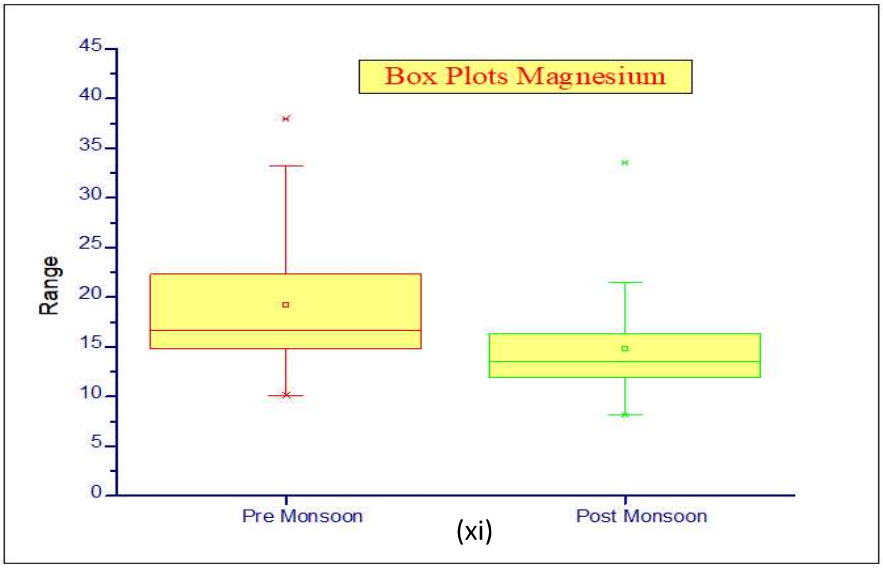
Box Plots Magnesium
Range
45
40
35
30
25
20
15
10
5
0
Pre Monsoon
Post Monsoon

(xi)

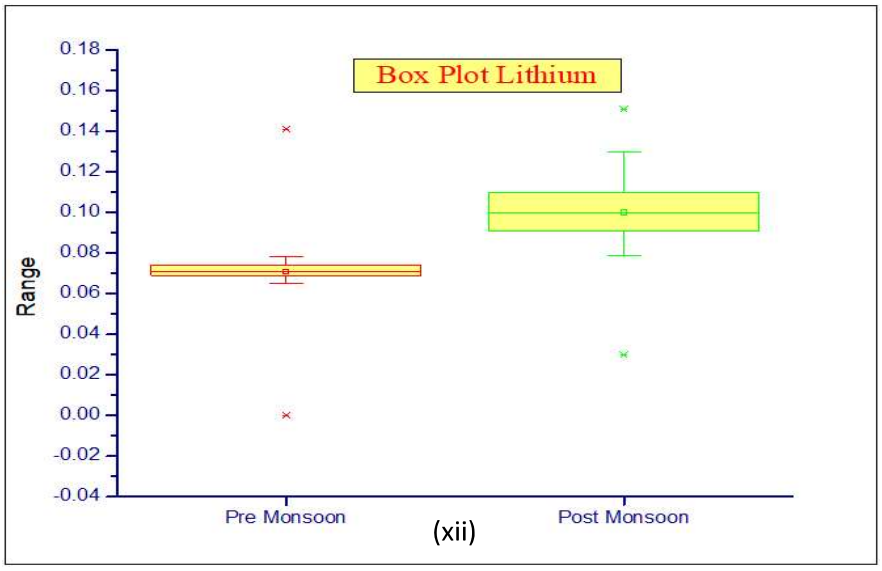
Box Plot Lithium
Range
0.18
0.16
0.14
0.12
0.10
0.08
0.06
0.04
0.02
0.00
-0.02
-0.04
Pre Monsoon
Post Monsoon

(xii)

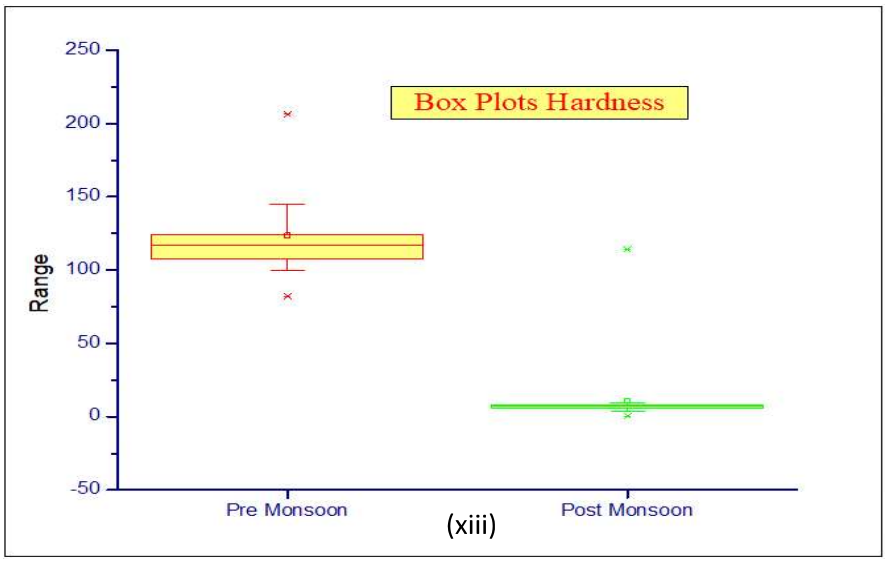
Box Plots Hardness
Range
250
200
150
100
50
0
-50
Pre Monsoon
Post Monsoon

(xiii)

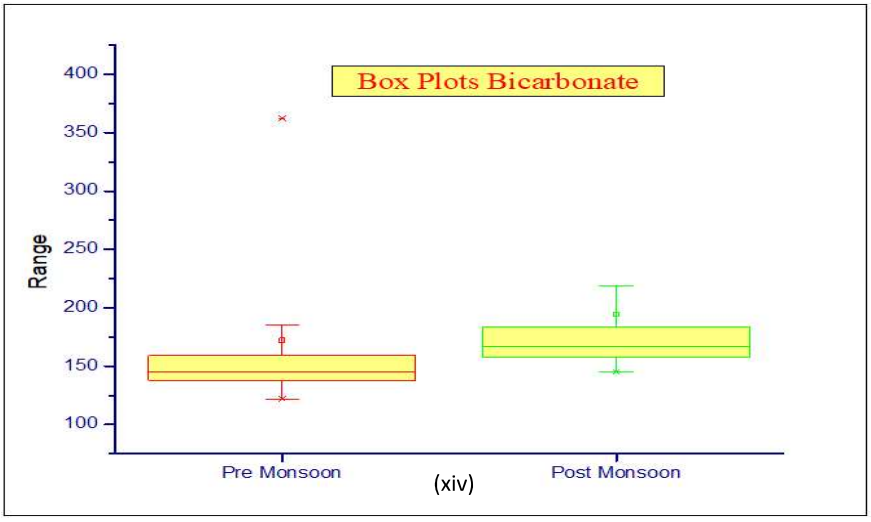
Box Plots Bicarbonate
Range
400
350
300
250
200
150
100
Pre Monsoon
Post Monsoon

(xiv)

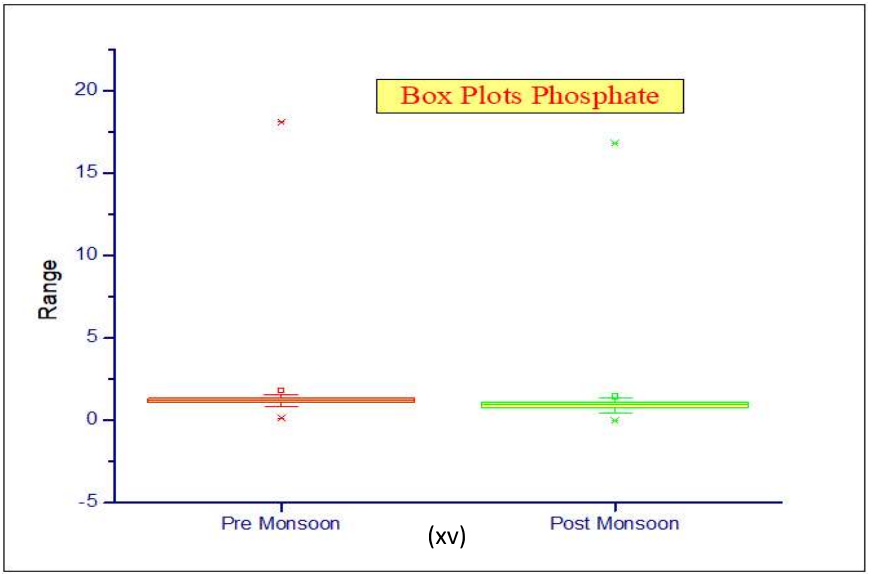
Box Plots Phosphate
Range
20
15
10
5
0
-5
Pre Monsoon
Post Monsoon

(xv)

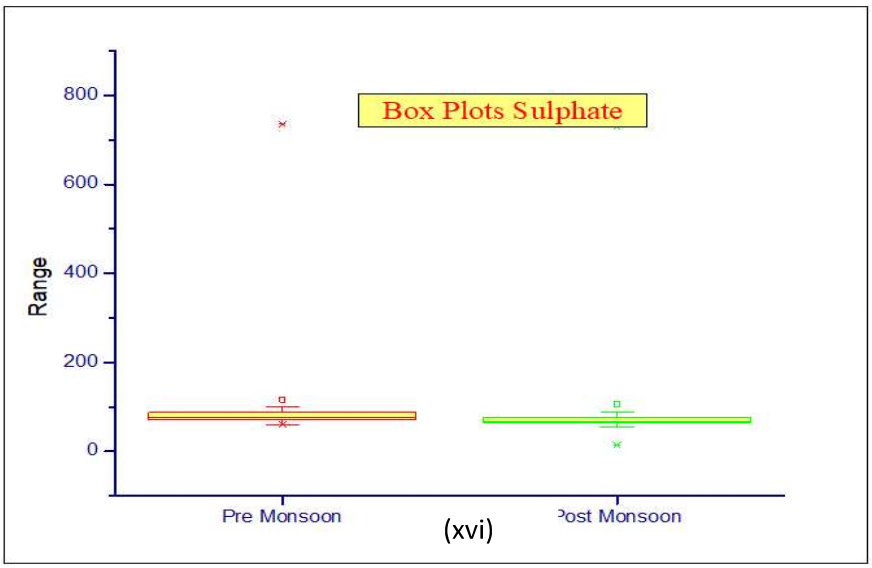
Box Plots Sulphate
Range
800
600
400
200
0
Pre Monsoon
Post Monsoon

(xvi)

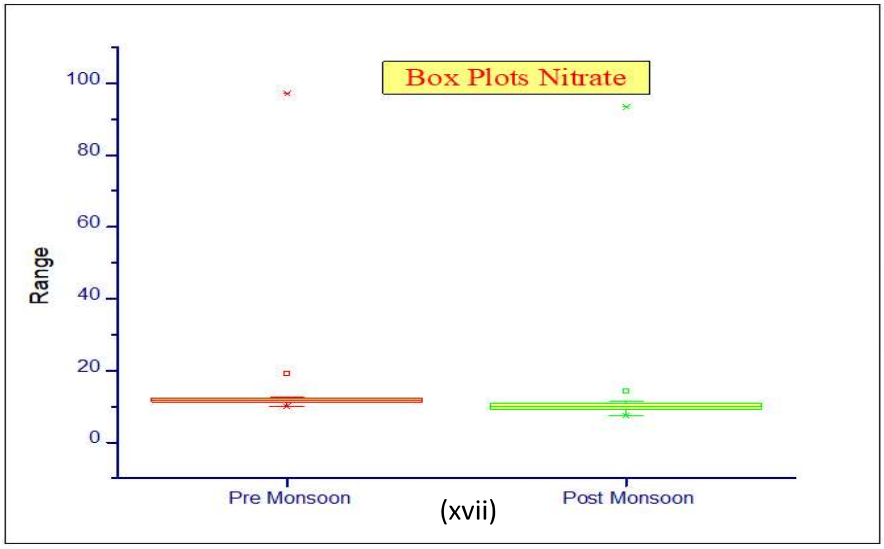

(xvii)

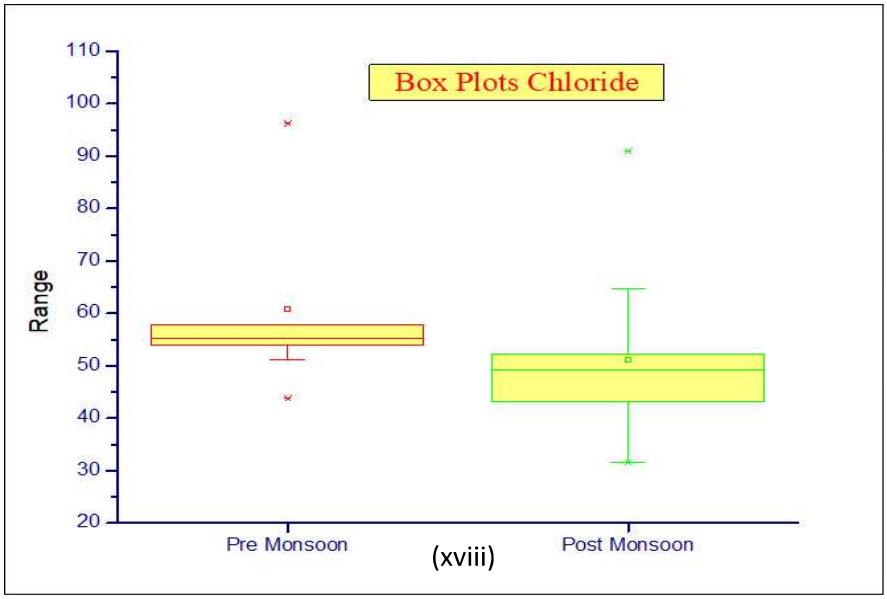

(xviii)

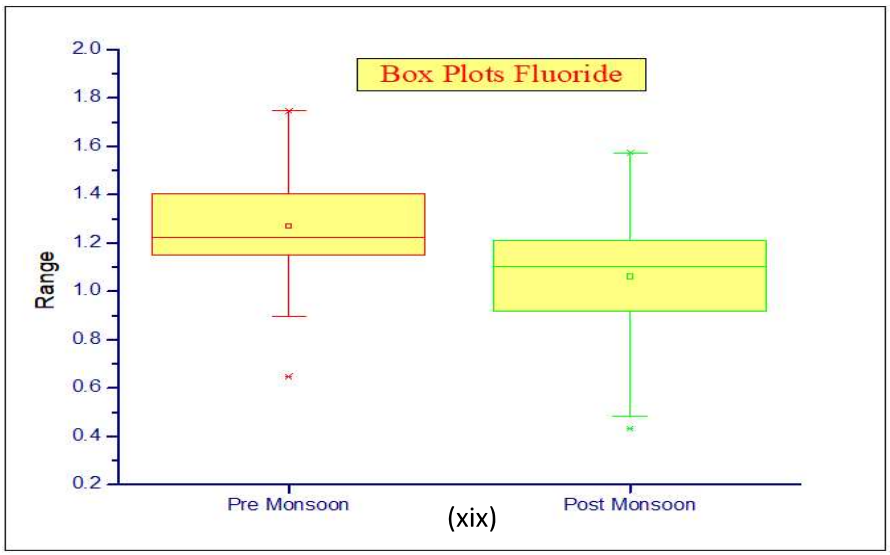

(xix)

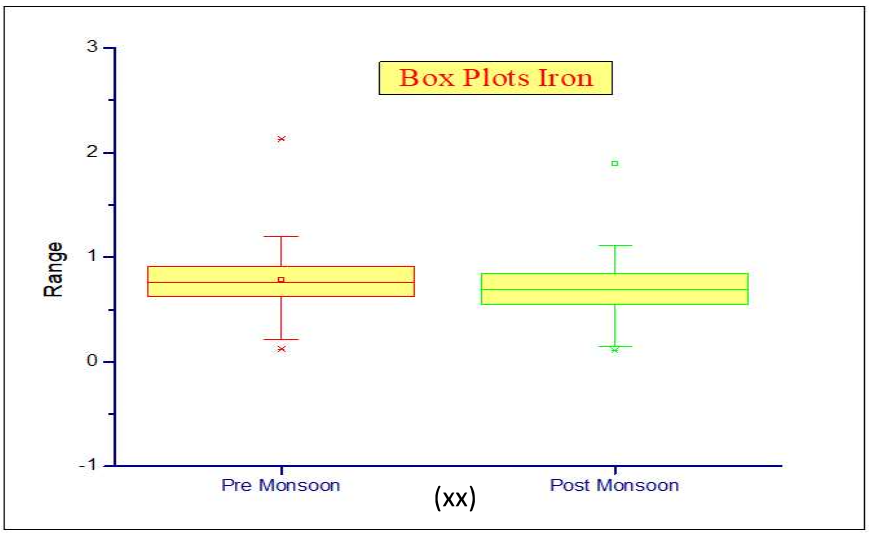
Box Plots Iron
Range
3
2
1
0
-1
Pre Monsoon
Post Monsoon

(xx)

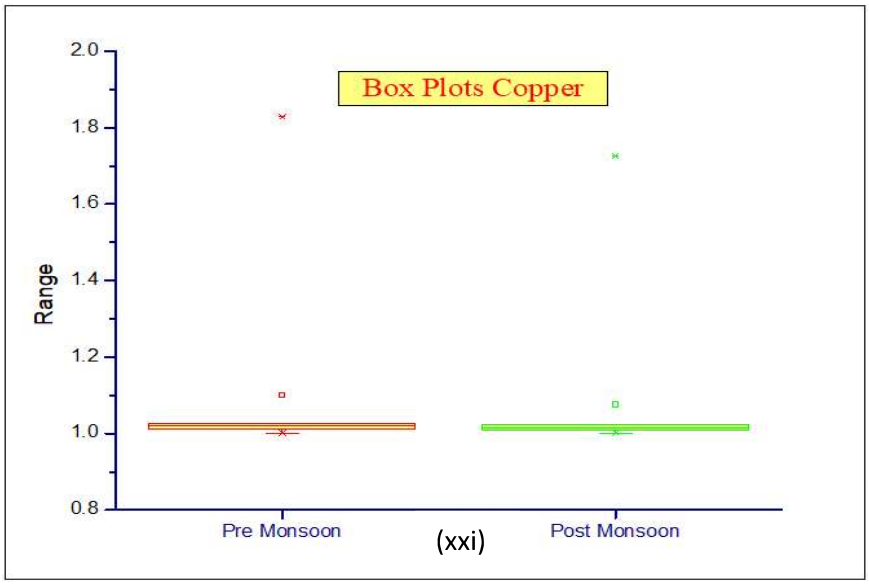
Box Plots Copper
Range
2.0
1.8
1.6
1.4
1.2
1.0
0.8
Pre Monsoon
Post Monsoon

(xxi)

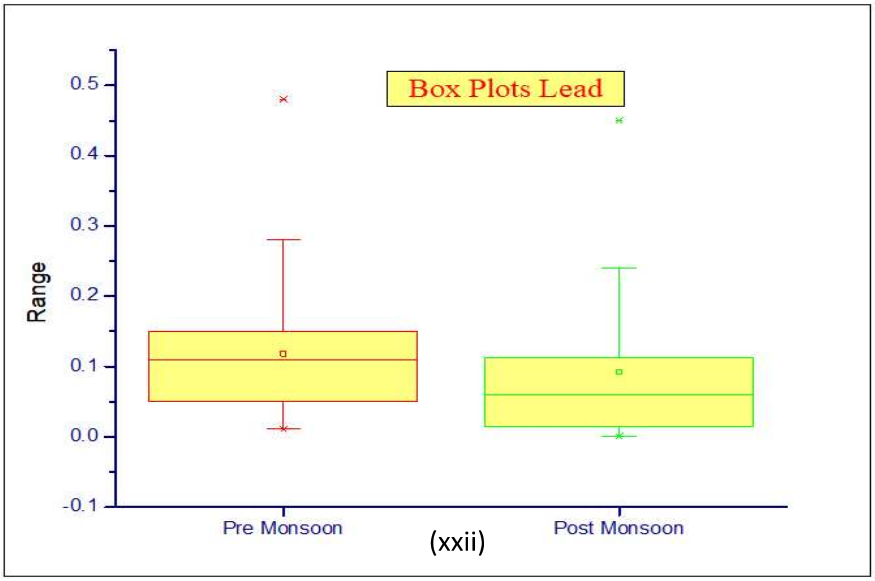
Box Plots Lead
Range
0.5
0.4
0.3
0.2
0.1
0.0
-0.1
Pre Monsoon
Post Monsoon

(xxii)

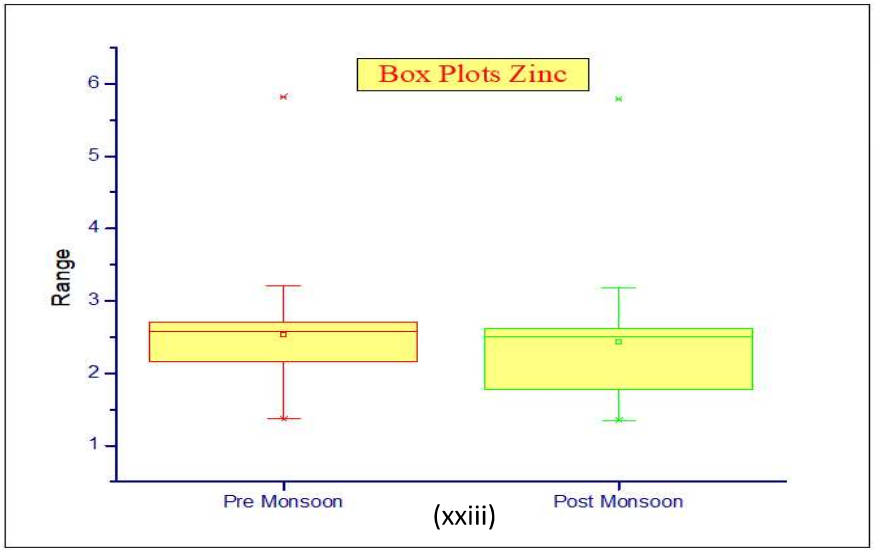

(xxiii)

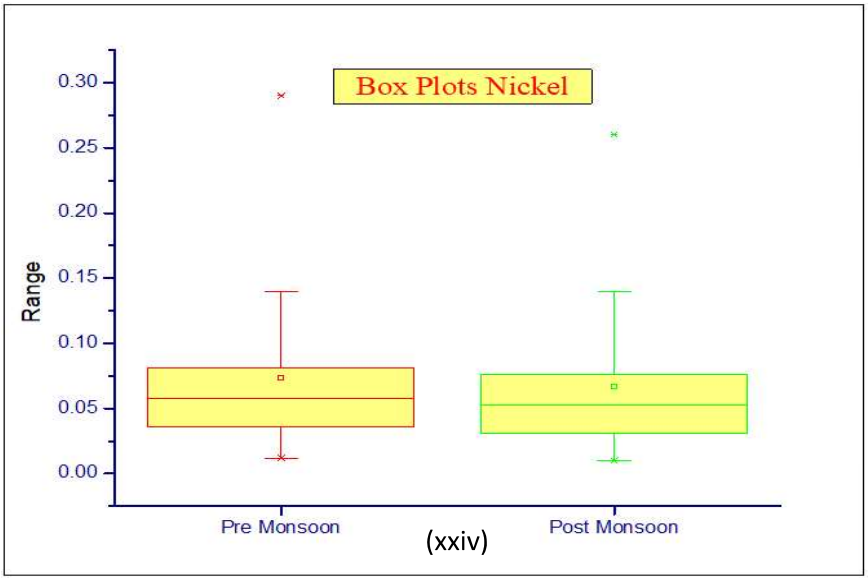

(xxiv)

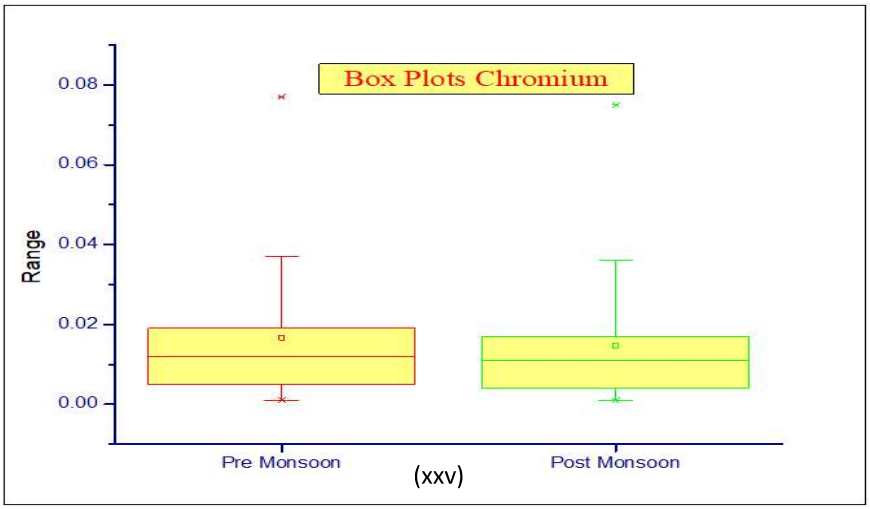

(xxv)

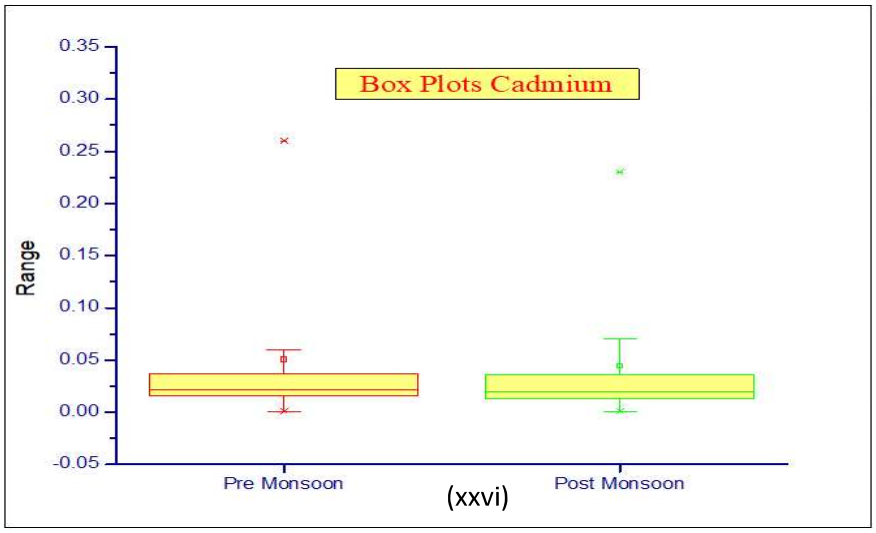

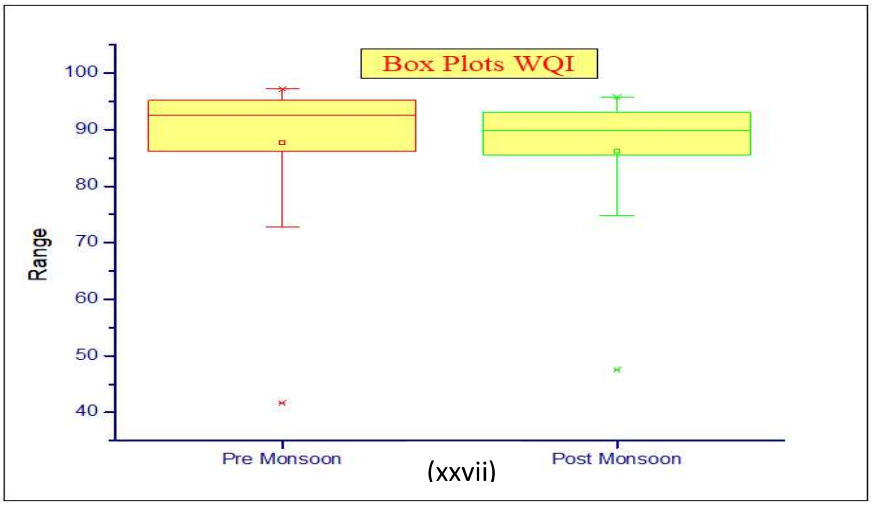

Fig 5.31 (i) to (xxvii) Box Plot Diagram of the Physico-chemical Parameters of water Samples of Study Area

As shown by Fig 5.31 (i) to (xxvii) for various water quality parameters along with the Water Quality Index, the comparative analysis of various parameters are shown separately for both pre and post monsoon dataset. It can be seen from Table A.1 and A.2 that the pH was slightly alkaline during the post monsoon season when compared with that of pre-monsoon season. Salinity and Oxidation Reduction Potential during post monsoon season was much less than that during pre-monsoon. However, Electrical Conductivity, Total Dissolved Solid, Total Suspended Solid and Bicarbonate values

during post monsoon season were quite more than that during pre-monsoon season. While the values of Chloride, Fluoride, Sulphate, Nitrate, Phosphate, Potassium and Magnesium during pre- monsoon season were higher than that of these during post monsoon season. The remaining ions such as Sodium, Calcium, Lithium and Hardness exhibit a higher value during post monsoon season than that during pre-monsoon season. Moving on to the heavy metals the value of Lead, Copper, Zinc, Nickel, Chromium and Cadmium during pre-monsoon season was higher than that during post monsoon season while Iron showcases a vice-versa scenario. Table A.1 to A.8 shows the concentration of these parameters during pre and post monsoon season.

5.2.3 Hierarchical Cluster Analysis (HCA)

Being an unsupervised pattern recognition technique, it reveals the intrinsic structure of a dataset, without making a prior assumptions about the data to classify the objects of the system into categories or clusters based on their similarity (Vega et al 1998). It is one of the most common approaches to chronologically categorize the most similar objects into groups and step by step forming higher clusters. Here, the similarity is maximum within the group while it is minimum amongst the group. However, the Euclidean distance is commonly used as a distance coefficient showcasing the similarity between two samples while the ‘distance’ is represented by the ‘difference’ between analytical values from both of the samples (Otto, 1998). Here, in this study, Hierarchical Cluster Analysis was executed on the dataset during pre and post monsoon season using Ward’s method with squared Euclidean distances as a measure of similarity. This method employs the evaluation of variance approach for scrutinizing the distances between clusters while endeavoring to trivialize the sum of squares between any two clusters forming at each step. The result of Hierarchical Cluster Analysis is presented in form of a dendrogram catering the visual summary of the agglomeration processes, depicting a picture of the

clusters and their similarity, with a dramatic reduction in dimensionality of the original data set (Shrestha et al 2007). In this study, Hierarchical Cluster Analysis is used to classify the 60 sampling sites into clusters on the basis of Water Quality Index during pre and post monsoon season to spatially examine the pattern of Water Quality Index during both the seasons. The spatial variability of Water Quality Index during both the season was ascertained from Hierarchical Cluster Analysis, using the linkage distance, reported as Dlink/Dmax, which shows the quotient between the linkage distances for a particular case divided by the maximal linkage distance. The quotient is then multiplied by 100 as a way to standardize the linkage distance represented on the y-axis (Wunderlin et al 2001, Simeonov et al 2004, Singh et al 2004).

In this study, the result obtained during pre-monsoon reason showed that the whole results of 60 sites were divided into four clusters. Group 1 consists of a maximum number of sampling locations covering almost all the sampling sites of Govind Ballabh Pant reservoir. However, the minimum number of sampling locations i.e. only 2 locations were locations were included in Group 4. In Group 2 also many sampling locations were included but their number was less than those present in Group 1. Moving on to Group 3, this Group consists of only 3 sampling sites on the basis of similarity of water quality index present among them. It can be depicted from Fig 5.32.

During the post monsoon season, the dendrogram generated consists of three clusters or groups. Here too, like the pre-monsoon season, the Group 1 consists of a maximum number of sampling locations with most of the sampling sites of Govind Ballabh Pant reservoir. Group 2 consists of very few sampling locations as can be depicted from the Fig 5.33. However, again the Group 3 constituted of only 2 locations i.e. Balia Nala and Motwani Dam showing the highest degree of similarity amongst these locations. Both the Dendrograms for pre and post monsoon season were constructed on the basis of Similarity

amongst the Water Quality Index for the 60 sampling locations present in and around the Govind Ballabh Pant reservoir in the area under study. The dendrogram obtained from Hierarchical Cluster Analysis for both the seasons are shown by Fig 5.32 and Fig 5.33.

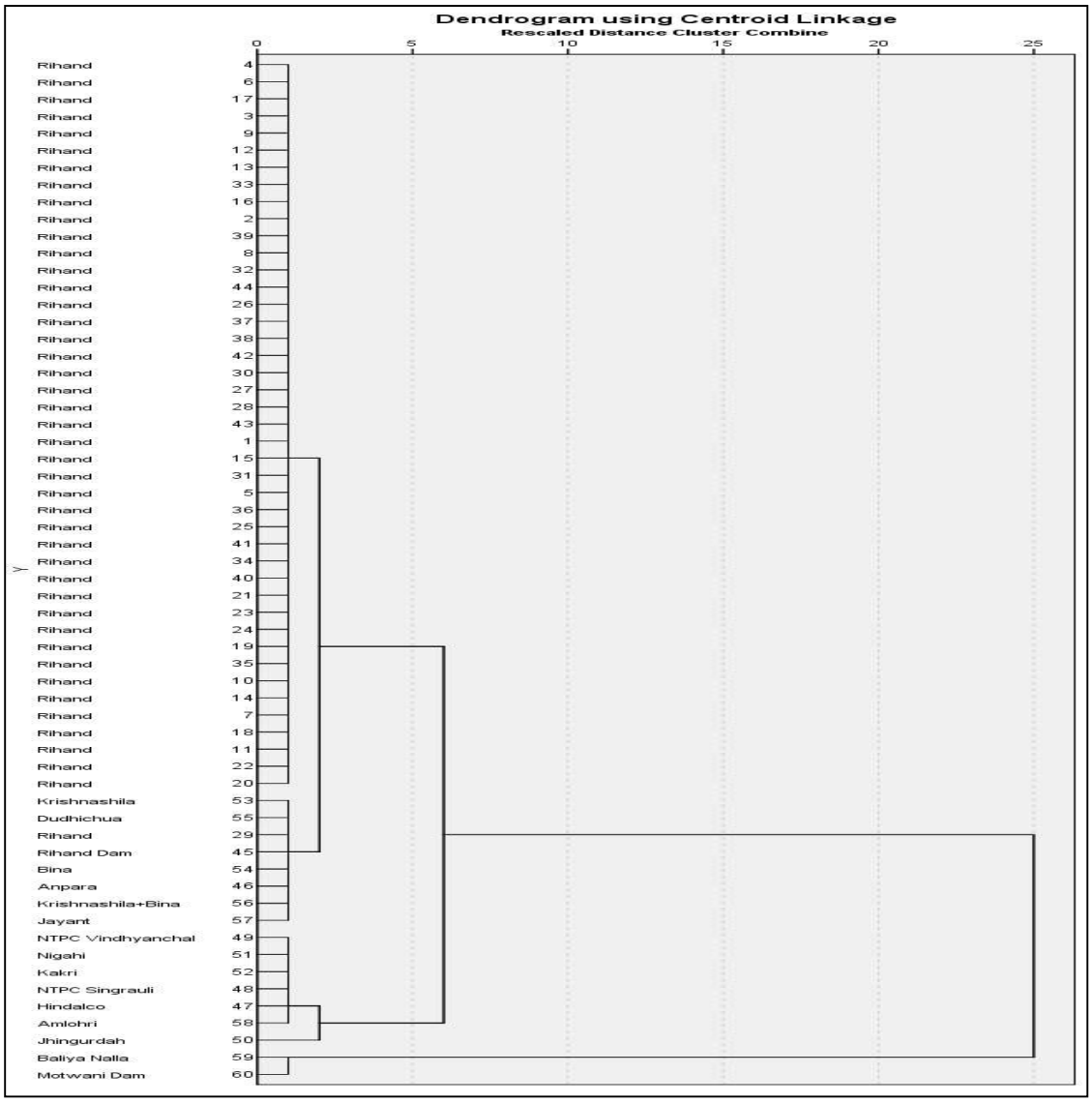

Fig 5.32 Dendrogram of the HCA based on WQI of the Sampling Sites during pre monsoon season

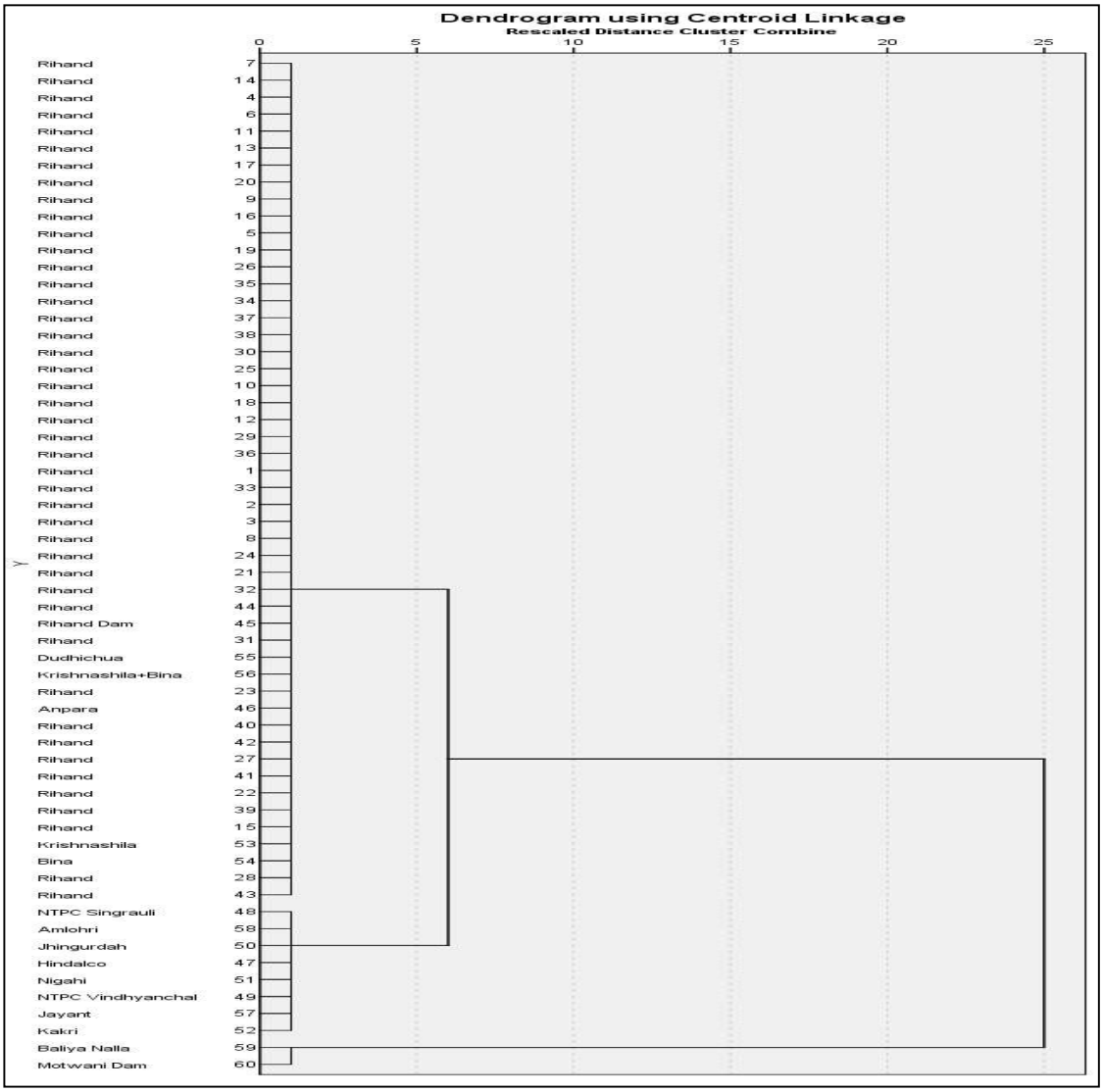

Fig 5.33 Dendrogram of the HCA based on WQI of the Sampling Sites during post monsoon season

5.2.4 Piper Diagram

As water flows in streams, reservoirs or lakes it passes through various lithological units thereby acquiring the chemical composition of the rocks present in the area due to interaction of rocks with surface water. In order to describe the chemical composition of this water, the term hydro-geo-chemical facies is used to express the chemical composition of water (either surface or groundwater) that differs due to interaction with the surrounding rocks. Hydro-geo-chemical facies are generally distinct zones that have

cation and anion concentration are described within defined composition categories (Ophari & Toth, 1989). Since, the chemical composition of surface water is mainly dependent on the geology as well as geochemical processes & anthropogenic activities taking place in the area under study therefore representation of these facies through Piper Diagram becomes convenient. Hydro-geo-chemical facies can be classified on the basis of dominant ions using the Piper's trilinear diagram (Ali et al 2018). Hydro-geo-chemical facies enable a convenient subdivision of water composition by identifiable categories and reflects the effect of chemical processes occurring between the minerals within the surface rock units and the groundwater (Piper, 1944). It permits the cation and anion composition of many samples to be represented on a single graph in which major grouping or trends in the data can be distinguished visually (Freeze & Cherry, 1979). The classification of these cations and anions in terms of percentage is ascertained by the domain in which they occur on the diagram. The Piper diagram used in this study has been constructed separately for both pre and post monsoon season to represent the presence of major hydro-geo-chemical facies present in the area during both the seasons. The Diagram is shown by Fig 5.34 and Fig 5.35.

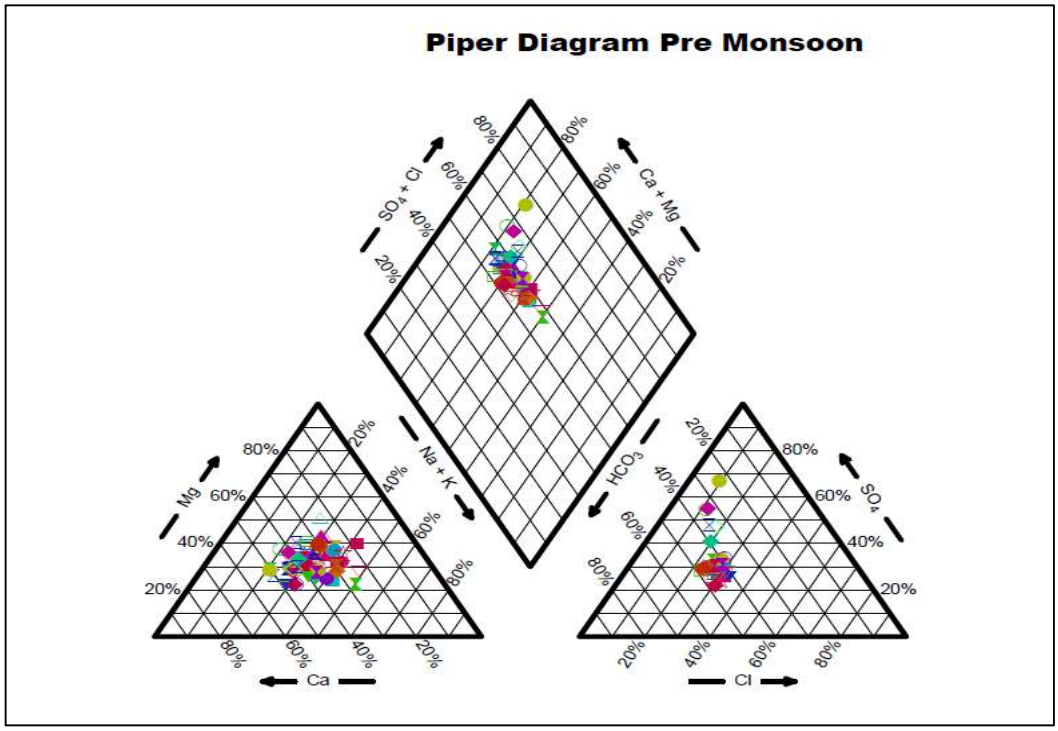

Fig 5.34 Piper diagram for describing the hydro-geo-chemical facies variations during pre-monsoon season

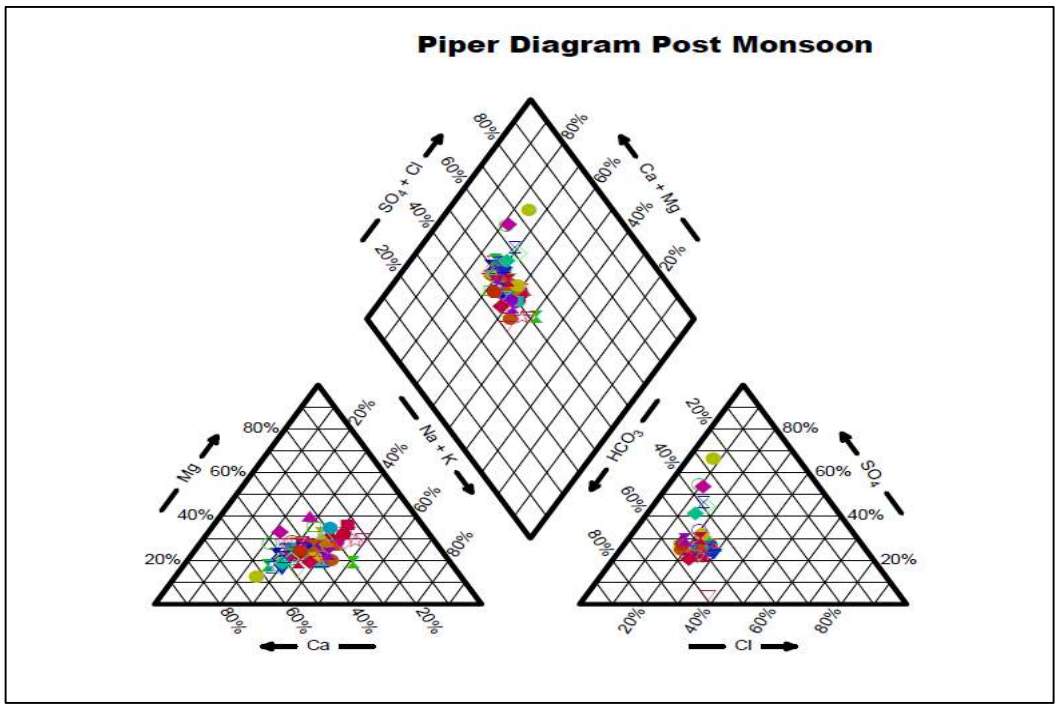

Fig 5.35 Piper diagram for describing the hydro-geo-chemical facies variations during post monsoon season

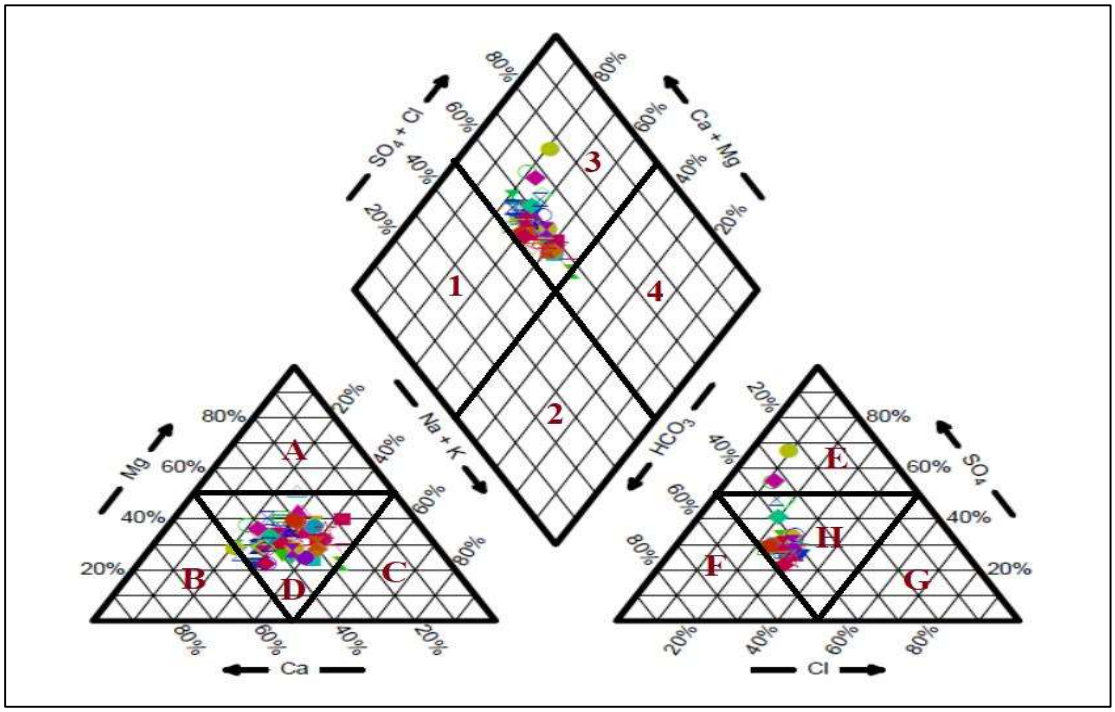

Fig 5.36 Modified Piper Plot of the Classification Scheme for hydro-geo-chemical facies variations during pre-monsoon season.

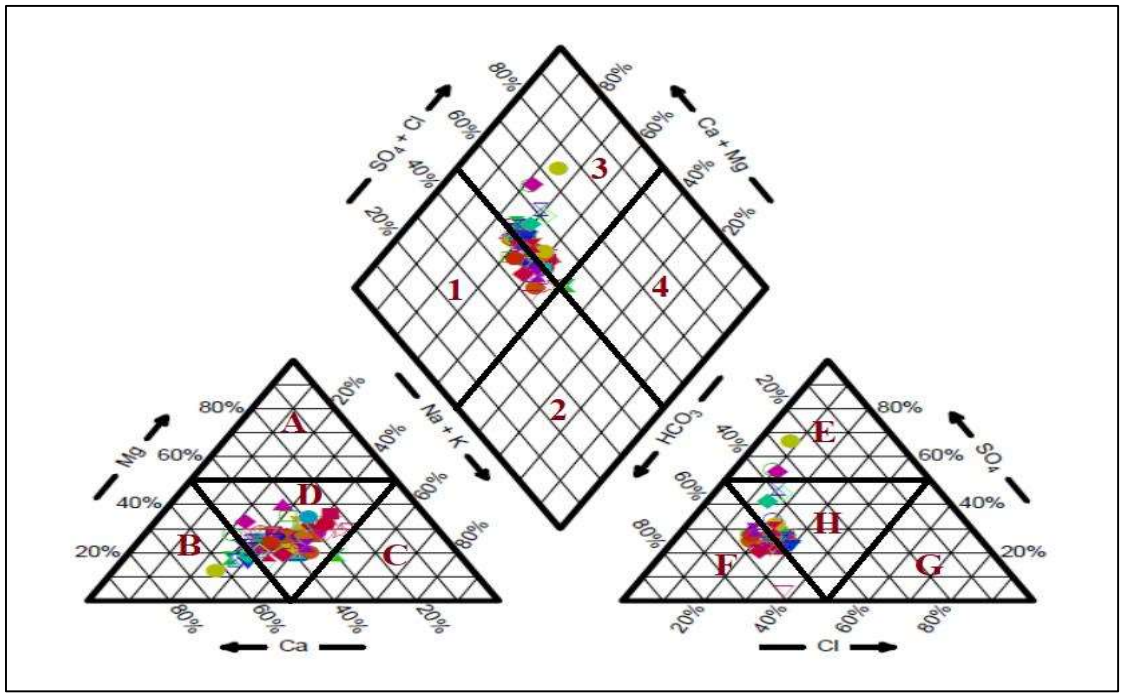

Fig 5.37 Modified Piper Plot of the Classification Scheme for hydro-geo-chemical facies variations during post monsoon season.

The Legends used in Fig 5.36 and 5.37 has been listed below as follows:-

A - Magnesium type

B - Calcium type

C - Sodium or Potassium type

D - No dominant type

E - Sulphate type

F – Bicarbonate type

G - Chloride type

H - No dominant type

1 – $CaMg\text{-}HCO_3$

2 – $NaK\text{-}HCO_3$

3 – $Ca\text{-}Mg\text{-}Cl\text{-}SO_4$

4 – $NaCl\text{-}SO_4$

The Piper diagram basically consists of 2 triangles & a diamond shaped plot. The right triangular part of the diagram shows major anions like Chloride, Sulphate, Bicarbonate and Carbonate while the left triangle is constituted by the presence of major cations like Calcium, Magnesium, Sodium & Potassium. These ions are plotted in terms of percentage on both the triangles respectively. The diamond shaped part of the diagram present between the two triangles represents the composition of water by a single point which is the convergence point of the projected point from the right & left triangle in the diamond field consisting of cation & anions.

During pre-monsoon season 6% of the water samples collected from the study area falls under the Calcium type while the rest 94% of the samples were in no dominant type in cation facies. Conversely 5% of the samples fell into Bicarbonate type, 3% into Sulphate type and rest 92% of the samples occurred in No dominant type in Anion facies. The plot of chemical data on the diamond shaped part of the piper diagram reveals that all the water samples collected from the study area falls under field 3 having $Ca\text{-}Mg\text{-}Cl\text{-}SO_4$ groups as major constituents. The predominance of this group indicates the presence of

anthropogenic activities in the area along with the geology of the study area which is dominated by presence of Calcite and Dolomite rocks thereby revealing the interaction of these rocks with the surface water present in the area.

Moving on to the post monsoon season, the piper plot of the season, 20% of the samples falls under Calcium type while the remaining 80% of the water samples collected occurred under No dominant type in the cation facies. In anion facies, 30% of the water samples falls under Bicarbonate type while 5% of the samples collected fall under Sulphate type. However, the remaining 65% of the samples were in No dominant type. The Diamond shaped part of the plot shows that nearly 40% of the samples collected from the study area falls under Ca-Mg-HCO_3 indicating the process of dissolving minerals present in the vicinity of the area. The remaining 60% of the water samples fall under Ca-Mg-Cl-SO_4 group like that during the pre-monsoon season showing the presence of anthropogenic activities due to presence of mining and thermal power plant in the area as well as the dominance of Calcite & Dolomite lithology in the geology of the study area. Fig. 5.36 and Fig. 5.37 shows the Modified Piper Plot of the Classification Scheme for hydro-geo-chemical facies variations during pre-monsoon and post monsoon season respectively.

5.3 Spectral characterization of Land Use/Land Cover classes

Being considered as one of the most indispensable sources for providing data about the natural resources present in the area under study, Land Use/Land Cover (LU/LC) acts as a major technique for classification of the area into various classes. The software used for these detections are ERDAS Imagine 2014 and ArcGIS 10.1. LU/LC classes are quintessentially depicted from the satellite imageries which are acquired, processed, enhanced and digitized to produce False Color Composite (FCC) of the image which in turn is classified through supervised digital image classification using Maximum Likelihood Classifier Approach. According to the above said methodology, this classification process converts all the pixels present in the image into a number of classes automatically as commanded by the user. This methodology quantifies patterns of spectral responses sent by the unknown pixel of the imagery into their respective classes, therefore making it one of the most accurate techniques of image classification. Since, the identification of various objects present in the satellite imagery of the area under study is depicted by the means emission or reflectivity of radiations measured and recorded by the sensor and ultimately representing as an image result. Identifying these targets by perceiving the difference between the objects and their backgrounds is based on visual interpretation of elements such as tone, shape, size, pattern, texture, shadow & association. Recollecting information about the object present in the imagery on the basis of elements of visual interpretation further enables us to analyze and interpret the satellite imagery efficiently. Here, in this study the satellite image was interpreted to portray six LU/LC classes viz:- Habitation, Hilly Area/Forest, Mining Area, Water bodies, Fallow/Barren and Crop land for five different years starting from 1988 to 2018. This study employs land use/land cover analysis by implementing temporal Landsat FCC data

of 1988, 1996, 2005, 2016 and 2018. These LU/LC maps were produced by the technique of visual interpretation of multispectral satellite data from Landsat 5 MSS of 06 February1988, 27 January 1996, 04 February 2005 and Landsat 8 OLI of 19 February 2016 and 24 February 2018. The dataset used in the classification for all the five years belongs to approximately the same month because of the reason to achieve minimum contrast in spectral signatures. The errors occurring in the interpretation of the dataset were rectified, enhanced and processed to finally obtain the LU/LC maps for the years 1988, 1996, 2005, 2016 and 2018.

The acquired satellite data is classified by LU/LC fundamentally on the essence of distinctive image attribute and applied domain comprehensions. Since, in this study six classes are classified for each of the year under LU/LC, therefore each class has its own unique spectral characteristic which allows it to get delineated from any other class. The habitation class is represented by Red tone, smooth texture and recognizable pattern with regular to irregular boundary having exquisite demarcation junction with the adjoining classes present in the LU/LC map. The Hilly area/Forest is recognized by purple tone, rough texture, contiguous to non-contiguous pattern having irregular shape associated with high relief. Mining areas were identified by yellow tone, smooth texture with a distinctive linear recognizable pattern having an extended shape coupled with a standard geometrical boundary. Water bodies are distinguished by dark blue tone having smooth texture accompanied by ragged shape possessing precise delineation boundary contact with adjoining Land use/Land cover classes in association with contiguous pattern. Barren/Fallow land is discerned by its greyish tone, rough texture, irregular shape accompanied with high to moderate relief and contiguous pattern. The last class i.e. Cropland is apprehended by green tone, smooth to medium texture, scattered pattern,

irregular boundary with non-uniform distribution. These spectral characterization of LU/LC classes are represented below in Fig:-

5.4 Land Use /Land Cover Analysis (1988)

In the year 1988, the total spread of water body area in the region of study was found to be 419.67 km^2 as mapped from Landsat 5 MSS Satellite image on 06 February 1988 comprising of about 15.27% of the total area under study. This mainly encompasses Govind Ballabh Pant reservoir along with the tributaries of fresh river water used for replenishing water to the reservoir required both for industrial or domestic supply in the area. However, the class covering the least amount of area is represented by Habitation Class of the LU/LC map. Here, it covers an area of about 8.14 km^2 embracing an area of about 0.296% of the total area taken into consideration. The next category which covers the second lowest area amongst the total area under study is Mining Area which constitutes about 15.19 km^2 of the total area forming 0.553% of the area under study. Following this, is the turn of the Cropland in terms of area covered. This category constitutes an area of about 374.19 km^2, an area of about 13.61% of the total area covered under the study for analysis of LU/LC classes. Contrary to this, comes the turn of categories comprehending the majority of the area covered under the LU/LC map. The class embracing the maximum amount of the area is Fallow/Barren which is about 41.19% of the total area under study. Accompanying this is the turn of Hilly Area/Forest category covering an area of about 799.38 km^2 which is equivalent to a percentage of about 29.08% of the total area taken into account. These classes/categories derived from LU/LC map of 1988 from Landsat 5 MSS satellite is shown in Table 5.2 below:-

LU/LC Category (1988)	Area (km^2)	Area (%)
Fallow/ Barren	1132.55	41.19
Hilly Area/ Forest	799.38	29.08
Water bodies	419.67	15.27
Cropland	374.19	13.61
Mining Area	15.19	0.553
Habitation	8.14	0.296
Total Area	**2749.14**	**100**

Table 5.2 Land Use Land Cover Statistics (1988)

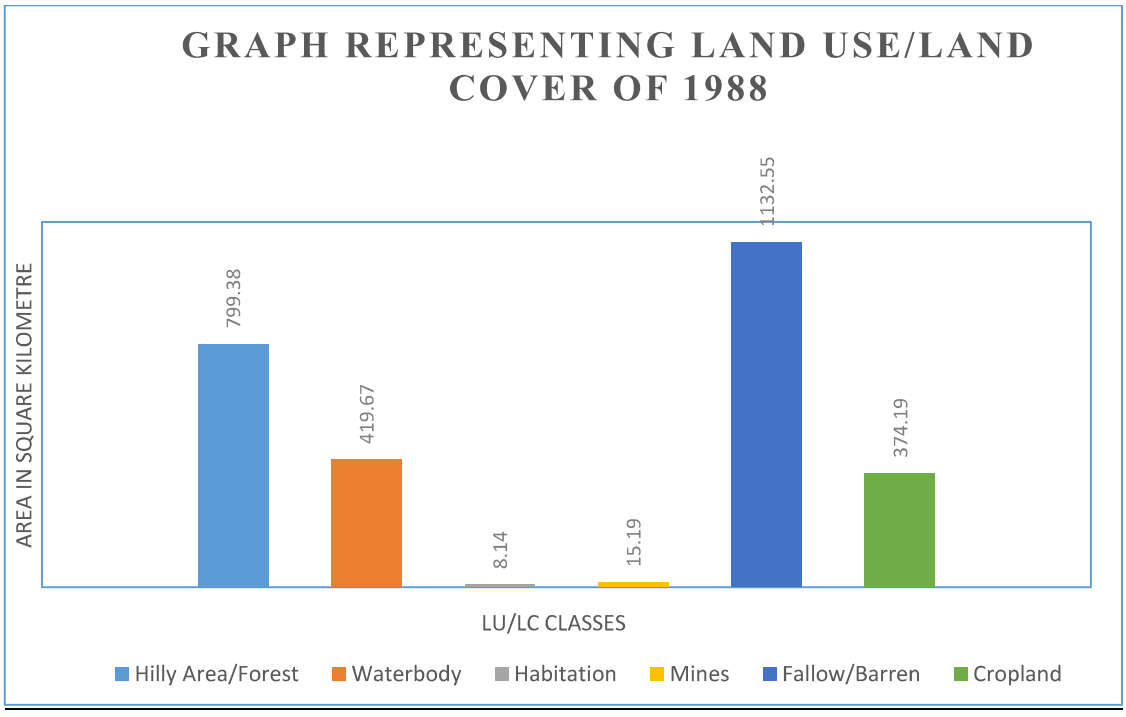

Fig 5.38 Graph representing Land Use/ Land Cover Classification for the year 1988

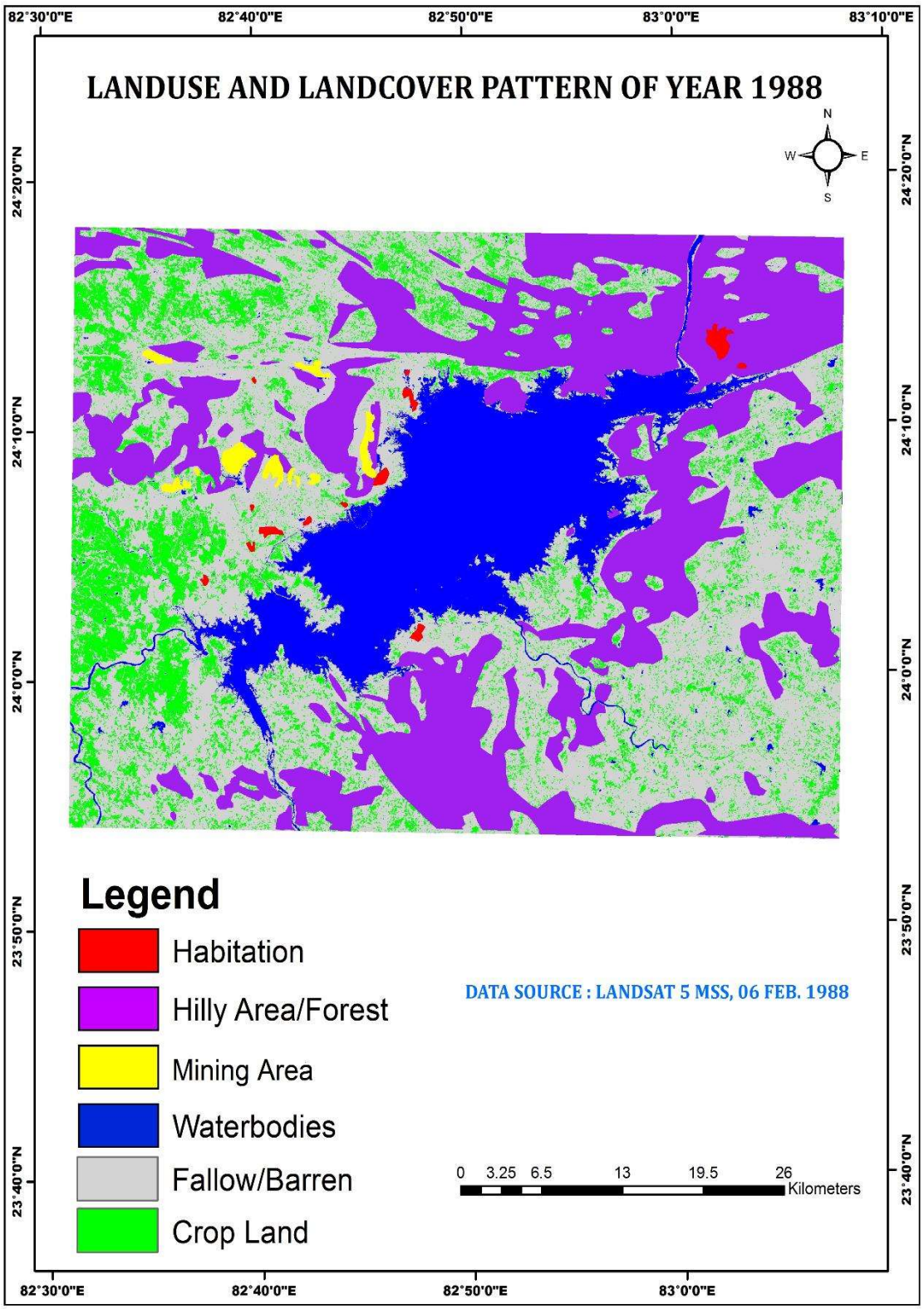

Fig 5.39 Land Use/ Land Cover Map of study area based on Landsat 5 MSS (1988)

5.5 Land Use /Land Cover Analysis (1996)

In the year 1996, the Landsat 5 MSS geocoded FCC satellite imagery of 27 Jan 1996 was interpreted for LU/LC mapping comprising a total area of 2749.14 km^2. The LU/LC classification suggests that the major part of the map is occupied by fallow/Barren class i.e. an area of about 1101.66 km^2 making up a percentage of 40.07% of the total area taken into consideration. Although there was reduction in the area covered by barren class from the year 1988 to 1996 but still it makes up the dominant class out of all the six classes taken into consideration. The next class which follows it is the Hilly Area/Forest category procuring 27.4%, an approximate area of about 753.35 km^2 of the total area employed in the study, though this class too showed a significant depletion in the area owned by the class from the year 1988 to 1996. Succeeding this, is the class consisting of water bodies comprising an area of about 392.45 km^2 analogizing 14.28% of the total area under study. This category too, unlike the previous two classes, exhibits a contraction in the area covered by the class during the year 1988 from the current year (1996). These reductions in the above three classess shows increased involvement of anthropogenic activities in the area under study. LU/LC statistics indicates that during the year 1996, changes prevailed with increase in area in the LU/LC classes exhibited in form of increase in the other three classes where cropland displayed maximum increase in area from the preceding imagery encompassing an area of about 468.33 km^2 contriving 17.04% of the total area under contemplation. Following this trend of increase in area, the next class which comes into consideration is the class of mining area embracing an area of about 23.76 km^2 equivalent to 0.864% of the overall area under study. The last class which accompanies this trend is the Habitation category enclosing an area of about 9.56 km^2 devising 0.348% of the aggregate area taken into evaluation. Table 5.3 represents the classes divided from LU/LC map through Landsat 5 MSS data of 1996.

LU/LC Category (1996)	Area (km^2)	Area (%)
Fallow/ Barren	1101.66	40.07
Hilly Area/ Forest	753.35	27.4
Water bodies	392.45	14.28
Cropland	468.33	17.04
Mining Area	23.76	0.864
Habitation	9.56	0.348
Total Area	**2749.14**	**100**

Table 5.3 Land Use /Land Cover Statistics (1996)

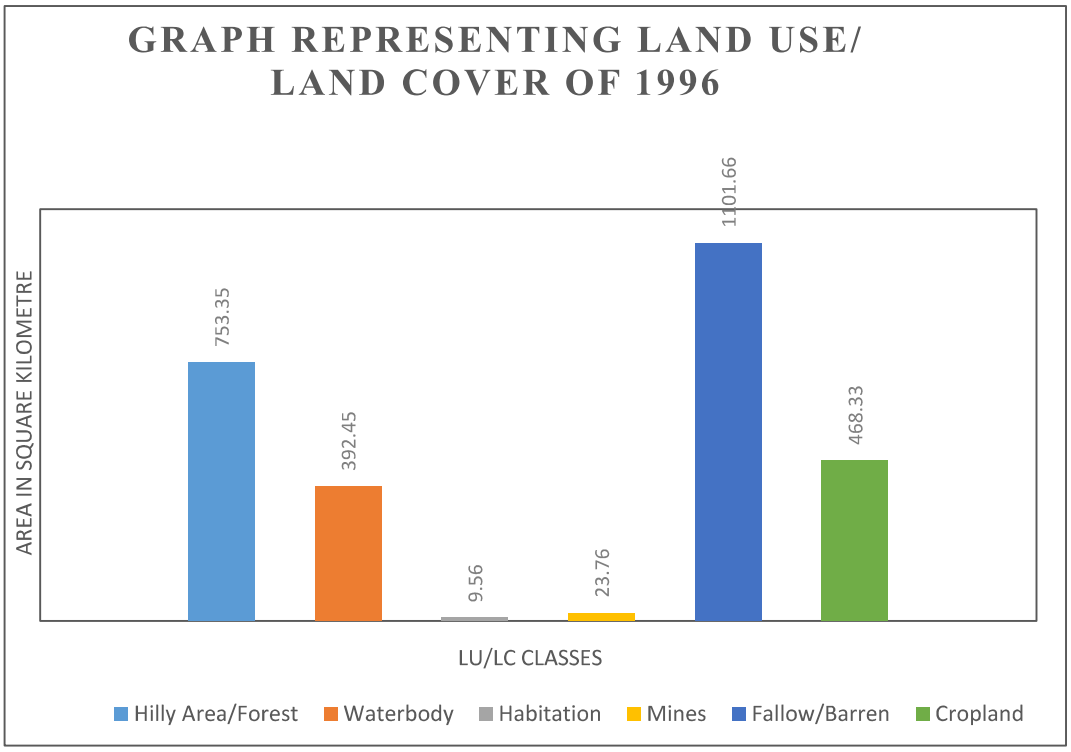

Fig 5.40 Graph representing Land Use/ Land Cover Classification for the year 1996

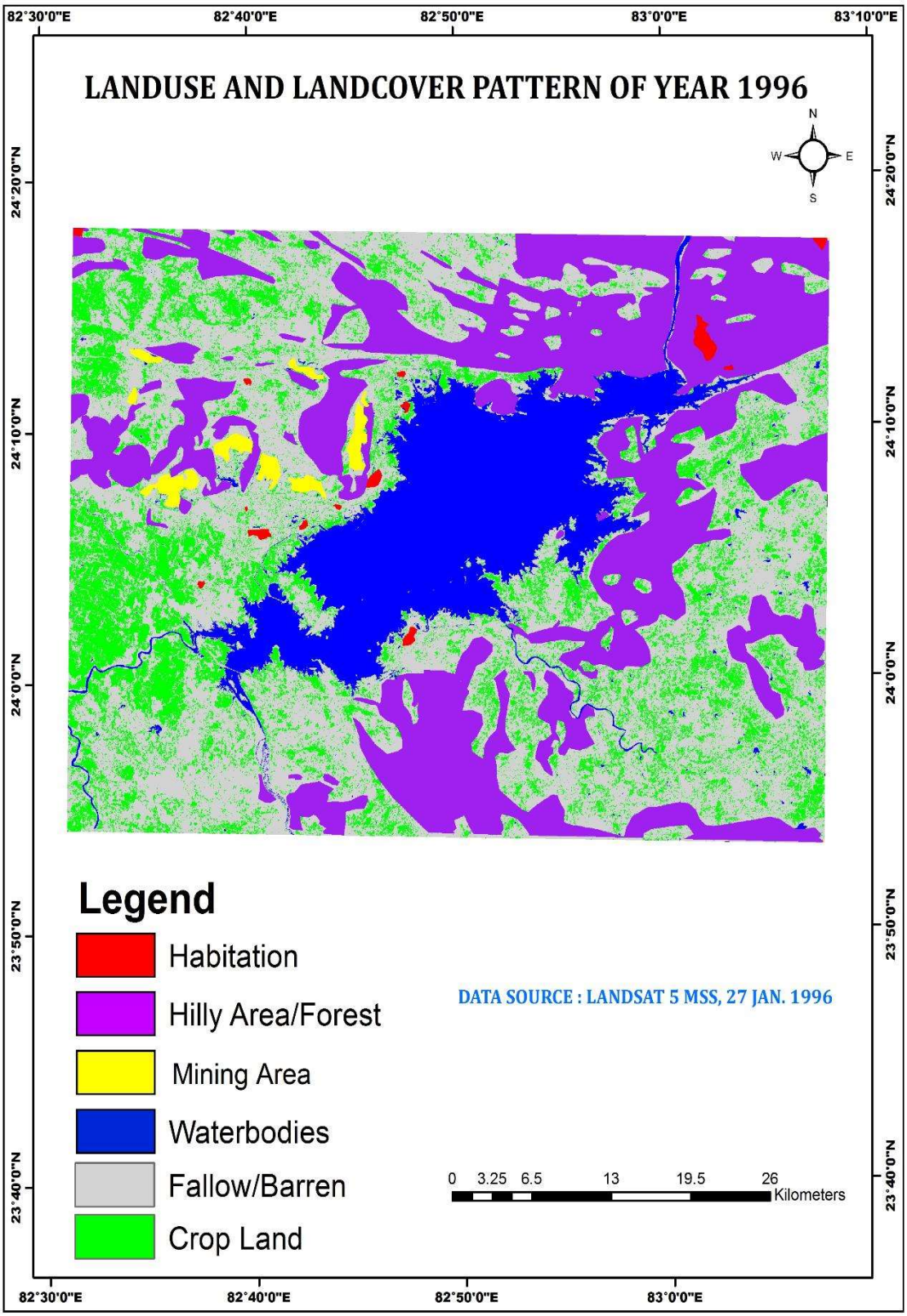

Fig 5.41 Land Use/ Land Cover Map of study area based on Landsat 5 MSS (1996)

5.6 Land Use /Land Cover Analysis (2005)

Landsat 5 MSS geocoded FCC of 04 February 2005 having spatial resolution of 30m with path 142 and row 43 was manoeuvred which propound that out of the six classes used in the LU/LC map of this year, the dominant class was again that of the Fallow/Barren area enclosing an area of about 1284.45 km^2 corresponding to about 46.72% of the total area under study. Although in the previous two maps this was a decrease in its area but the area in this year present in this class has increased significantly from that of the year 1996. The next class which occupies the majority of the area after this class is the Hilly/Forest area, though it showed the continuous decrease in the area when compared with the other two LU/LC maps but still it is one of the dominant classes in terms of area under study. This class surrounds an area of about 719.36 km^2 analogous to about 26.17% of the total area under investigation. Unlike the previous imagery, the area covered by cropland was found to be 396.56 km^2 constituting about 14.42% of the total area under evaluation. However, this class exhibited a sudden decrease in area under it varying from the preceding classification which manifested an increase in area from that of the year 1988. Succeeding this trend of decrease in area, water bodies like the two antecedent classifications follows the same tendency of decrease in area in the current LU/LC classification too. This particular category occupied an area of 307.04 km^2 and estimated percent of 11.17% of total area. Opposing this lean, the other two categories displayed an increase in area under them when compared with the last two LU/LC maps representing mining area enclosed an area of 28.51 km^2 i.e. 1.04% of the total area. While the class entitling habitation in the classification constitute an area of 13.2 km^2 making up a percent of 0.48% of the area used under the study. LU/LC derived from Landsat 5 MSS (2005) is shown in Table 5.4

LU/LC Category (2005)	Area (km^2)	Area (%)
Fallow/ Barren	1284.45	46.72
Hilly Area/ Forest	719.36	26.17
Water bodies	307.04	11.17
Cropland	396.56	14.42
Mining Area	28.51	1.04
Habitation	13.2	0.48
Total Area	**2749.14**	**100**

Table 5.4 Land Use /Land Cover Statistics (2005)

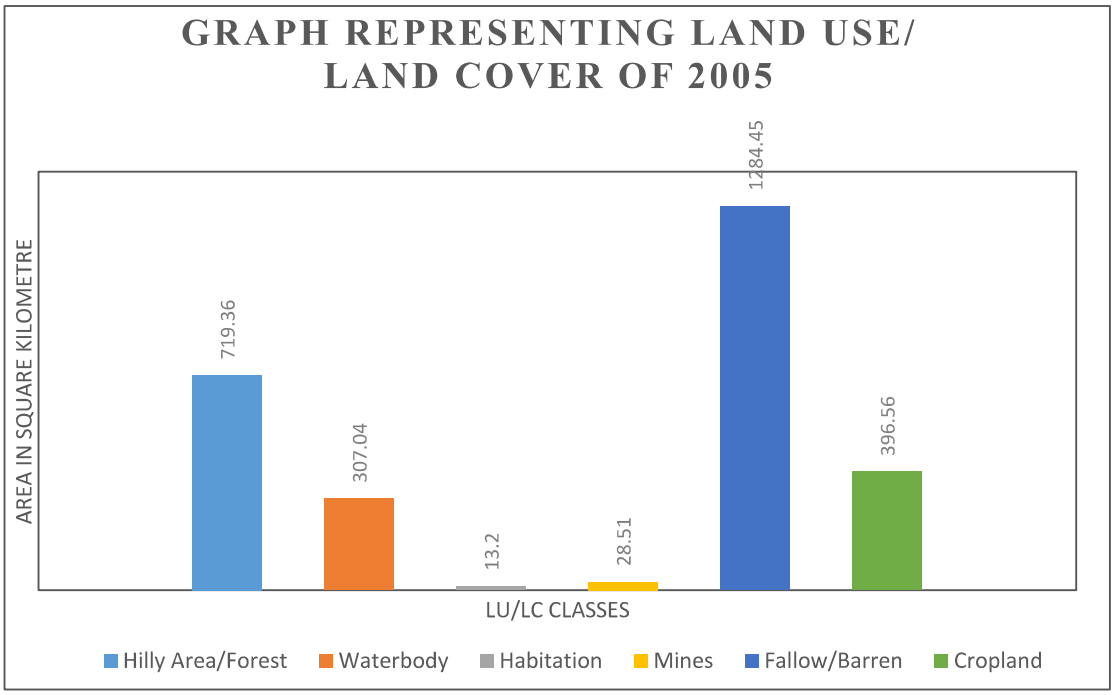

Fig 5.42 Graph representing Land Use/ Land Cover Classification for the year 2005

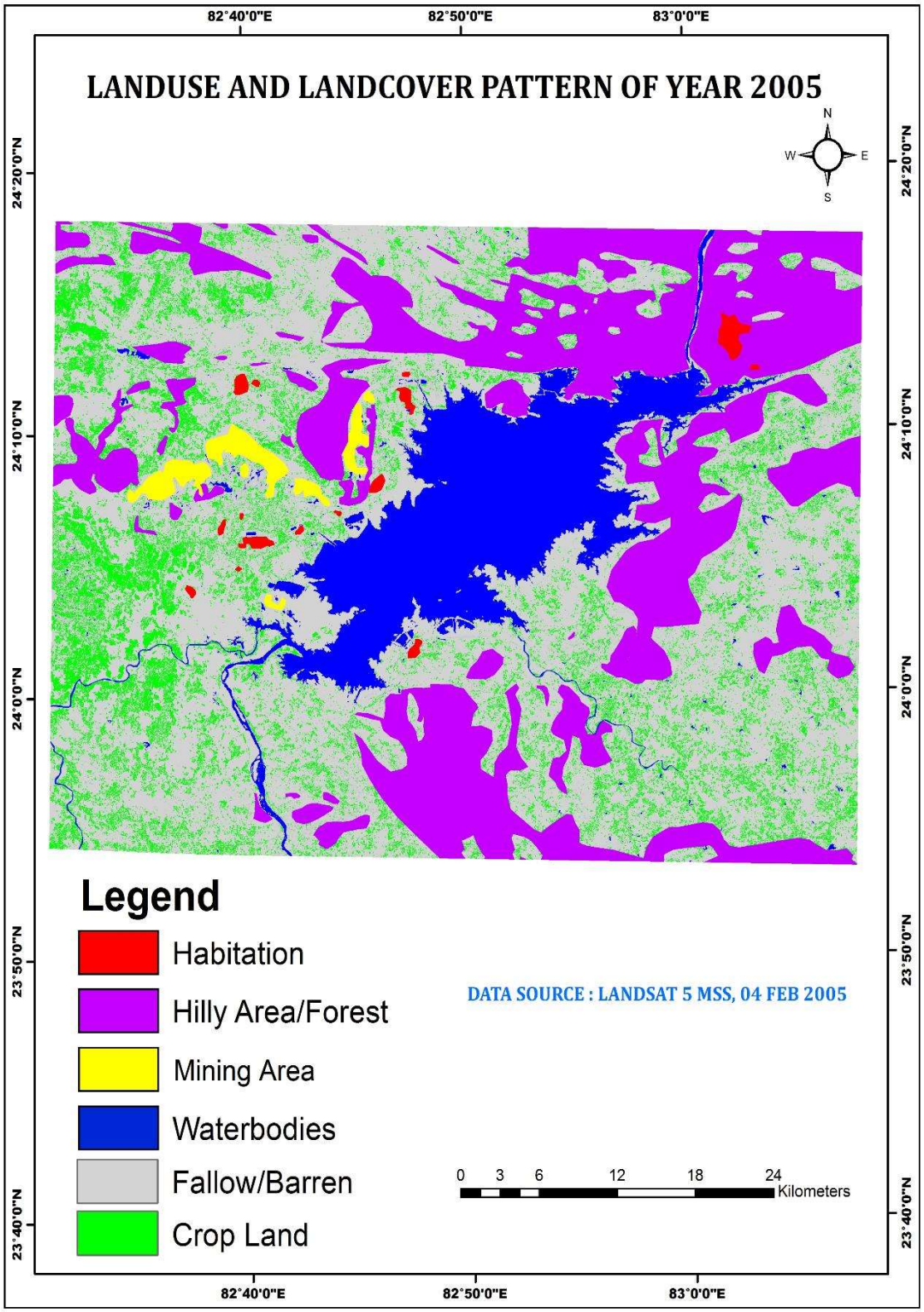

Fig 5.43 Land Use/ Land Cover Map of study area based on Landsat 5 MSS (2005)

5.7 Land Use /Land Cover Analysis (2016)

In the year 2016, the total area recorded from geocoded FCC of 19 February 2016 having spatial resolution of 30m resolution with path 142 and row 43 Landsat 8 OLI/TIRS satellite image was approximately 2749.14 km^2 encompassing six categories of LU/LC classification. During this year, the Fallow/Barren land class covers an area of about 1230.08 km^2 exhibiting the maximum area under it amongst the all six classes with a percentage of 44.74% showing a decrease from the precedent LU/LC classification. However, the second class enveloping the next highest area was that of the Hilly/Forest area encompassing an area of 683.93 km^2 forming 24.88% displaying the continuous decreasing trend which it showed during the preceding LU/LC classification. The next class covering the maximum area is that of the Cropland which unlike its quondam classification expressed a converse course of expansion in area under it with an area of about 435.22 km^2 constituting 15.83% of the total area under study. The upcoming class i.e. the class exhibiting water bodies unexpectedly showed a divergent result from its precursory LU/LC maps. During the current classification the area covered by it was approximately 315.53 km^2 constituting 11.47% of the total area taken under consideration. The remaining two categories which follow the increasing trend from the first LU/LC classification of the year 1988 are represented by Mining area and Habitation classes. The category indicating Mining area covers an area of 67.89 km^2 analogue to an approximately 2.47% of the total area under study while Habitation incorporates an area of about 16.42 km^2 equivalent to 0.597% of the entire area taken into account. LU/LC classification acquired from Landsat 8 OLT/TIRS (2016) is shown in Table 5.5

LU/LC Category (2016)	Area (km^2)	Area (%)
Fallow/ Barren	1230.08	44.74
Hilly Area/ Forest	683.98	24.88
Water bodies	315.53	11.47
Cropland	435.22	15.83
Mining Area	67.89	2.47
Habitation	16.42	0.597
Total Area	**2749.14**	**100**

Table 5.5 Land Use /Land Cover Statistics (2016)

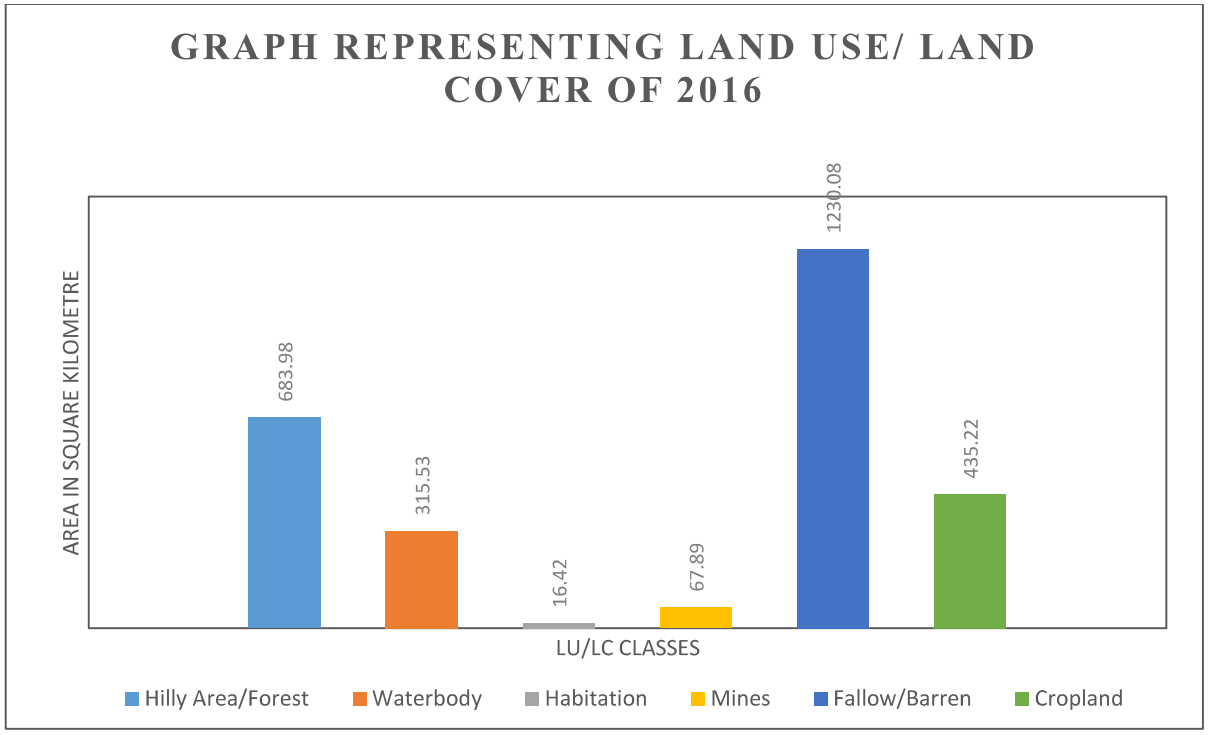

Fig 5.44 Graph representing Land Use/ Land Cover Classification for the year 2016

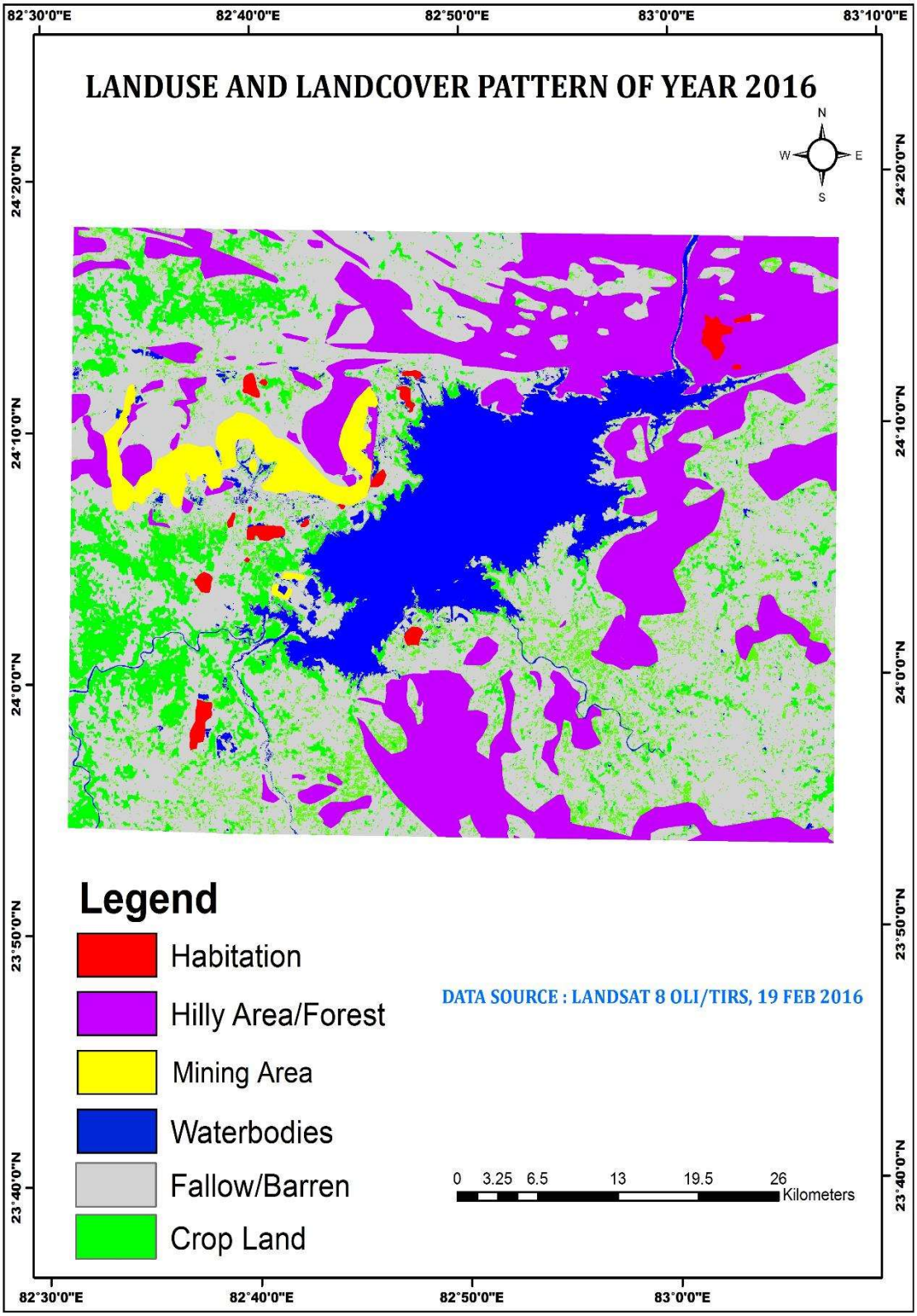

Fig 5.45 Land Use/ Land Cover Map of study area based on Landsat 8 OLI/TIRS (2016)

5.8 Land Use /Land Cover Analysis (2018)

Landsat 8 OLI/TIRS geocoded FCC of 24 February 2018 has been interpreted for LU/LC mapping again with a total area of 2749.14 km^2 having six classes. Major part i.e. 46.48% is occupied by Follow/Barren land which constitutes about 1277.72 km^2 proclaiming an increase from the proceeding LU/LC map of the year 2016. The next dominant class which is represented by the Hilly/Forest area forms an area of 673.79 km^2 corresponding to 24.51% exhibiting a continuous decreasing trend from 1988 to 2018. Following this decreasing trend as stated for the above class, Cropland too expressed a decline in area covered under this class. The area under it is approximately 351.79 km^2 making up 12.79% of the total percentage of area involved in study. Succeeding to it, is the category of water body covering an area of 335.63 km^2 analogous to 12.21% demonstrating an expansion in its area prevalent to the forms LU/LC classification (for the year 2016). Accompanying this, are the two categories of Mining area and Habitation respectively conveying an increase in area for both the classes as shown during the previous years. Mining area envelops an area of about 85.21 km^2 corresponding to 3.1% of the total area shown in the study while Habitation enclose 0.909% of the total area which is equivalent to about 24.98 km^2 of the area under study. LU/LC classification obtained from Landsat 8 OLI/TIRS (2018) is shown in Table 5.6

LU/LC Category (2018)	Area (km^2)	Area (%)
Fallow/ Barren	1277.72	46.48
Hilly Area/ Forest	673.79	24.51
Water bodies	335.63	12.21
Cropland	351.79	12.79
Mining Area	85.21	3.1
Habitation	24.89	0.909
Total Area	**2749.14**	**100**

Table 5.6 Land Use /Land Cover Statistics (2018)

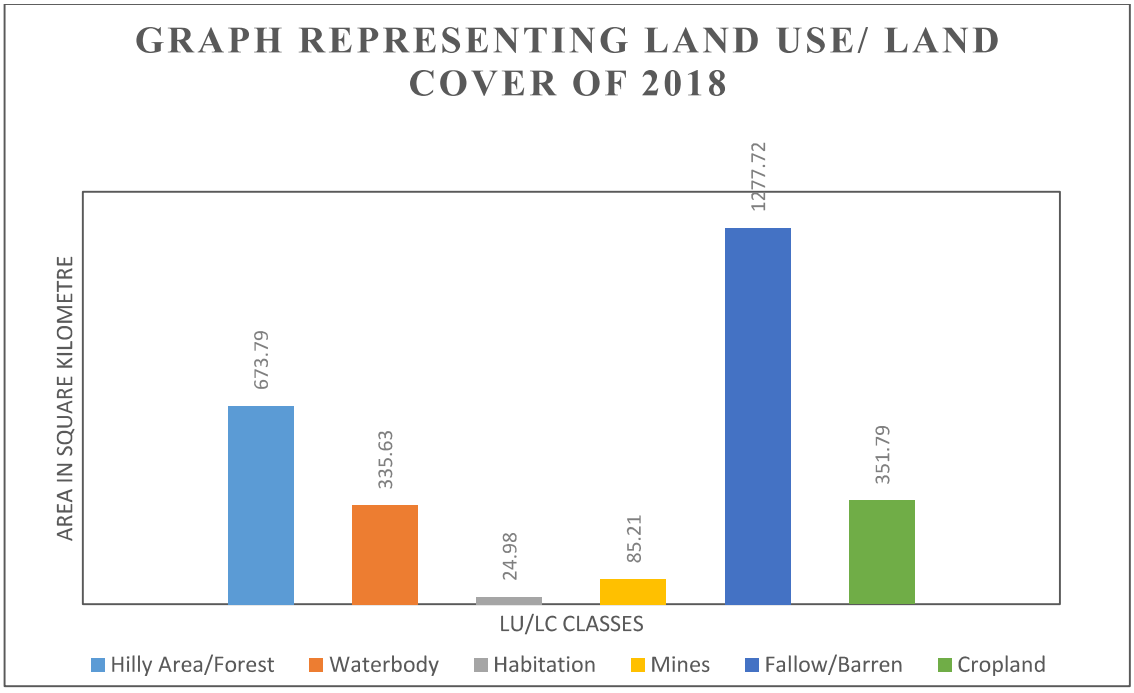

Fig 5.46 Graph representing Land Use/ Land Cover Classification for the year 2018

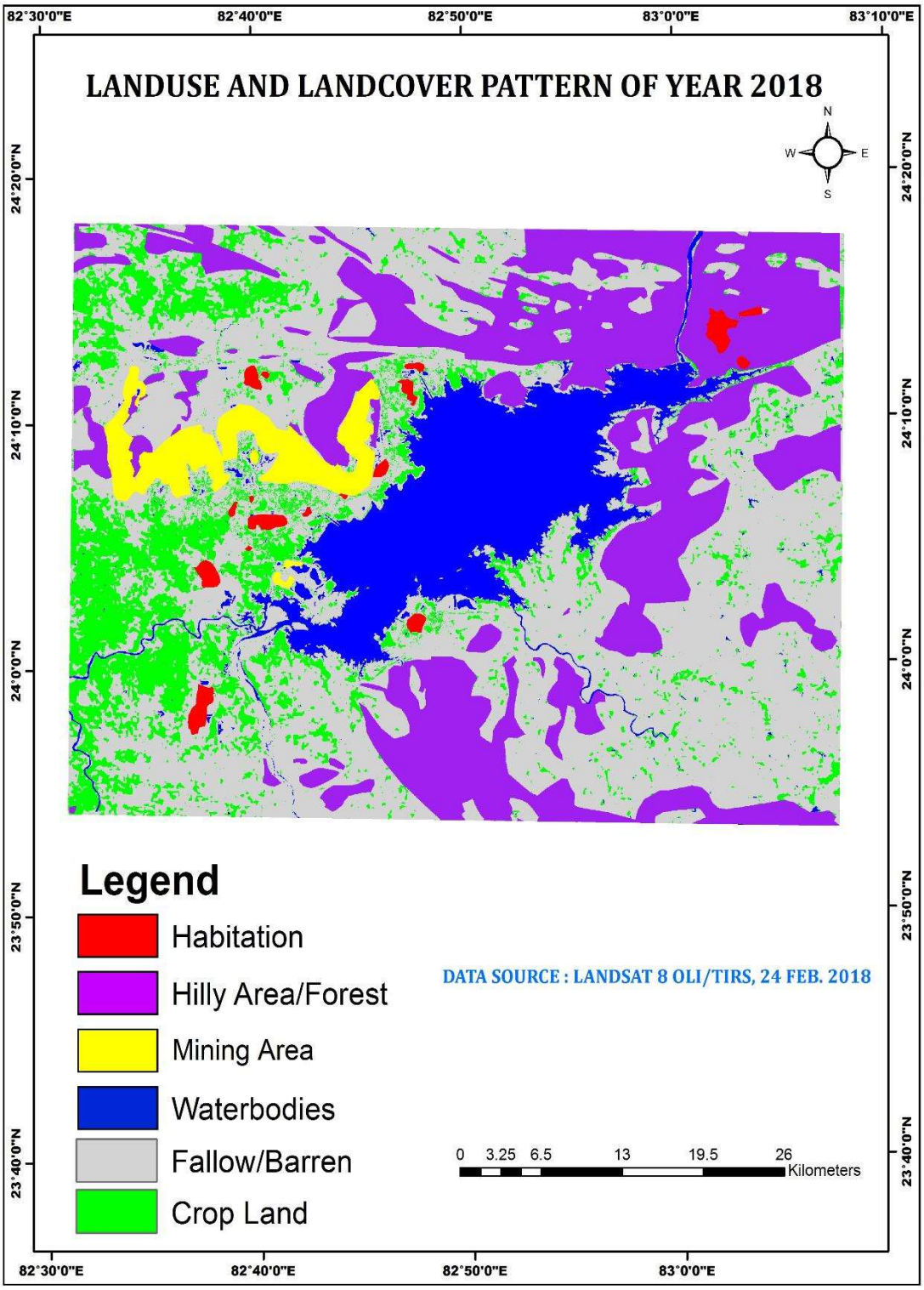

Fig 5.47 Land Use/ Land Cover Map of study area based on Landsat 8 OLI/TIRS (2018)

5.9 Land Use /Land Cover Change (1988-1996-2005-2016-2018)

LU/LC changes are the consequences of the interaction between socioeconomic, institutional and environmental factors posing an impact on the functioning of socioeconomic and environmental systems (Lesschen et al 2005). LU/LC changes comprises the transformation of various land cover classes used in the study. Here, in this study, the LU/LC change for the year 1988-1996-2005-2016-2018 has been analyzed to interpret the influence of LU/LC changes on the various classes of the LU/LC classification and especially on the water body of the study area. Significant changes have occurred during 1988-1996-2005-2016-2018 period due to natural or anthropogenic activities. Area statistics of each of the six categories of LU/LC classification for the year 1988, 1996, 2005, 2016 and 2018 has been computed in the Table 5.7 to analyze the change in each category over a time span of 30 years in terms of the extent of Area in km^2 and percentage. The notable LU/LC changes noticed during 1988-1995-2005-2016-2018 are discussed below:-

Land Use/ Land Cover Categories	**Land Use/ Land Cover (1988)**		**Land Use/ Land Cover (1996)**		**Land Use/ Land Cover (2005)**		**Land Use/ Land Cover (2016)**		**Land Use/ Land Cover (2018)**	
	Area (km^2)	**Area (%)**	**Area (km^2)**	**Area (%)**	**Area (km^2)**	**Area (%)**	**Area (km^2)**	**Area (%)**	**Area (km^2)**	**Area (%)**
Hilly/Forest	799.4	29.08	753.35	27.4	719.36	26.17	683.9	24.88	673.8	24.51
Water body	419.7	15.27	392.45	14.28	307.04	11.17	315.5	11.47	335.6	12.21
Habitation	8.14	0.296	9.56	0.348	13.2	0.48	16.42	0.597	24.98	0.909
Mining Area	15.19	0.553	23.76	0.864	28.51	1.04	67.89	2.47	85.21	3.1

Fallow/Barren	1132.55	41.19	1101.7	40.07	1284.5	46.72	1230.08	44.74	1277.72	46.48
Cropland	374.2	13.61	468.33	17.04	396.56	17.04	435.2	15.83	351.8	12.79
Total Area	2749.14	100	2749.14	100	2749.14	100	2749.14	100	2749.14	100

Table 5.7 Statistics showing Land Use/ Land Cover Change Analysis during 1988-1996-2005-2016-2018 period

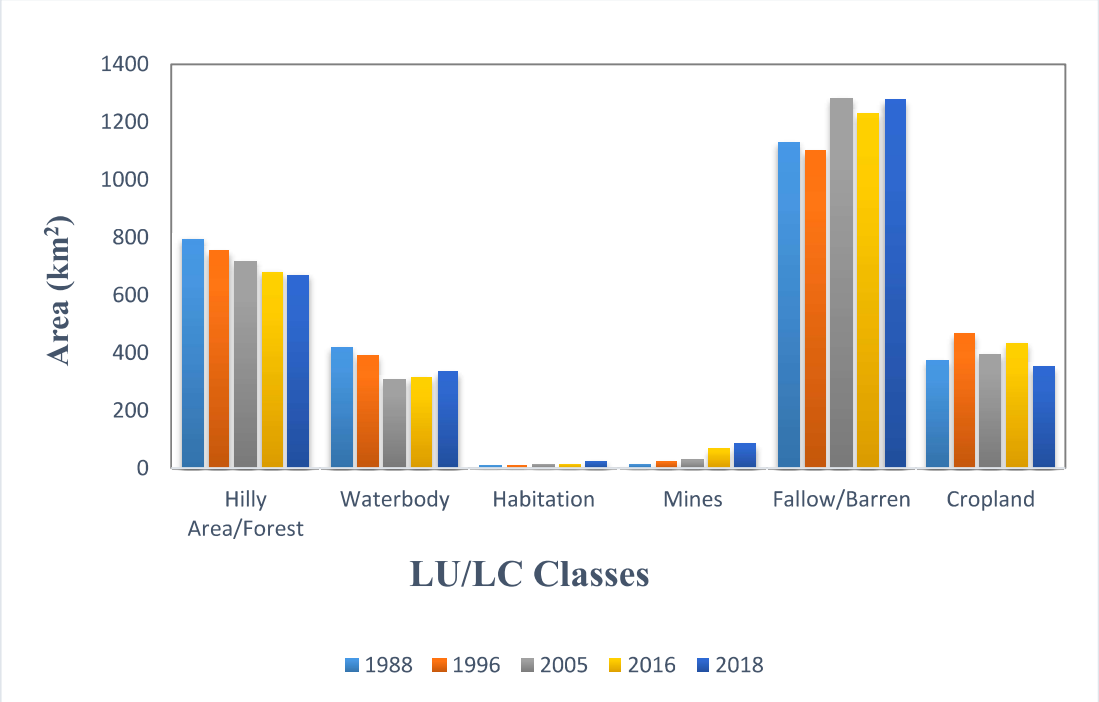

Fig 5.48 Graph representing various Land Use/ Land Cover Classes in square kilometers

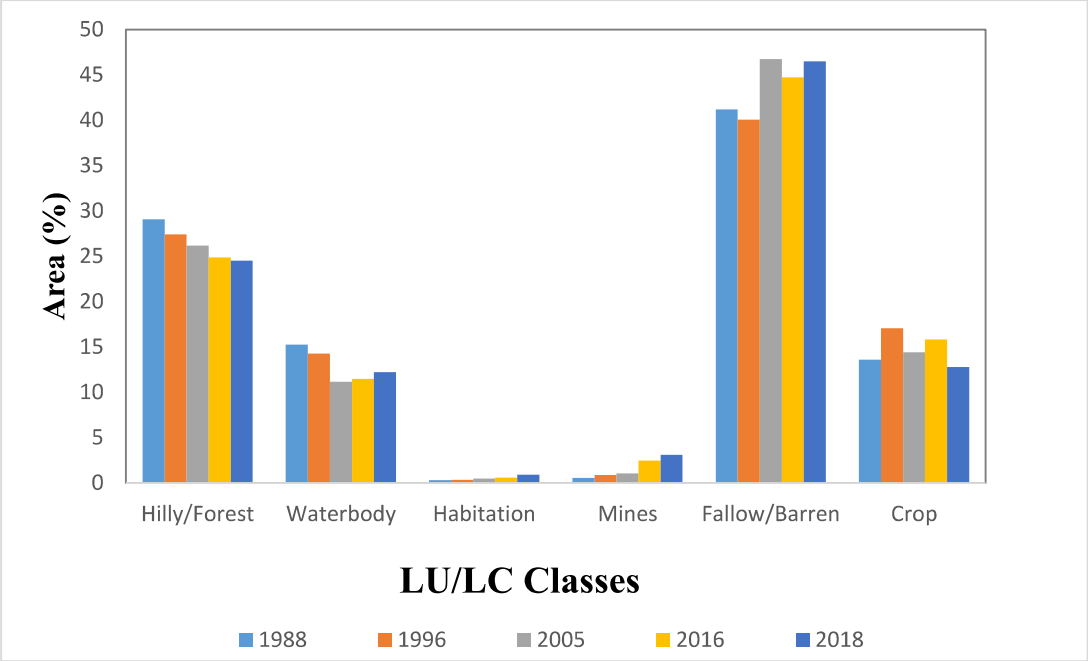

Fig 5.49 Graph representing various Land Use/ Land Cover Classes in percentage (%)

As it can be seen from the Table, that during all the five years of the study, the maximum and minimum area were covered by Fallow/Barren land and Habitation respectively. The changes observed in Fallow/Barren land is most in correspondence with changes in Cropland. During the year 1988 the amount of area enveloped by it was 1132.55 km^2 or 41.19%. However, during 1988-1996 period it shows a considerable decrease in its coverage by 2.73% i.e. 30.89 km^2 as the area occupied under it during 1996 was 1101.66 km^2. Thereafter, during the period of 1996-2005, it was found that unlike the previous time span it manifested a contrasting trend of increase in area under this class which is about 182.79 km^2 or 16.5% while the area under it was found to be 1284.45 km^2 during the year 2005. In the year 2016 the total area covered by it was 1230.08 km^2 again showing an opposite trend from its previous map i.e. a decrease of 54.37 km^2 or 4.23%. Following this, is the year 2018 where the area engaged under it was 1277.72 km^2 exhibiting an increase of 47.64 km^2 or 3.87% from the year 2016 although the total increase in area during 1988-2018 was approximately 145.17 km^2 or 12.82% .

The next class which covers the second highest area after Fallow/Barren land is Hilly/Forest land class which showed a continuous decreasing trend during the time span of 30 years. As it can be concluded from the Table, a decrease of 125.59 km^2 or 15.71% was found during this period. In the year 1988, the area under it was 799.38 km^2 or 29.08% of the total area enveloped under study while during 1996 there was a slight decrease of 46.03 km^2 or 5.76% from the year 1988. During 2005, the area under it was 719.36 km^2 following a decreasing trend of 4.51% or 33.99 km^2 from the preceding year. In 2016, the area encompassing the class was 683.98 km^2 revealing a decrease of 35.38 km^2 or 4.92% while the same trend was also observed in 2018 where there was a decrease of 10.19 km^2 or 1.49% from the year 2016 while incorporating an area of 673.79 km^2 under it.

The third class which falls in majority after the above two classes is the class of water body where up to the year 2005 there was decrease in its area coverage while the last two LU/LC classifications showed a positive trend of increase under it. During the year 1988, the area covered involved in it was 419.67 km^2 or 15.27% of the total area, though during 1996 the area of coverage was 392.45 km^2 which showed a decrease by 27.22 km^2 or 6.49%. The year 2005 too expressed a considerable decrease of 85.41 km^2 or 21.76% from 1988 and covering an area of 307.04 km^2. Opposite to the above three years, the year 2016 exhibited an increase in area of 8.49 km^2 or 2.77% while the area covered by it is 315.53 km^2. During the year 2018, the area inhabited by it was 335.63 km^2 showing an increase of 20.1 km^2 or 6.37%. Though, the overall decrease in area during 1988-2018 was 84.04 km^2 or 20.03%

The next class in majority is the cropland category where a hap-hazard trend of increase and decrease was observed while there was a decrease of 22.4 km^2 or 5.99% during the time span of 30 years. The year 1988 has an area of 374.19 km^2 under it is equivalent to

13.61%. During the year 1996, the area covered by it was 468.33 km^2 showing an increase of 94.14 km^2 or 25.16% while the year 2005 has an area of 396.56 km^2 under it exhibiting a negative trend of 71.79 km^2 or 15.33%. In 2016, an increase of 38.66 km^2 or 9.75% was observed with a total area of 435.22 km^2. The year 2018, showed a decrease of 83.43 km^2 or 19.17% with an overall area of 351.79 km^2 out of the 2749.14 km^2 area under study.

The last two classes which were in minority amongst all the 6 classes are Mining area and Habitation which are in one way or the other inter-related to each-other showing an overall increase in both the classes during the time span of 30 yrs. Amongst the two, the most considerable and reasonable change was observed in the Mining Area where there was a change of 70.02 km^2 or 82.17% increase from 1988-2018. An area of 15.19 km^2 was involved in it during 1988 i.e. 0.553% of the total area under study. The year 1996, has an area of 23.76 km^2 showing an increase of 8.57 km^2 or 56.41% while the year 2005 occupied an area of 28.51 km^2 exhibiting an increase of 4.76 km^2 or 16.67%. During the year 2016, the area covered by it was around 67.89 km^2 revealing an increase of 39.38 km^2 or 58.00% while the year 2018 employed an area of 85.21 km^2 with an increase of 17.32 km^2 or 25.51%.

The last class i.e. Habitation, having the minimum coverage under it showed an area of about 8.14 km^2 i.e. 0.296% of the total area under study during the year 1988. The year 1996, exhibited an increase of 1.42 km^2 or 17.44% having a total area of 9.56 km^2 under it. Following this was also the year 2005 where the increase was 3.64 km^2 or 38.08% with a total area of 13.2 km^2. During the year 2016, the area of incorporation was 16.42 km^2 exhibiting an increase of 3.22 km^2 or 24.4% while the year 2018 revealed an increase of 8.56 km^2 or 52.13% with an area of 24.98 km^2 was observed. However, the overall change or increase during 1988-2018 was found to be 16.84 km^2 or 67.41% showing an increase

in population thereby increasing the amount of habitation in the area due to various industries present in the area under study.

5.10 Change Detection Analysis

Change Detection can be defined as the procedure of recognizing dissimilarity in the situation of an entity or event by distinguishing it at different times. This process critically includes the quantification of temporal effects using datasets. The change detection analysis is considered as a useful tool for the interpretation of LU/ LC change over a time span of thirty years. It can be considered as a convenient instrument for the analysis of damage assessment, change in LU/ LC Analysis, monitoring of shifting agriculture, study of changes in vegetation phenology, crop stress detection, disaster monitoring, snow melt measurements, assessment of deforestation, day/night analysis of thermal characteristics and other environmental changes (Adeniyi 1980). Though, there are two methods for computation of change detection i.e. pre classification change detection and post classification comparison change detection. This study involves post classification change detection techniques. This method is based on the principle of comparison of individual classified images of different time periods. The post classification comparison method can not only locate the changes but also provide "from-to" change information and also minimize the problem caused by the variation in sensor and atmospheric condition (Singh 1989, Jensen 2004). This method employs the processing, classification and registration of satellite imageries of different years with the change in extent of different land use classes during in extent of different land use classes during the period 1988-2018 was examined and enumerated. This change detection map was produced by overlay analysis of land use maps of the years 1988 and 2018 and statistics related to it were generated to convey the distinctive nature of the change between the dates of imagery.

In this study, using ArcGIS 10.1 software a change detection map along with the statistics have been generated to access the major changes and land transformation in the study area during 1988-2018. The result obtained shows that 2088.06 km^2 or 75.95% of the area remain unchanged. From the Table 5.7 it can be concluded that out of the land cover types which are converted other types during the period 1988-2018, Cropland to Fallow/Barren land has the largest value compared with the other converted areas i.e. 198.56 km^2 or 7.23% of the total area under study. The area converted from Fallow/Barren land to Cropland was next in majority with 155.62 km^2 or 5.67% followed by Hilly/Forest land to Fallow/Barren land with 99.81 km^2 or 3.63%. The categories succeeding this category is the Water body to Fallow/Barren land, Fallow/Barren land to mines, Hilly/Forest land to mining area and Water body to Cropland with 65.01 km^2, 38.63 km^2, 30.89 km^2 and 26.59 km^2 respectively or 2.36%, 1.41%, 1.12% and 0.97% respectively. On the other hand, the area converted from Mining Area to Habitation was the smallest i.e. 0.009 km^2 or 0.00033% of the total area under study. This was followed by Mining area to Hilly/Forest, Water body to Habitation, Hilly/Forest to water body, Fallow/Barren land to Hilly/Forest land, Mining area to water body and Mining area to Cropland with 0.04 km^2, 0.16 km^2, 0.22 km^2, 0.25 km^2, 0.65 km^2 and 0.94 km^2 respectively or 0.0016%, 0.0058%, 0.0079%, 0.009%, 0.024% and 0.034% respectively. The categories which possess intermediary changes are Water body to Mining Area, Cropland to Water Body, Cropland to Habitation, Cropland to Hilly / Forest Area, Hilly/Forest Area to Cropland, Mining Area to Fallow/Barren land, Fallow/Barren land to Water body, Crop land to Mining Area and Fallow/Barren land to Habitation with 1.03 km^2, 1.06 km^2, 1.37 km^2, 2.18 km^2, 2.53 km^2, 4.27 km^2, 5.18 km^2, 6.75 km^2, 6.50 km^2 and 12.79 km^2 respectively or 0.038%, 0.039%, 0.05%, 0.08%, 0.092%, 0.16%, 0.19%, 0.25%, 0.23% and 0.47%. Based on the results, it could be concluded that these changes are mainly caused by

anthropogenic activities with few amounts of natural activity involved in it in the study area. The changes are depicted through the Graph and Figure below.

Categories	Area (km^2)	Area (%)
Unchanged	2088.06	75.95
Hilly/Forest-water body	0.22	0.0079
Hilly/Forest-habitation	2.18	0.08
Hilly/Forest-mines	30.89	1.12
Hilly/Forest - fallow/barren	99.81	3.63
Hilly/Forest-cropland	4.27	0.16
Water body-Hilly/Forest	0.25	0.009
Water body- habitation	0.16	0.0058
Water body-Mines	1.03	0.038
Water body-Fallow/Barren	65.01	2.36
Water body-cropland	26.60	0.97
Mines -Hilly/Forest	0.04	0.0016
Mines –water body	0.65	0.024
Mines - habitation	0.009	0.00033
Mines -fallow/barren	5.18	0.19
Mines -Cropland	0.94	0.034
Fallow/Barren-water body	6.75	0.25
Fallow/Barren- habitation	12.79	0.47
Fallow/Barren-mines	38.64	1.41

Fallow/Barren-crop	155.62	5.67
Crop -hilly/forest	2.53	0.092
Crop –water body	1.06	0.039
Crop - habitation	1.37	0.05
Crop -mines	6.49	0.23
Crop -fallow/barren	198.56	7.23
Total area	**2749.14**	**100**

Table 5.8 Land Transformation Statistics from 1988 to 2018.

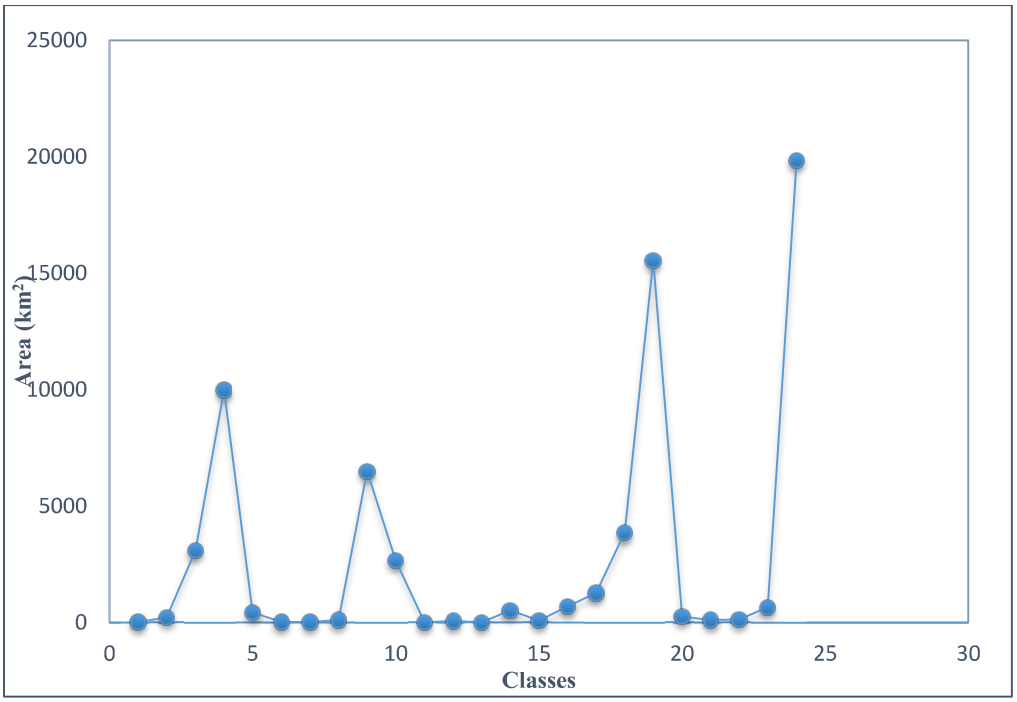

Fig 5.50 Graph representing Land Transformation Statistics from 1988-2018

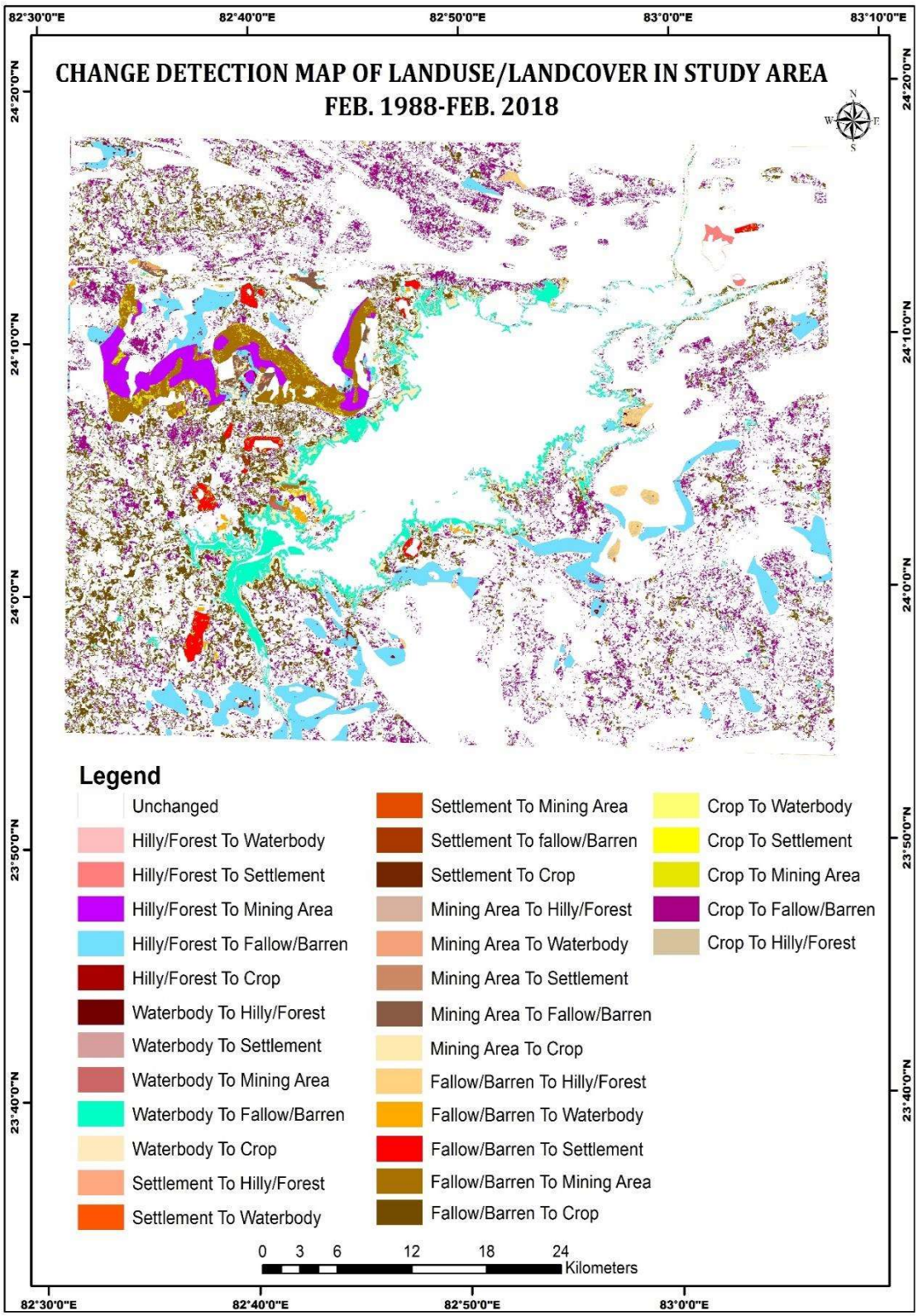

Fig 5.51 Change Detection Map of study area (1988-2018)

5.11 Volume Estimation of Govind Ballabh Pant reservoir

Due to the continuous pouring of sediments in the reservoir the complications of reservoir sedimentation is increasing relentlessly. This causes the amassing of sediments in the reservoir thereby affecting the ecological balance of the area and hence causing the loss of flora and fauna of the region. The sedimentation of the reservoir is mainly caused by human activities including the mining and other industrial activities in and around the reservoir. These sediments are the ultimate source of potential chemical and biological pollutants (Apitz et al 2005). Worldwide the siltation of the reservoir causes an annual loss of 0.5-1% of the total reservoir storage capacity thus affecting the catchment area of the reservoir as well as the local population dependent on it for fulfillment of their basic needs. Therefore, proper and incessant monitoring should be adopted to examine the change in volume of the reservoir over a particular timespan. Since, relocation of Total Suspended Solid plays a consequential role in estimating the volume of the reservoir both spatially and temporally hence, it's constant tracking should be done. In order to analyze the account of Total Suspended Solid deposition in the reservoir proper examination of the reservoir should be done based on long time series analysis. Many studies have been performed to calculate the storage capacity of the reservoir due to deposition of sediments. For example Ortt, VanRyswick & Wells, 2007 used echo sounding data to calculate the storage capacity of the reservoir since 1942 but none of the studies have been performed to calculate the volume of Govind Ballabh Pant reservoir. Therefore, to assess the impact of sedimentation on the volume of the reservoir, remote sensing and GIS plays an important role for performing detailed, fast and easy computation to extract the information about the reservoir and integrating them with other data to obtain the estimated volume of the reservoir over a particular timespan.

Since water storage capacity & water surface area of reservoir is the function of the water level elevation (Fuska et al 2017). Therefore, using this concept in particular the storage capacity loss of the reservoir has been monitored using TIN model creation from the data obtained over a time span of 20 years. Here, the storage capacity of the reservoir has been computed from the interpolated surfaces. The difference between the estimated volume of the reservoir has been analyzed by evaluating the difference between the volume of reservoir during the year 1998 to 2018. This difference in volume has been esteemed using the DEM Krigging and TIN approaches in ArcGIS software. The study hence utilizes ASTERGDEM (30m) for interpolating spatially for comparing the volume of reservoir for a time span of 20 years (1998 to 2018).

The volume of water present in reservoirs or lakes is influenced by the water balance between the influx through inflow of river, precipitation pouring of industrial effluents or through domestic discharge and outflux through percolation of groundwater, river outflow or withdrawal for industrial or domestic use. Therefore, its estimation using the difference of these influx and outflux is difficult hence, its measurement through direct methods such as remote sensing becomes easy. Traditionally, the volume of the reservoir was estimated using onsite measurement techniques such as bathymetric measurement using maps or it's evaluation using quantification in water level. Since, this method is neither cost effective nor accurate so it is quite difficult to measure the volume of a reservoir using this method. The use of DEM (Digital Elevation Model) has appeared as a powerful tool for the study of hydrological & geological lakes or reservoirs (Wang et al 2005). As DEMs help in examination and monitoring of reservoir automatically therefore it helps in furnishing guided detailed survey of the reservoir. Therefore, the information obtained through DEM helps in reducing the time and labour when compared with conventional methods.

The volume of the reservoir was computed by structuring the elevation matrix of the area by providing regular grid DEM data sampled at regular intervals in x,y planes. After this, these obtained points were merged to provide the perimeter and surface area of the reservoir. With the help of these coordinates obtained the reservoir terrain TIN was derived. Due to the presence of random coordinates on specific surfaces, TIN based DEM is computationally efficient. During the computation of TIN based DEM, the presence of depression and elevation were specially taken care by substituting them through the presence of appropriate intersect between them for precise measurement of reservoir capacity.

In this study, the volume of the reservoir was estimated by using the predetermined surface areas and the corresponding reservoir depths D, the surface area depth (A-D) relationship was derived and used to calculate the reservoir capacity (V) (Takeuchi 1997). The results for estimating the volume of the reservoir for four years were then calculated from DEM by multiplying the water level surface difference raster with the grid cell area. The elevation used for this computation ranges between 54.08 to 22.64m for the year 1998, for the year 2013 it ranges between 28.02 to 61.91m, 16.45 to 89.81m in the year 2016 and 25.21 to 114.86m for the year 2018. These figures help in establishing the relationship between volume-depth. Using this relationship the volume of the reservoir in the year 1998 was 30.72 km^3 while that during the year 2013 was 27.31 km^3. During the year 2016 the volume estimated was found to be 25.97 km^3 and during the year 2018 it was 25.12 km^3. The difference in volume during the year 1998 and 2013 was 3.41km^3 and during 2016 & 2018 the difference in volume was found to be 0.85 km^3. Therefore, it can be depicted from the result that the volume of the reservoir showed a considerable decrease during the time span of 2 years i.e. 2016 to 2018 which is due to increase in mining and other industrial activities in the area during this time span as can be observed

from Land Use/ Land Cover pattern during the year 2016 and 2018. However, the difference in volume between the year 1998 and 2018 was found to be 5.6km^3 again showing the decrease in volume of reservoir due to increase in mining activities as well as other activities like agricultural practices and habitation in the area as can be correlated with the Land Use/ Land Cover pattern during these years.

Thus, it can be seen from the results of volume estimation that TIN based DEM can be used as an alternative for conventional methods for simulation, designing and future monitoring of the reservoir. The same DEM model can be applied for any type of terrain for the construction, planning & designing of the reservoir. Therefore, TIN based DEM is thus used in the study for estimating the difference in volume of the reservoir during the time span of 20 years i.e. 1998 to 2018. The volume estimation of the study area can be depicted from Fig. 5.52 to Fig. 5.55 the year 1998 to 2018.

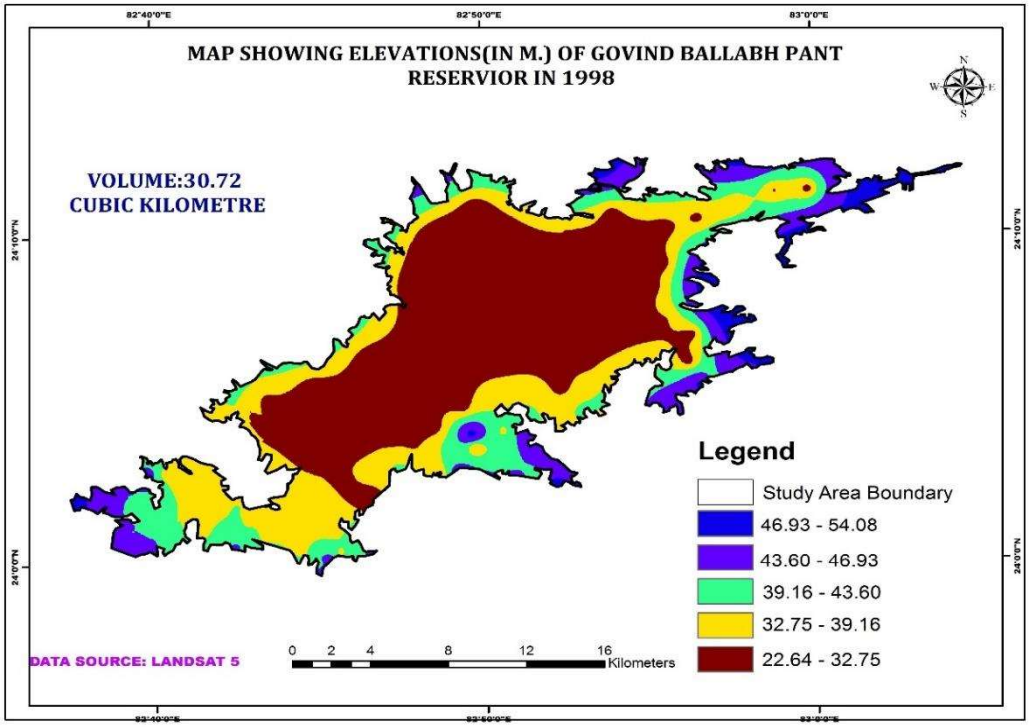

Fig 5.52 Estimation of Govind Ballabh Pant reservoir volume during 1988

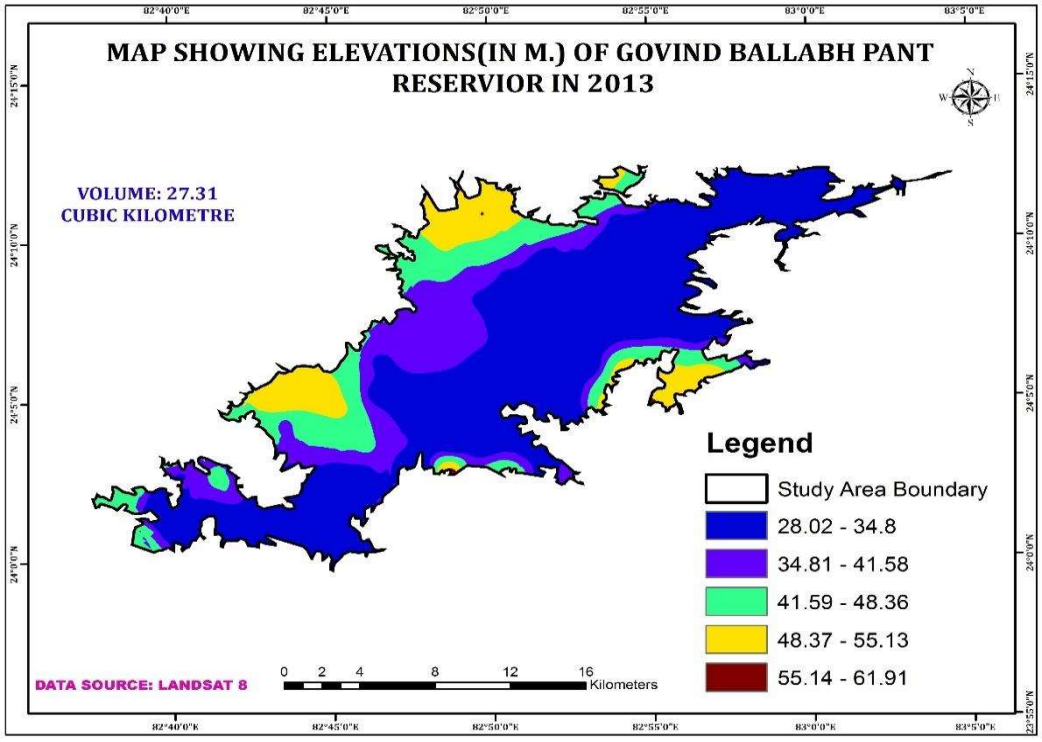

Fig 5.53 Estimation of Govind Ballabh Pant reservoir volume during 2013

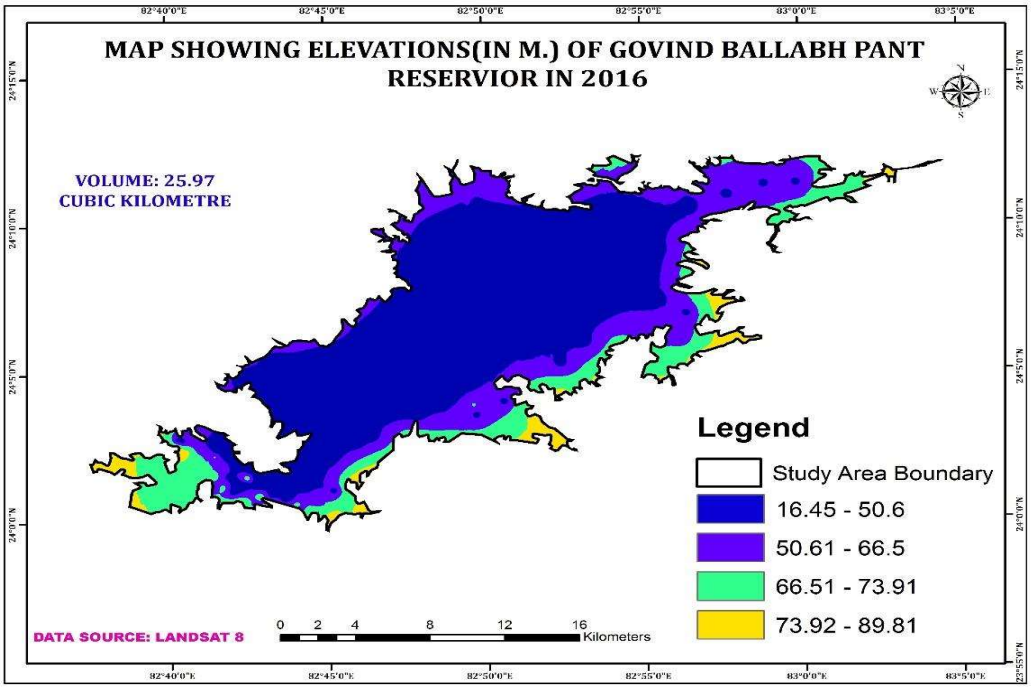

Fig 5.54 Estimation of Govind Ballabh Pant reservoir volume during 2016

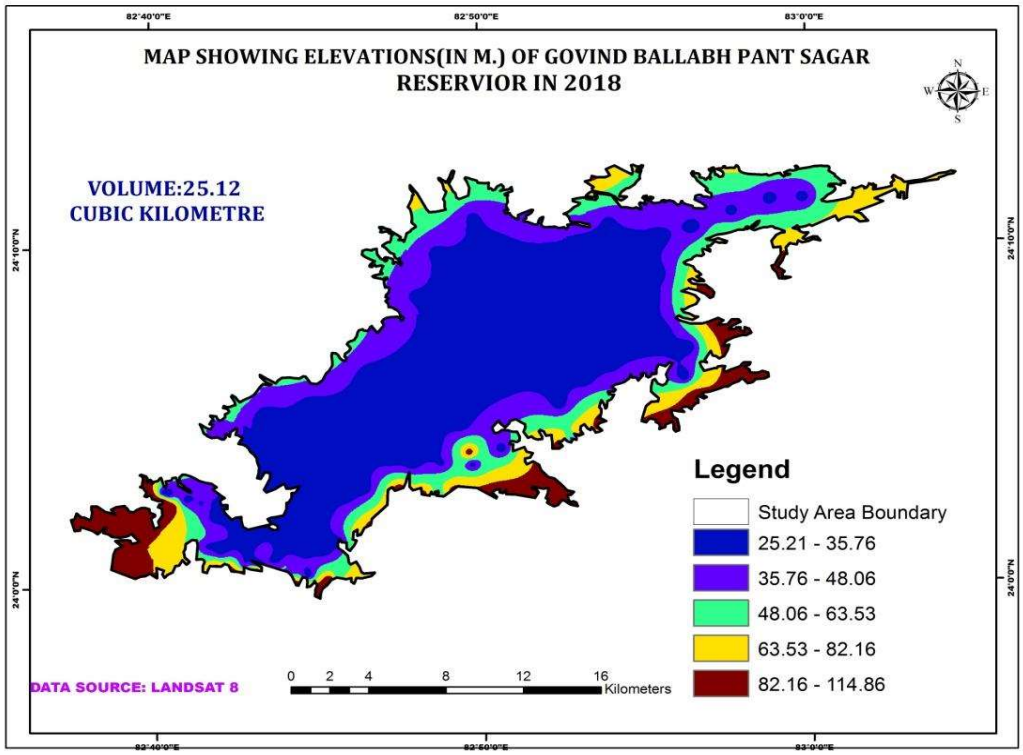

Fig 5.55 Estimation of Govind Ballabh Pant reservoir volume during 2018

As a result of mining, reclamation of mined land is increasing which in turn is decreasing the siltation problem of rivers and reservoirs of the area. However, the increase in siltation rate in reservoir i.e. reduction in volume of the reservoir is mainly due to major rivers disposing off water into the reservoir.

Hence, this chapter presents the stepwise analysis of the objectives and discusses the findings of the research in terms of its wider applicability and current state of art. The next chapter describes about the management of water pollution through phytoremediation at Balia Nala which is pouring its water directly into the Govind Ballabh Pant reservoir.